4-15-2019 10:00 AM

Valuation and Risk Management of Some Longevity and P&C Insurance Products

Yixing Zhao
The University of Western Ontario

Supervisor
Mamon, Rogemar
The University of Western Ontario

Graduate Program in Statistics and Actuarial Sciences
A thesis submitted in partial fulfillment of the requirements for the degree in Doctor of Philosophy

Abstract

Numerous insurance products linked to risky assets have emerged rapidly in the last couple of decades. These products have option-embedded features and typically involve at least two risk factors, namely interest and mortality risks. The need for models to capture risk factors' behaviours accurately is enormous and critical for insurance companies. The primary objective of this thesis is to develop pricing and hedging frameworks for option-embedded longevity products addressing correlated risk factors. Various methods are employed to facilitate the computation of prices and risk measures of longevity products including those with maturity benefits. Furthermore, in order to be prepared for the implementation of the new International Financial Reporting Standards (IFRS) 17, the thesis's secondary objective is to provide a methodology for computing risk margins under the impending regulatory requirements. This is demonstrated using a property and casualty (P&C) insurance example and taking advantage of P&C data availability.

To accomplish the above-mentioned objectives, five self-contained but related research works are undertaken and described as follows. (i) A pricing framework for annuities is constructed, where interest and mortality rates are both stochastic and dependent. The short-rate process and the force of mortality follow the two-factor Hull-White model and Lee-Carter model, respectively. (ii) The framework in (i) is further developed by adopting the Cox-Ingersoll-Ross model for the short-rate process to price guarantee annuity options (GAOs). The change of measure technique together with the comonotonicity theory is utilised to facilitate the computation of GAO prices. (iii) A further modelling framework extension is attained by considering a two-decrement model for GAO's valuation and risk measurement. Interest rate, mortality and lapse risks are assumed correlated and they are all modelled as affine-diffusion processes. Risk measures are calculated via the moment-based density method. (iv) We introduce a regime-switching set up for the valuation of guaranteed minimum maturity benefits (GMMBs). A hidden Markov model (HMM) modulates the evolution of risk processes and the HMM-based filtering technique is employed to generate the risk-factor models' parameter estimates. An analytical expression for GMMB value is derived with the aid of the change of measure technique in combination with a Fourier-transform approach. (v) Finally, a paid-incurred chain method is customised to model Ontario's automobile claim development triangular data set over a 15-year period, and the moment-based density method is applied to approximate the distributions of outstanding claim liabilities. The risk margins are determined through risk measures as prescribed by the IFRS 17. Sensitivity analysis is performed for risk margins using the bootstrap method.

Keywords: stochastic model, mortality, interest rate, guaranteed annuity option, guaranteed minimum benefit, comonotonicity, change of numéraire, hidden Markov model

Co-Authorship Statement

Two chapters (i.e., Chapters 3 and 4) of this thesis have already been published. The remaining chapters are now in manuscript form and under review in various peer-reviewed journals. I hereby declare that the research outputs incorporated in this thesis are the direct results of my main research works and efforts during the course of my PhD studies.

- The research materials in Chapter 2 are based on a manuscript with citation details

  'Zhao, Y. and Mamon, R., Annuity valuation under dependent risk factors'.

  This manuscript has been accepted for publication in the *Japan Journal of Industrial and Applied Mathematics*.

- The research results featured in Chapter 3 are the main bulk of an article with citation details

  'Zhao, Y. and Mamon, R. (2018), An efficient algorithm for the valuation of guaranteed annuity options with correlated financial and mortality risks, *Insurance: Mathematics and Economics,* 78 1-12.'

- The contents of Chapter 4 were used as basis for a full paper having the citation details

  'Zhao, Y., Mamon, R. and Gao, H. (2018). A two-decrement model for the risk measurement of a guaranteed annuity option. *Econometrics and Statistics,* 8, 231-249.'

- Chapter 5 is a modified version of a manuscript that is presently under second review in the *North American Actuarial Journal* and it has the citation details

  'Zhao, Y. and Mamon, R., The valuation of a guaranteed minimum maturity benefit under a regime-switching framework.'

- A manuscript with citation details

  'Zhao, Y. and Mamon, R., Setting risk margin for claims liabilities in accordance with IFRS 17 '

is under second review in *ASTIN Bulletin: The Journal of the International Actuarial Association* and its contents constitute Chapter 6 of this thesis.

An integrated-article format is employed in line with Western's thesis guidelines. Each chapter in this thesis can be read independently as it does not rely on other chapters. Therefore, every chapter is deemed to be self-contained and can stand on its own; in addition, the notations used are defined and described at the beginning of each chapter. As the first author of all manuscripts incorporated in this thesis, I am responsible for the development of modelling set-up, the implementation of algorithms, and the completion of the manuscripts. The research plan, model formulation, and empirical analysis of all aforementioned work are guided and supervised by Dr. Rogemar Mamon. Some computing insights along with certain risk-factor modelling considerations were provided by Dr. Huan Gao; they emanated from her elemental conceptualisation and served as starting points of Chapter 4.

I certify that this thesis is fully a product of my own work. This was conducted from September 2015 to present under the supervision of Dr. Rogemar Mamon at *The* University *of* Western Ontario.

This work is dedicated to my parents.
Thank you for your unflinching support, love and encouragement.

Acknowledgements

First and foremost, I would like to express my special appreciation and thanks to my supervisor, Dr. Rogemar Mamon, for his undiminished motivation, continued support and unfailing patience throughout my entire graduate education. His professionalism, meticulous supervision, immense knowledge and scientific insights not only ensured the accomplishment of my research work, but also enhanced my problem-solving and other transferable skills, which are invaluable for my future's work and study.

I would also like to thank my thesis committee members: Dr. Tak Kuen Siu, Dr. Shu Li, Dr. Jiandong Ren and Dr. Xingfu Zou for their insightful comments and constructive suggestions on this dissertation. Moreover, I am grateful to the outstanding faculty and staff at the Department of Statistical and Actuarial Sciences (DSAS) for their support in various capacities. I also acknowledge the financial support provided by DSAS and the MITACS-Accelerate program.

Many thanks to Joe Cheng and his staff at JSCP for their profound industry insights, professional advice and precious guidance during the time of my internship work in Toronto. The skills I learnt from them and the experience I gained from the internship has helped me broaden my horizon and enable a better understanding of the connection between my research work and its potential for impact in the industry.

I also thank all of my colleagues and friends in Canada. They never hesitated to offer me their moral support and encouragement. The cheerful moments shared with them together will absolutely be part of happy memories and enduring friendships for the years to come.

Last but not least, I would like to convey my immense gratitude to my parents for their selfless love. They have provided me with an unfailing support and continued encouragement to persevere in pursuing what I love most: research and academic endeavours. Certainly, this big milestone would not have been possible without them.

Contents

List of Figures

List of Tables

Chapter 1

Introduction

1.1 Research motivation and objectives

The importance of managing longevity risk in the pension sector has become more profoundly pronounced in recent years as improvements in mortality have continued. Governments, insurance companies and individuals must deal with longevity risk in order to to provide stable and dependable social security for the populace. Many innovations were introduced by the insurance industry and the capital markets to facilitate the hedging and transfer of longevity risk. Such financial innovations are in the form of new investment products including mortality-catastrophe bonds, longevity bonds, longevity swaps, and mortality-forward contracts, amongst others.

The International Longevity Risk and Capital Markets Solutions Conferences were held to discuss and analyse these longevity-related developments in their impact to the economy and financial markets. In 2008, the Institutional Life Services and the Institutional Life Administration were launched to serve as life settlements' trading platform and clearing house. The Life and Longevity Markets Association was established in 2010 to promote the development of a liquid market involving longevity- and mortality-related risks. The volume of transactions and amounts of longevity products all around the world have grown dramatically in recent years. Academic researches on longevity risk also made headway in the analysis of capital markets that accommodate the trading of longevity-linked contracts. Specifically, ideas on the use of longevity bonds to hedge longevity risk in the capital market have been promoted, and they cover the following themes: developing longevity-linked markets, pricing longevity-linked products and derivative, mortality indices, longevity risk in pension plans and pension systems, natural hedging of longevity risk, and mortality

modelling.

Stochastic models, which are mathematical tools for estimating and predicting random events over time, are necessary to support the investigation of longevity risk. They have been widely used in many research areas such as engineering, natural sciences, economics, and business. Financial innovations, needing random models, entail the creation of many insurance products with option-embedded features such as guaranteed annuity options and equity-linked annuities. Uncertainty arises from future liability in these products and must be taken into consideration when pricing and hedging them. This uncertainty could lead to huge losses and liquidity problem for insurance companies. Hence, it is important to model and include these risks explicitly in the actuarial valuation. Considering the similarities of these insurance products to financial derivatives, option-pricing theory in conjunction with stochastic modelling could be relied upon. Typically, the interest, mortality and lapse risks are assumed independent of each other ease computational hurdles. Nonetheless, the correlations between these risks are should not be ignored especially when there is strong empirical evidence.

The International Accounting Standards Board issued the new International Financial Reporting Standard in May 2017, which is now commonly known as IFRS 17. It will replace IFRS 4 on the accounting of insurance contracts. It will come into effect on 01 January 2022. IFRS 17 introduces a new measurement model for insurance contracts and will give users of financial information a whole new perspective on insurance companies' financial statements. Therefore, new methods for calculating risk margins for claims adherent to IFRS 17 are desired.

The specific aims of this thesis consist of the following: (i) Propose suitable pricing and hedging frameworks for longevity products with investment guarantee where the correlation between risks are explicitly modelled. (ii) Facilitate the valuation of insurance products with the aid of change of measure technique and comonotonicity theory. (iii) Determine various risk measures and compare them quantitatively. (iv) Perform sensitivity analyses and investigate the impact of each factor on prices and risk measures of insurance products. (v) Develop a risk-margin calculation method that meets the requirement of IFRS 17.

1.2 Literature review

This section provides an overview of pertinent stochastic modelling and its applications to capture the time-series behaviours of interest, mortality, lapse rates supporting the valuation and risk management of insurance products.

1.2.1 Stochastic modelling of interest rate

Stochastic models in finance can be traced back to the 1900s when Bachelier [1] utilised Brownian motion to model stock price movements in the Paris Stock Exchange and to study the option markets. In Vasiček [23], an equilibrium interest rate model was in introduced for the short rate process based on the Ornstein-Uhlenbeck specification having a mean-reverting feature. The Vasiček interest rate model continues to have a significant influence in the current financial modelling. Widening the interest-rate model choices, Cox et al. [4] developed the Cox-Ingersoll-Ross (CIR) short-rate interest model based on a square-root diffusion, thereby avoiding non-negativity of the process but still maintaining mean reversion.

An alternative methodology to modelling interest rates is the no-arbitrage approach. Under this approach, a model is designed to match today's term structure of interest rates. The first no-arbitrage model of interest rate term structure was developed by Ho and Lee [10] in which the drift term is a function of time and is calculated analytically by using forward rates. Hull and White [11] extended the Vasiček model so that it fits the initial term structure exactly. In Hull and White [12], a two-factor model is proposed, where the mean-reverting level is a stochastic process. The Hull-White two-factor model is able to replicate richer patterns of term structure movements and volatilities than the one-factor models.

Further model flexibility could be obtained using regime-switching processes for interest rates; normally, the Markov chain either in discrete or continuous time drives the evolution of parameters. The work of Hamilton [9] pioneered the application of a regime-switching technique to economic modelling. Elliott and Mamon [8] presented a Markovian interest rate model with a complete term structure characterisation. The proof is given via the Unbiased Expectation Hypothesis and change of measure technique. An explicit analytical expression for the bond price under the Heath-Jarrow-Morton approach in a Markovian market environment was also derived.

1.2.2 Stochastic modelling of mortality rate and lapse rate

In traditional frameworks, the probabilities of death, which are used in life insurance premium and reserve calculations, are assumed deterministic and obtained using observed data. However, with medical and health care advances, the future uncertainty on morality rate remains unabated.

The first account of using stochastic processes to model the movement of mortality rates appears to originate from the work of Lee and Carter [15]. In their paper, the logarithms of mortality rates are modelled as a linear function of a time-varying index with age-dependent parameters. The time-varying index can describe the variation of mortality patterns over time. The least-squares solution to the model were obtained by employing the singular-value decomposition method. Predictions of mortality and other life table variables were also derived and presented. The concept that allowing uncertainty in the mortality rate by modelling it as a stochastic process inspires subsequent research works on stochastic mortality based LC model.

Cairns et al. [3] compared quantitatively eight stochastic mortality models. In their paper, a model was developed to capture the improvement of mortality at higher ages. The cohort effects were also taken in to account. They also pointed out that the most suitable model for different cohorts might be different as well.

A Markovian regime-switching (RS) model incorporating mortality state switches into mortality dynamics is developed in Milidonis et al. [21]. In their paper, the error term of the time-varying index in the LC model is modelled as a regime-switching process. It was highlighted that RS models have the capacity to describe the timing of a structural change in death rates and the duration of each regime.

Modelling lapse rates appropriately is also important in the management of the assets and liability of insurance companies. The risks arising from lapsation could threaten the insurer's liquidity and force the selling of their assets. Eling and Kochanski [7] gave a comprehensive review of lapse-rate modelling in life insurance.

De Giovanni [5] built a Rational-Expectation model to describe lapse rates. In his paper, the interest rate follows the CIR model and the price of a insurance product embedded with surrender option was carried out via numerical approximation of the two-space-dimensional

parabolic partial differential equation. Loisel and Milhaud [18] proposed a stochastic model for lapse rate with a bi-modal distribution. Numerical results were carried out and showed that the lapse rate distribution could affect appreciably the reserves of the company and forecasts of its economic capital needs.

1.2.3 Stochastic modelling in actuarial valuation and risk measurement

The rapid emergence of complex insurance products with option-embedded features necessitates all the more reason to apply and advance stochastic modelling in finance and actuarial science. Ballotta and Haberman [2] considered the fair valuation of guaranteed annuity options (GAOs) but with independent financial and insurance risks.

Following Jalen and Mamon [14], an integrated framework was proposed for the valuation of contingent claims with correlated interest and morality risks. They relaxed the assumption of independence between two risks and assume that both interest and mortality rates follow affine-type stochastic process. The survival benefit can be priced in an analytically tractable way in conjunction with the change of measure technique.

Both Liu et al. [16] and Liu et al. [17] developed a generalised pricing framework for GAOs. In their framework, two risks are assumed dependent and the short rate follows the Vasiček model whilst the mortality rate follows the non-mean-reverting process in Luciano and Vigna [19]. A simplified for the GAO price was derived by using the change of measure technique. The numerical results showed that their proposed method has highly efficient and accuracy.

Deelstra et al. [6] proposed a GAO pricing set up based on the approach in Liu et al. [17]. They considered multi-factor models for the interest and mortality rates under some generalised affine settings. Specifically, a Wishart affine model, which allows a non-trival dependence between the mortality and the interest rates, was taken into consideration.

A hidden Markov model (HMM) is also employed in actuarial valuation. In Shen and Siu [22], an HMM was developed for valuing longevity bonds incorporating jumps in both the short rate and force or mortality. An exponential affine form solution of the longevity bond price in terms of the fundamental matrix solutions to linear, matrix-values ODEs is derived. Ignatieva et al. [13] presented a regime-switching framework for pricing and

hedging Guaranteed Minimum Benefits (GMBs). Semi-closed form solutions for prices and the Greeks for GMBs are derived and computed efficiently using the Fourier-Space Timestepping algorithm.

1.3 Structure of the thesis

This thesis comprises seven chapters. The current chapter (Chapter 1) gives an overview of recent stochastic models used in finance and insurance. The succeeding chapters make up a collection of five related research papers. Chapter 2 presents a model setting for the valuation of annuities that assumes dependent financial and mortality risks. In Chapter 3, we propose a pricing framework addressing correlated interest and mortality risks. The change of measure technique and comonotonicity theory are employed to facilitate the valuation of a guaranteed annuity option(GAO). We introduce a two-decrement model for the valuation and risk measurement of a GAO in Chapter 4. Chapter 5 introduces a regime-switching framework for a guaranteed minimum maturity benefit (GMMB). Filtering technique is utilised to estimate model parameters. In Chapter 6, we devise a method to determine risk margins in line with the new accounting standard referred to as IFRS 17. Finally, some concluding remarks and future directions are outlined in Chapter 7. The contents of Chapters 2-6 are briefly reviewed below.

1.3.1 Annuity valuation under correlated risks

A pricing framework for annuity valuation is considered, where the dependence between interest and mortality risk factors is modelled explicitly. The calculation is facilitated by combining the change of measure and comonotonic-based methods to obtain accurate approximation of the survival probability's quantile and hence annuity value. We demonstrate that our approach is significantly more efficient than the usual simulation under a stochastic setting. The interest rate is governed by a two-factor Hull-White model to capture current levels of very low and even the possibility of negative rates occurring in some countries post-2008 financial crisis. The mortality rate evolves in accordance with a continuous-time version of the Lee-Carter (LC) model.

1.3.2 An efficient algorithm for the valuation of a guaranteed annuity option with correlated financial and mortality risks

We introduce a pricing framework for a GAO, where both the interest and mortality risks are correlated. We assume that the short rate and the force of mortality follow the Cox-Ingersoll-Ross (CIR) and LC models, respectively. Employing the change of measure technique, we decompose the pure endowment into the product of the bond price and survival probability, thereby easing computational burden in the evaluation of the annuity expression. With the aid of the dynamics of interest and mortality processes under the forward measure, we construct an algorithm based on comonotonicity principles to estimate the quantiles of survival probability and annuity rate. The comonotonic upper and lower bounds in the convex order are used to approximate the annuity and GAO prices and henceforth avoiding the simulation-within-simulation problem. Numerical illustrations show that our algorithm gives an efficient and practical method to estimate GAO values.

1.3.3 A two-decrement model for the valuation and risk measurement of a guaranteed annuity option

The lapse risk arising from the termination of policies, due to a variety of causes, has significant influence on the prices of contracts, liquidity of an insurer and the reserves necessary to meet regulatory capital. We address in an integrated way the problem of pricing and determining the capital requirements for a GAO when lapse risk is specifically embedded in the modelling framework. In particular, two decrements are considered in which death and policy lapse occurrences with their correlations to the financial risk are explicitly modelled. A series of probability measure changes is employed and the corresponding forward, survival, and risk-endowment measures are constructed. This approach superbly circumvents the rather slow "simulation-within-simulation" pricing procedure under a stochastic setting. Our implementation illustrates that our proposed approach cuts down the Monte-Carlo technique's average computing time by 99%. Risk measures are determined using the moment-based density method and benchmarked with the Monte-Carlo simulation. Our numerical results also indicate that depending on the risk metric used (e.g., VaR, CVaR, various forms of distortion risk measures) and the correlation between the interest and lapse rates, the capital requirement may substantially change, which could be either an increase or decrease up to 50%.

1.3.4 The pricing of a guaranteed minimum maturity benefit under regime-switching framework

The global insurance markets have become more sophisticated in recent times in response to the evolving needs of population that tends to live longer. Policy holders desire the benefits of longevity/mortality protection whilst taking advantage of investment growth opportunities in the equity markets. As a result, insurers incorporate payment guarantees in new insurance products known as equity-linked contracts whose values are dependent on prices of risky assets. A GMMB is now common in many equity-linked contracts. We develop an integrated pricing framework for a GMMB focusing on segregated fund contracts. More specifically, we construct hidden Makov models (HMMs) for a stock index as well as interest and mortality rates. The dependence between these risk factors are characterised explicitly. We assume that the stock index follows a Markov-modulated geometric Brownian motion whilst the interest and mortality rates have Markov-modulated affine dynamics. A series of measure changes is employed to obtain a semi-closed form solution for the GMMB price. The Fourier-transform method is applied to numerically approximate the prices more efficiently. Recursive HMM filters are developed for our model calibration. We provide numerical investigations to show the accuracy of GMMB prices and an extensive analysis is included to examine systematically how risk factors affect the GMMB value.

1.3.5 Setting risk margin for claims liabilities in accordance with IFRS 17

In IFRS 17, the general approach for liability measurement is the Building Block Approach (BBA). Under the BBA, the value of the contract is the sum of four components: (i) total future cash flows, (ii) time value of the future cash flows, (iii) risk margins, and (iv) contractual service margin. In this thesis, we address the computation of risk margin for claims liability. In IFRS 17, there is no explicit recommendation for the method in calculating the risk margin, which is defined as the compensation that insurers require for bearing the uncertainty in the amount and timing of cash flows.

We employ the paid-incurred chain model proposed in Merz and Wüthrich [20] to model the claim triangular data. The moment-based density approximation is used to approximate the distribution of losses as the years progress. Risk measures including value at risk, conditional tail expectation and cost of capital are applied to compute risk margins of claim liabilities. Historical data on the aggregate Ontario automobile insurance claims are used

to examine the appropriateness and accuracy of our approach. The results are compared with those obtained from some traditional methods. A sensitivity analysis for risk margins is performed using the bootstrap method.

References

[1] L. Bachelier. Theory of speculation. *The random character of stock market prices*, 1018:17–78, 1900.

[2] L. Ballotta and S. Haberman. The fair valuation problem of guaranteed annuity options: The stochastic mortality environment case. *Insurance: Mathematics and Economics*, 38(1):195–214, 2006.

[3] A. Cairns, D. Blake, K. Dowd, G. Coughlan, D. Epstein, A. Ong, and I. Balevich. A quantitative comparison of stochastic mortality models using data from England and Wales and the United States. *North American Actuarial Journal*, 13(1):1–35, 2009.

[4] J. Cox, J. Ingersoll, and S. Ross. A theory of the term structure of interest rates. *Econometrica*, 53(2):385–407, 1985.

[5] D. De Giovanni. Lapse rate modeling: A rational expectation approach. *Scandinavian Actuarial Journal*, 2010(1):56–67, 2010.

[6] G. Deelstra, M. Grasselli, and C. Van Weverberg. The role of the dependence between mortality and interest rates when pricing guaranteed annuity options. *Insurance: Mathematics and Economics*, 71:205–219, 2016.

[7] M. Eling and M. Kochanski. Research on lapse in life insurance: What has been done and what needs to be done? *Journal of Risk Finance*, 14(4):392–413, 2013.

[8] R. Elliott and R. Mamon. A complete yield curve description of a Markov interest rate model. *International Journal of Theoretical and Applied Finance*, 6(04):317–326, 2003.

[9] J. Hamilton. A new approach to the economic analysis of nonstationary time series and the business cycle. *Econometrica*, 57(2):357–384, 1989.

[10] T. Ho and S. Lee. Term structure movements and pricing interest rate contingent claims. *Journal of Finance*, 41(5):1011–1029, 1986.

[11] J. Hull and A. White. Pricing interest-rate-derivative securities. *Review of Financial Studies*, 3(4):573–592, 1990.

[12] J. Hull and A. White. Numerical procedures for implementing term structure models II: Two-factor models. *Journal of Derivatives*, 2(2):37–48, 1994.

[13] K. Ignatieva, A. Song, and J. Ziveyi. Pricing and hedging of guaranteed minimum benefits under regime-switching and stochastic mortality. *Insurance: Mathematics and Economics*, 70:286–300, 2016.

[14] L. Jalen and R. Mamon. Valuation of contingent claims with mortality and interest rate risks. *Mathematical and Computer Modelling*, 49(9):1893–1904, 2009.

[15] R. Lee and L. Carter. Modeling and forecasting US mortality. *Journal of the American Statistical Association*, 87(419):659–671, 1992.

[16] X. Liu, J. Jang, and S.M. Kim. An application of comonotonicity theory in a stochastic life annuity framework. *Insurance: Mathematics and Economics*, 48(2):271–279, 2011.

[17] X. Liu, R. Mamon, and H. Gao. A generalized pricing framework addressing correlated mortality and interest risks: A change of probability measure approach. *Stochastics: An International Journal of Probability and Stochastic Processes*, 86(4):594–608, 2014.

[18] S. Loisel and X. Milhaud. From deterministic to stochastic surrender risk models: Impact of correlation crises on economic capital. *European Journal of Operational Research*, 214(2):348–357, 2011.

[19] E. Luciano and E. Vigna. Non mean reverting affine processes for stochastic mortality, 2005. URL `https://ssrn.com/abstract=724706`.

[20] M. Merz and M. Wüthrich. Paid–incurred chain claims reserving method. *Insurance: Mathematics and Economics*, 46(3):568–579, 2010.

[21] A. Milidonis, Y. Lin, and S. Cox. Mortality regimes and pricing. *North American Actuarial Journal*, 15(2):266–289, 2011.

[22] Y. Shen and T. Siu. Longevity bond pricing under stochastic interest rate and mortality with regime-switching. *Insurance: Mathematics and Economics*, 52(1):114–123, 2013.

[23] O. Vasiček. An equilibrium characterization of the term structure. *Journal of Financial Economics*, 5(2):177–188, 1977.

Chapter 2

Annuity contract valuation under dependent risks

2.1 Introduction

Both the decline of future mortality rates and uncertainty in the term structure of interest rates neccessitate an improved framework for the pricing of annuity contracts. The associated computational challenge arising from such a framework and complexity of the risk-factor models are primary considerations. Thus, there is a need to balance between the desire for closed-form or tractable pricing representation and the sophistication of both mortality and financial risk processes with correlation structures.

We shall utilise a mortality model with a good fitting performance to empirical data and an interest rate model that adequately describe short-term dynamics. A computationally efficient algorithm will be developed to characterise the future annuity values. The aim is to go around the "simulation-within-simulation" problem involved in a correlated stochastic framework. The principle of our aim is related to that in Dowd et al. [8]. Our work on the correlated modelling set up for annuity pricing is akin to the objectives of Zhao and Mamon [23], Gao et al. [9], Liu et al. [16], and Jalen and Mamon [13], amongst others. Independence between mortality and financial risks is no longer a realistic assumption. Dhaene et al. [7], for example, asserted that independence under the physical world is not hereditary under the risk-neutral world. Also, as an ageing population puts burden on national security systems, there is now clarity on the impact of life and health insurance markets on the financial markets. A pertinent analysis focusing on the combined effect of random mortality and interest rates in the context of a portfolio of deferred annuities is given in [17].

In this chapter, we adopt the two-factor Hull-White model [12] for the interest rate process, which has a better performance than the one-factor Vasicek model in fitting the rates' initial term structure; see also [11]. The two-factor HW model is able to generate as well a wider class of yield curves and volatility term structures observed in the market. In light of the current developments of very low interest rates and in some countries they can become negative, it is reasonable and justified to utilise the HW model. In Denmark, Sweden, Switzerland and Japan, for example, a negative rate applies on commercial banks' excess funds held on deposit in each central bank. The rationale for lower and negative interest rates comes from an economic policy that discourages investors from buying the local currency; the act of buying more tends to push its value up. Near-zero and negative rates also curb deflation that was recently experienced in those countries; see [21] for further discussion. For mortality projections, we employ the Lee-Carter (LC) [14] model. Unfortunately, there is no closed-form solution for the survival probability under the LC model, and extensive simulation is required. In lieu of simulation, nonetheless, we utilise the general idea in Denuit and Dhaene [5] to construct comonotonic upper- and lower-bound approximations for the survival quantiles. These are sharp approximations with remarkable precision without implementing any Monte-Carlo (MC) simulation.

The main problem that we are addressing is how to deal with the sum of dependent random variables, which is the case for the conditional expected present value of a life annuity. Pertinent comonotonicity concepts will aid us in re-expressing this sum into a more mathematically tractable form. Analytical approximations for the quantiles of the life annuity's conditional expected present value will be derived. This chapter will proceed as follows. Section 2.2 presents the correlated mortality and interest rate models, and the annuity function under a change of numéraire. Comonotonic approximations are given in section 2.3. Section 2.4 highlights numerical illustrations for the efficient computations of the survival probability and approximation for the annuity rate. Some final remarks are provided in Section 2.5.

2.2 The pricing problem and framework

2.2.1 Correlated modelling

We define the short rate r_t and the force of mortality μ_t under a filtered probability space $(\Omega, \mathcal{F}_T, \{\mathcal{F}_t\}, \mathbb{Q})$, where $\mathbb{Q}$ is risk-neutral and $\{\mathcal{F}_t\}$ is the joint filtration generated by r_t and μ_t. The way a risk-neutral measure is selected for the r_t or the corresponding market prices of risk for r_t (and also mortality) is broadly discussed in Biffis et al. [1]. The r_t process follows the two-factor HW model, which gives an analytically tractable bond price, via the stochastic differential equations (SDEs)

$$\begin{aligned} \mathrm{d}r_t &= [\theta(t) + u_t - a r_t]\,\mathrm{d}t + \sigma_1\,\mathrm{d}W_t^1 \\ \mathrm{d}u_t &= -b u_t dt + \sigma_2\left(\rho_1\,\mathrm{d}W_t^1 + \sqrt{1-\rho_1^2}\,\mathrm{d}W_t^2\right), \end{aligned} \tag{2.1}$$

where u_t is the stochastic mean-reverting level for some initial value, and a, b, σ_1, σ_2 and ρ_1 are positive constants. In (2.1), W_t^1 and W_t^2 are two independent standard Brownian motions; and $\theta(t)$ is deterministic, which can be used to match the initial term structure. The HW model is flexible and can accommodate a hump volatility structure that is often observed in the cap market.

The mortality index κ_t will be modelled in accordance with the Lee and Carter's continuous-time specification [14]. In particular, the force of mortality μ_t is driven by κ_t satisfying

$$\mathrm{d}\kappa_t = c\,\mathrm{d}t + \xi\,\mathrm{d}Z_t, \tag{2.2}$$

where c is constant, ξ is a positive constant, and Z_t is a standard Brownian motion correlated with W_t^1. The dependence between the interest and mortality rates is achieved by means of the correlation coefficient ρ_2£ between r_t and κ_t, i.e., through

$$\mathrm{d}W_t^1\,\mathrm{d}Z_t = \rho_2\,\mathrm{d}t.$$

So, for any $\rho_2 \neq 0$, we have

$$Z_t = \rho_2 W_t^1 + \sqrt{1-\rho_2^2}W_t^3$$

and it must be noted that W_t^1, W_t^2 and W_t^3 are independent standard Brownian motions. The joint filtration generated by the adapted processes r_t, u_t and μ_t is defined as $\mathcal{F}_t := \mathcal{F}_t^{W_t^1} \vee \mathcal{F}_t^{W_t^2} \vee \mathcal{F}_t^{W_t^3}$.

In Liu et al. [15] and the references therein, a decrease of adult mortality could cause a decline of interest rate as in the case of pre-industrial England. Such a result relied upon the

life-cycle hypothesis in which higher life expectancy implies less farmer impatience leading to more investment in land fertility and higher production per acre. It was documented that agricultural production and capital rates of return have their empirical patterns coincide fairly well. Furthermore, the importance of a pricing framework that allows dependence between mortality and interest rates is noted. This is because real-world independence between two risk factors does not carry forward to valuation-world independence.

Our model construction under a risk-neutral measure $\mathbb{Q}$ is a starting assumption. Interested readers are referred to Biffis et al. [1] on how to adjust mortality dynamics to reflect the market price of mortality risk from $\mathbb{P}$ to $\mathbb{Q}$. The supposition that the $\mathbb{Q}$-dynamics of μ_t equals its dynamics under the real probability measure $\mathbb{P}$ is valid only when interest and mortality risks are driven by independent Brownian motions. Notwithstanding this caveat, we shall bypass the necessary adjustment and simply use parameters obtained from calibrating a mortality model under the real world. Our main focus is on showing the computational efficiency of our algorithm for annuity valuation. Besides, as Hardy [10] indicated, current market statistics that are used to back out the risk-neutral measure may not contain adequate information as life and annuity contracts have longer maturities than traded options. Current market conditions and prices are insufficient when analysing future annuity cash flows. Thus, reliance on real-world estimates, with appropriate adjustment, may still make better sense for longevity products.

2.2.2 Mortality model

Mortality evolution is a function of both age x and time t, and it is linked to future survival probabilities dependent on κ_t. The LC model describes how the the logarithm of the central mortality rate μ_{xt} behaves and affected by two age-specific covariates and a time-varying component. In particular,

$$\log \mu_{xt} = \Gamma_x + \Psi_x \kappa_t + \epsilon_{xt}. \tag{2.3}$$

In equation (2.3), Γ_x is the average of $\log \mu_{xt}$ over time; changes in $\log \mu_{xt}$ are driven by the dynamics of κ_t and the sensitivity of changes at age x is modulated by Ψ_x; and ϵ_{xt} is the error term. Additionally, $\exp(\Gamma_x)$ influences the general shape of the mortality schedule whilst Ψ_x explains which age-specific rates decline more rapidly or slowly over time due to changes in κ_t. For a given age x, we assume Γ_x and Ψ_x remain constant over time and modulates κ_t in (2.2). The survival probability, given μ_{xt}, is

$$S_x(t, T) = e^{-\int_t^T \mu_{x+s,s}\, \mathrm{d}s}, \tag{2.4}$$

which is a random variable. When pricing, we need to evaluate

$$P_x(t,T) := \mathbb{E}\left[\mathbb{I}_{\{\tau \geq t\}} | \mathcal{M}_t\right] = \mathbb{E}\left[S_x(t,T) | \mathcal{M}_t\right] = \mathbb{E}\left[e^{-\int_t^T \mu_{x+s,s}\,\mathrm{d}s} | \mathcal{M}_t\right], \tag{2.5}$$

where $\{\mathcal{M}_t\}$ is the filtration generated by μ_{xt}.

2.2.3 Interest-rate model

When r_t is given by equation (2.1), closed-form pricing solutions to bond and bond forwards/futures could be obtained. The price at time t of a \$1 zero-coupon bond that matures at time T ($t \leq T$) is

$$B(t,T) = \mathrm{E}^{\mathbb{Q}}[e^{-\int_t^T r_s\,\mathrm{d}s} | \mathcal{F}_t] = e^{-A(t,T)r_t - C(t,T)u_t + D(t,T)}, \tag{2.6}$$

where

$$A(t,T) = \frac{1 - e^{-a(T-t)}}{a},$$

$$C(t,T) = \frac{1}{a(a-b)} e^{-a(T-t)} - \frac{1}{b(a-b)} e^{-b(T-t)} + \frac{1}{ab}$$

and $D(t,T)$ satisfies the ordinary differential equation

$$\frac{\partial D}{\partial t} - A\theta_t + \frac{1}{2}\left(\sigma_1^2 A^2 + \sigma_2^2 C^2 + 2\rho_1\sigma_1\sigma_2 AC\right) = 0.$$

Risk-neutral parameters are recovered using current market prices of bonds; see for example, Rodrigo and Mamon [19] on how to solve the inverse problem of backing out model parameters from bond market prices. However, if past short-term interest rate data are used for model calibration, then the parameter estimates obtained are under the physical measure $\mathbb{P}$. Consequently, the market price of risk must be defined or determined.

The two-factor HW model is equivalent to a two-additive-factor Gaussian model. It has analytic bond price solution, and both the mean and variance of the interest rate process have tractable expressions. Equation (2.1) has the solution

$$\begin{aligned} r_t = r_0 e^{-at} + \frac{u_0}{b-a}\left(e^{-at} - e^{-bt}\right) + \int_0^t \theta(s) e^{-a(t-s)}\,\mathrm{d}s + \int_0^t \Big(\sigma_1 e^{-a(t-s)} \\ + \frac{\rho_1\sigma_2}{b-a}\left(e^{-a(t-s)} - e^{-b(t-s)}\right)\Big)\mathrm{d}W_s^1 + \frac{\sqrt{1-\rho_1^2}\sigma_2}{b-a}\int_0^t \left(e^{-a(t-s)} - e^{-b(t-s)}\right)\mathrm{d}W_s^2 \end{aligned}$$

and yields the respective mean and variance

$$r_0 e^{-at} + \frac{u_0}{b-a}\left(e^{-at} - e^{-bt}\right) + \int_0^t \theta(s) e^{-a(t-s)}\,\mathrm{d}s$$

and

$$\frac{(\sigma_1^2(b-a)^2 + \sigma_2^2 - 2\rho_1\sigma_1\sigma_2(b-a))}{2a(b-a)^2}\left(1 - e^{-2at}\right) + \frac{\sigma_2^2}{2b(b-a)^2}\left(1 - e^{-2bt}\right)$$
$$- \frac{2\rho_1\sigma_1\sigma_2(b-a) + 2\sigma_2^2}{(a+b)(b-a)^2}\left(1 - e^{-(a+b)t}\right).$$

2.2.4 Annuity and the change of numéraire

Let $\tau(x,t)$ be the remaining lifetime random variable, and for convenience set the current time to $t = 0$. A survival benefit of \$1 to be paid at time T to a life aged x at time $t < T$ has the fair value

$$M(t,T) = \mathrm{E}^{\mathbb{Q}}[e^{-\int_t^T r_u\,\mathrm{d}u} \cdot \mathbb{I}_{\{\tau \geq T\}} | \mathcal{F}_t] = \mathbb{I}_{\{\tau \geq t\}} \cdot \mathrm{E}^{\mathbb{Q}}[e^{-\int_t^T r_u\,\mathrm{d}u} e^{-\int_t^T \mu_{x+u,u}\,\mathrm{d}u} | \mathcal{F}_t]. \tag{2.7}$$

The indicator $\mathbb{I}_{\{\tau \geq t\}}$ in equation (2.7) emphasises that a pure endowment's value is conditional on (x) being alive at time t . An annuity is a series of periodic payments of survival benefits of \$1. Hence, the risk-neutral value of $a_x(T)$, conditional on (x) surviving at time T, is

$$a_x(T) = \sum_{n=1}^{\infty} \mathrm{E}^{\mathbb{Q}}[e^{-\int_T^{T+n} r_u\,\mathrm{d}u} e^{-\int_T^{T+n} \mu_{x+v,v}\,\mathrm{d}v} | \mathcal{F}_T] = \sum_{n=1}^{\infty} M(T, T+n). \tag{2.8}$$

The future trajectory of the risk factors, namely, r_t and κ_t from time T will determine the conditional expected present value of the life annuity. Although the force of mortality is commonly modelled by adopting the financial-theory approach as noted in Cairns et al. [3], the force of mortality here is indirectly specified by the time-varying mortality index κ_t. The LC model is selected here because of its impressive empirical performance e.g., [14], and it has become a mortality forecasting benchmark. LC's lack of tractability is circumvented here by offering instead closed-form approximations for the survival probabilities.

A change-of-measure technique is employed, with the bond price $B(t,T)$ as the numéraire, to evaluate the pure endowment dependent on correlated interest and mortality rates. A martingale measure $\widetilde{\mathbb{Q}} \sim \mathbb{Q}$ on $\mathcal{F}_T$ corresponding to $B(t,T)$ is called the forward measure, and it is constructed as

$$\left.\frac{d\widetilde{\mathbb{Q}}}{d\mathbb{Q}}\right|_{\mathcal{F}_T} = \frac{\exp\left(-\int_0^T r_u\,\mathrm{d}u\right)}{\mathrm{E}\left[\exp\left(-\int_0^T r_u\,\mathrm{d}u\right)\right]}.$$

As in Xi and Mamon [22], an application of the Bayes' rule for conditional expectation gives

$$M(t,T) = B(t,T)\mathrm{E}^{\widetilde{\mathbb{Q}}}\Big[\mathbb{I}_{\{\tau\geq T\}}\Big] = B(t,T)\mathrm{E}^{\widetilde{\mathbb{Q}}}\Big[e^{-\int_t^T \mu_{x,x+v}\,\mathrm{d}v}\Big|\mathcal{F}_t\Big]. \tag{2.9}$$

Equation (2.9) tells us that the pure endowment is a product of the bond price and the survival probability under $\widetilde{\mathbb{Q}}$.

Remark: *We shall derive the dynamics of μ_t under $\widetilde{\mathbb{Q}}$. In the succeeding discussion, as the subscript x does not affect the model dynamics, it is removed from μ to avoid clutter of notation.*

Similar to the results from the Appendix of Mamon [18], the standard Brownian motion under $\widetilde{\mathbb{Q}}$ can be written as

$$\mathrm{d}\widetilde{W}_t^1 = \mathrm{d}W_t^1 + (\sigma_1 A(t,T) + \rho_1\sigma_2 C(t,T))\,\mathrm{d}t, \quad \mathrm{d}\widetilde{W}_t^2 = \mathrm{d}W_t^2 + \sigma_2\sqrt{1-\rho_1^2}C(t,T)dt \quad \text{and}$$
$$\mathrm{d}\widetilde{W}_t^3 = \mathrm{d}W_t^3.$$

From (2.2), the dynamics of κ_t under $\widetilde{\mathbb{Q}}$ is

$$\begin{aligned}\mathrm{d}\kappa_t &= c\,\mathrm{d}t + \xi\left(\rho_2\,\mathrm{d}\widetilde{W}_t^1 - \rho_2\left(\sigma_1 A(t,T) + \rho_1\sigma_2 C(t,T)\right)\mathrm{d}t + \sqrt{1-\rho_2^2}\,\mathrm{d}\widetilde{W}_t^2\right)\\ &= (-\xi\rho_2\sigma_1 A(t,T) - \xi\rho_2\rho_1\sigma_2 C(t,T) + c)\,\mathrm{d}t + \rho_2\xi\,\mathrm{d}\widetilde{W}_t^1 + \xi\sqrt{1-\rho_2^2}\,\mathrm{d}\widetilde{W}_t^2\\ &= (-\xi\rho_2\sigma_1 A(t,T) - \xi\rho_2\rho_1\sigma_2 C(t,T) + c)\,\mathrm{d}t + \xi\,\mathrm{d}\widetilde{Z}_t,\end{aligned} \tag{2.10}$$

where $\widetilde{Z}_t = \rho_2\widetilde{W}_t^1 + \sqrt{1-\rho_2^2}\widetilde{W}_t^3$. Given an initial value κ_0, the process κ_t has the integral representation

$$\begin{aligned}\kappa_t &= \kappa_0 + ct - \xi\rho_2\int_0^t (\sigma_1 A(v,T) + \rho_1\sigma_2 C(v,T))\,\mathrm{d}v + \xi\widetilde{Z}_t\\ &= \kappa_0 + ct - \xi\rho_2\left(\frac{t}{a} - \frac{1}{a^2}\left(e^{-a(T-t)} - e^{-aT}\right) + \frac{1}{a^2(a-b)}\left(e^{-a(T-t)} - e^{-aT}\right)\right.\\ &\quad \left. - \frac{1}{b^2(a-b)}\left(e^{-b(T-t)} - e^{-bT}\right) + \frac{t}{ab}\right) + \xi\widetilde{Z}_t,\end{aligned} \tag{2.11}$$

where $A(t,T) = \dfrac{1-e^{-a(T-t)}}{a}$ and $C(t,T) = \dfrac{1}{a(a-b)}e^{-a(T-t)} - \dfrac{1}{b(a-b)}e^{-b(T-t)} + \dfrac{1}{ab}$. Notice that the mortality index is a Brownian motion but with a time-varying drift now. Conse-

quently, μ_t follows the geometric Brownian motion with a functional form

$$\begin{aligned}\mu_t &= \exp\left(\Gamma_x + \Psi_x\kappa_t\right)\\ &= \exp\Bigg(\Gamma_x + \Psi_x\Bigg(\kappa_0 + ct - \xi\rho_2\Bigg(\frac{t}{a} - \frac{1}{a^2}\left(e^{-a(T-t)} - e^{-aT}\right)\\ &\quad + \frac{1}{a^2(a-b)}\left(e^{-a(T-t)} - e^{-aT}\right) - \frac{1}{b^2(a-b)}\left(e^{-b(T-t)} - e^{-bT}\right) + \frac{t}{ab}\Bigg) + \xi\widetilde{Z}_t\Bigg)\Bigg).\end{aligned}$$

Under $\widetilde{\mathbb{Q}}$ and with the aid of Itô's lemma, we get

$$\mathrm{d}\mu_t = \left(-\Psi_x\xi\rho_2\sigma_1 A(t,T) - \Psi_x\xi\rho_2\rho_1\sigma_2 C(t,T) + c\Psi_x + \frac{1}{2}(\Psi_x\xi)^2\right)\mu_t\,\mathrm{d}t + \Psi_x\xi\mu_t\,\mathrm{d}\widetilde{Z}_t. \quad (2.12)$$

From (2.5), the semblance between survival probability determination under $\widetilde{\mathbb{Q}}$ and zero-coupon bond price calculation in equation (2.6) is apparent. In (2.12), the drift term contains a deterministic function, whilst the diffusion term contains the term μ_t^β, where $\beta = 1$. As shown in Hull and White [11], models with a diffusion term of the form μ_t^β with $\beta = 0$ and $\beta = 0.5$ are analytically tractable in the sense of evaluating the conditional expectations of their discounted values. Hence, this tells us that a closed-form solution to the survival probability, driven by μ_t in (2.12), is not available. An alternative evaluation method for the survival probability, based on comonotonicity theory, will be provided.

2.3 Comonotonic approximation

2.3.1 Relevant background

We shall be dealing with the evaluation of discounted cash flows of the form

$$S = \sum_{i=0}^{n} \alpha_i e^{-Y_i}, \quad (2.13)$$

where $\alpha_i, i = 1, \ldots, n$ are real numbers. The expression $\exp(-Y_i)$ may refer to either a discounted value or a decrement process. A multivariate normal random vector $(Y_0, Y_1, \ldots, Y_{n-1})$ is at the core of our analysis. Equation (2.13), which is a series of dependent log-normal random variables, is instrumental so that we could invoke the results of Denuit et al. [6] for our proposed approximations.

A random vector $\mathbf{X} \equiv (X_1, X_2, \ldots, X_n)$ is comonotonic if there exists a random variable Z and monotonic functions $g_1, g_2, \ldots, g_n$, such that the distribution of $\mathbf{X}$ is $(g_1(Z), g_2(Z), \ldots, g_n(Z))$.

In other words, the random variables $X_1, X_2, \ldots, X_n$ are transformations of the same underlying random variable Z so that comonotonicity indicates a perfect positive dependence.

Suppose F_X is the distribution function of a random variable X. The inverse distribution function F_X^{-1} is given by

$$F_X^{-1}(p) = \inf\{x \in \mathbb{R} | F_X(x) \geq p\},$$

where $p \in [0, 1]$ is the X's p-th quantile. If F_X is continuous, the relation between the quantiles of X and $g(X)$ is

$$F_{g(X)}^{-1}(p) = g\Big(F_X^{-1}(p)\Big)$$

whenever g is a continuous and non-decreasing function. Similarly,

$$F_{h(X)}^{-1}(p) = h\Big(F_X^{-1}(1-p)\Big)$$

whenever h is a continuous and non-increasing function. From the quantile additivity property of comonotonic random variables,

$$F_{X_1+\ldots+X_n}^{-1}(p) = \sum_{i=1}^{n} g_i\left(F_Z^{-1}(1-p)\right)$$

provided g_i, $i = 1, \ldots, n$ are non-increasing. Hence, if the components of the sum are comonotonic then the aggregate sum's quantiles could be calculated without much difficulty. Clearly, comonotonic sum is tractable and aids in establishing with ease the distribution of equation (2.13).

2.3.2 Comonotonic lower bounds

Consider two random variables X and Y, and suppose $\mathbb{E}[(X-\zeta)^+] \leq \mathbb{E}[(Y-\zeta)^+]$, for all $\zeta \in \mathbb{R}^+$. Then, X is less than Y in the *stop-loss* order sense, denoted by $X \preceq_{sl} Y$, and this can also be viewed as an *increasing-convex* order. This is because for all non-decreasing and convex functions g, $X \preceq_{sl} Y \Leftrightarrow \mathbb{E}[g(X)] \leq \mathbb{E}[g(Y)]$. If $X \preceq_{sl} Y$ and $\mathbb{E}[X] = \mathbb{E}[Y]$ then we have a stochastic *convex ordering* denoted by $X \preceq_{cx} Y$.

When $X \preceq_{cx} Y$, X has lighter tails than those of Y; so, the the latter is more likely to have extreme values, larger variance, and risky-profile distribution. This concept together with comonotonicity is applied to create a version of $\mathbf{X}$ with a more risky profile for the upper bound, and a random vector with a less risky profile for the lower bound. Suppose the

marginal distribution of X_i and the corresponding cumulative distribution function F_i are known, given the random vector $(X_1, X_2, \ldots, X_n)$. Then,

$$\sum_{i=1}^{n} X_i \preceq_{cx} \sum_{i=1}^{n} F_i^{-1}(U),$$

where $U \sim \text{Uniform}(0, 1)$. Let $S_n^u := \sum_{i=1}^n F_i^{-1}(U)$ be the convex-order upper bound of $S_n := \sum_{i=1}^n X_i$.

Now, let $S_n^l := \sum_{i=1}^n \mathrm{E}[X_i|\Lambda]$ be the convex-order lower bound of $S_n := \sum_{i=1}^n X_i$. That is,

$$\sum_{i=1}^{n} \mathrm{E}[X_i|\Lambda] \preceq_{cx} \sum_{i=1}^{n} X_i,$$

for some random variable Λ. An accurate approximation will depend on the choice of Λ, and as revealed in Dhaene et al. [6], Vanduffel et al. [20] and Denuit [4], S_n's first-order Taylor's approximation could be chosen as a suitable Λ. This means that S_n^l is constructed by conditioning the $X_i's$ on Λ. Moreover, $\mathbb{E}[X_i|\Lambda]$'s are monotonic functions of Λ and have known distributions. Thus, S_n^l is a comonotonic sum.

2.3.3 Comonotonic bounds of survival probabilities

Equation (2.5) illustrates that the survival probability is a random variable whose values are conditional on κ_t. Our goal is the future survival probabilities' evaluation not relying on demanding and costly computations. Instead, closed-form bounds for the future survival probability random variable will be derived following the comonotonic principles outlined in Denuit and Dhaene's results [5]. In particular, the stop-loss upper and lower bounds satisfying $S_x^l \preceq_{sl} S_x \preceq_{sl} S_x^u$ will be developed.

We assume $\mu_{x+\epsilon}(t+\tau) = \mu_x(t) \quad \text{for} \quad 0 \leq \epsilon, \tau < 1$. That is, within each band of age and time, the force of mortality is constant. This implies

$$S_x(t, t+n) = \exp\left(-\sum_{j=0}^{n-1} \mu_{x+j}\right) = \exp\left(-\sum_{j=0}^{n-1} \exp(\Gamma_{x+j} + \Psi_{x+j}\kappa_{t+j})\right), \tag{2.14}$$

and μ_x has a log-normal distribution because κ_t is normally distributed. It should be noted that future survival probabilities are random variables with a dependence structure, and so we have to deal with a sum of correlated log-normal random variables whose distribution is not easy to determine. Nonetheless, we circumvent such difficulty with the comonotonic

bounds for $S_x(t, t+n)$.

Then, $S_x(t, t+n) = \exp(-S_n)$ if

$$S_n := \sum_{j=0}^{n-1} \exp(\Gamma_{x+j} + \Psi_{x+j}\kappa_{t+j}). \tag{2.15}$$

Consequently,

$$S_n = \sum_{j=0}^{n-1} \delta_j \exp(Y_j) \tag{2.16}$$

with $\delta_j = \exp(\Gamma_{x+j})$ and $Y_j = \Psi_{x+j}\kappa_{t+j}$.

The characterisation of the survival probability under $\widetilde{\mathbb{Q}}$ is paramount. Assuming a known κ_{t_0}, $Y_j \sim \mathcal{N}(\mu_{Y_j}, \sigma^2_{Y_j})$ where

$$\begin{aligned}
\mu_{Y_j} &= \mathrm{E}^{\widetilde{\mathbb{Q}}}[Y_j] \\
&= \Psi_{x+j}\left(\kappa_{t_0} + cj - \int_{t_0}^{t_0+j} (\xi\rho_2\sigma_1 A(v, t_0+n) + \xi\rho_2\rho_1\sigma_2 C(v, t_0+n))\,\mathrm{d}v\right) \\
\text{and} \quad \sigma^2_{Y_j} &= \mathrm{Var}^{\widetilde{Q}}[Y_j] = (\Psi_{x+j})^2 j\xi^2.
\end{aligned}$$

Define the convex-upper bound of S_n as

$$S^u_n = \sum_{j=0}^{n-1} \delta_j \exp(\mu_{Y_j} + \sigma_{Y_j} Z) \tag{2.17}$$

with $Z \sim \mathcal{N}(0,1)$ so that $S_n \preceq_{cx} S^u_n$. This yields $S_x(t, t+n) \preceq_{sl} \exp(-S^u_n)$.

Denote by Φ^{-1} the standard normal distribution's quantile function. The quantile function of S^u_n satisfies additivity by the comonotonicity property, i.e.,

$$F^{-1}_{S^u_n}(\epsilon) = \sum_{j=0}^{n-1} \delta_j \exp\left(\mu_{Y_j} + \sigma_{Y_j}\Phi^{-1}(1-\epsilon)\right). \tag{2.18}$$

For the convex-order lower bound of S_n, consider $S^l_n = \mathbb{E}[S_n|\Lambda_n]$. We condition on some random variable Λ_n to approximate S_n; and Λ_n is set as the first-order Taylor approximation of S_n. Hence,

$$\Lambda_n = \sum_{j=0}^{n-1} \delta_j Y_j, \tag{2.19}$$

which is a normal random variable. With the aid of the concept of moment-generating function, $\mathbb{E}[S_n|\Lambda_n]$ can be evaluated and this provides

$$S_d^l = \sum_{j=0}^{n-1} \delta_j \exp\left(\mu_{Y_j} + \rho_j[Y_j, \Lambda_n]\sigma_{Y_j} Z + \frac{1}{2}\left(1 - \rho_j[Y_j, \Lambda_n]\right)^2 \sigma_{Y_j}^2\right), \tag{2.20}$$

as the comonotonic lower-bound approximation for S_n. In (2.20), $\rho_i[Y_j, \Lambda_n]$, $j = 0, \ldots, n-1$, is the correlation coefficient given by

$$\rho_j[Y_j, \Lambda_n] = \frac{\mathrm{Cov}[Y_i, \Lambda_n]}{\sigma_{Y_i}\sigma_{\Lambda_n}}.$$

Thus, $\exp(-S_n^l) \preceq_{sl} S_x(t, t+n)$ holds. Again, by the quantile-additivity property and with S_n^l being the sum of comonotonic random variables, the quantile function of S_n^l is

$$F_{S_n^l}^{-1}(\epsilon) = \sum_{j=0}^{n-1} \delta_j \exp\left(\mu_{Y_j} + \rho_j[Y_j, \Lambda_n]\sigma_{Y_j}\Phi^{-1}(1-\epsilon) + \frac{1}{2}\left(1 - \rho_j[Y_j, \Lambda_n]\right)^2 \sigma_{Y_j}^2\right). \tag{2.21}$$

2.3.4 Approximation for the annuity rate

An annuity immediate is a series of survival benefits paying \$1 at time T for a life aged x. Its fair value is

$$\begin{aligned} a_x(T) &= \sum_{i=1}^{n} M(T, T+i) = \sum_{i=1}^{n} B(T, T+i)\mathrm{E}^{\widetilde{\mathbb{Q}}}\left[e^{-\int_T^{T+i}\mu_v \,\mathrm{d}v}\middle|\mathcal{F}_T\right] \\ &= \sum_{i=1}^{n} e^{-A(T,T+i)r_T - C(T,T+i)u_T + D(T,T+i)}\mathrm{E}^{\widetilde{\mathbb{Q}}}\left[e^{-\int_T^{T+i}\mu_v \,\mathrm{d}v}\middle|\mathcal{F}_T\right]. \end{aligned}$$

Clearly, $a_x(T)$ depends on the state, under $\mathbb{Q}$, of r_T, u_T and κ_T from (2.3.4).

The quantile functions obtained from the comonotonic approximations will facilitate the numerical computation of the expected n-year survival probability at time T. This is accomplished via

$$\mathrm{E}^{\tilde{\mathbb{Q}}}[S_x(T, T+n)|\mathcal{F}_T] = \int_0^1 F^{cm^{-1}}(p)\,\mathrm{d}p, \tag{2.22}$$

where $F^{cm^{-1}}$ denotes the lower or upper comonotonic bound of $S_x(T, T+n)$'s quantile function. Whenever κ_T, r_T and u_T are known, $a_x(T)$ is efficiently generated. To calculate at time $t = 0$ the expected value or quantile of $a_x(T)$, simulated vales of κ_T, r_T and u_T are necessary. The distribution of $a_x(T)$ under $\mathbb{Q}$ relies on (r_T, u_T, κ_T), which is a trivariate normal random variable with

$$\mathrm{E}^{\mathbb{Q}}[r_T] = r_0 e^{-aT} + \frac{u_0}{b-a}\left(e^{-aT} - e^{-bT}\right) + \int_0^T \theta(s)e^{-a(T-s)}\,\mathrm{d}s, \tag{2.23}$$

$$\mathrm{E}^{\mathbb{Q}}[u_T] = u_0 e^{-bT}, \tag{2.24}$$

$$\mathrm{E}^{\mathbb{Q}}[\kappa_T] = cT, \tag{2.25}$$

$$\begin{aligned}\mathrm{Var}^{\mathbb{Q}}[r_T] = &\frac{(\sigma_1^2(b-a)^2 + \sigma_2^2 - 2\rho_1\sigma_1\sigma_2(b-a))}{2a(b-a)^2}\left(1 - e^{-2at}\right) \\ &+ \frac{\sigma_2^2}{2b(b-a)^2}\left(1 - e^{-2bt}\right) \\ &- \frac{2\rho_1\sigma_1\sigma_2(b-a) + 2\sigma_2^2}{(a+b)(b-a)^2}\left(1 - e^{-(a+b)t}\right),\end{aligned} \tag{2.26}$$

$$\mathrm{Var}^{\mathbb{Q}}[u_T] = \frac{\sigma_2^2}{2b}\left(1 - e^{-2bT}\right), \tag{2.27}$$

$$\mathrm{Var}^{\mathbb{Q}}[\kappa_T] = \xi^2 T, \tag{2.28}$$

$$\mathrm{Cov}^{\mathbb{Q}}[r_T, u_T] = \left(\frac{\rho_1\sigma_1\sigma_2}{a+b} + \frac{\sigma_2^2}{(b-a)(a+b)}\right)\left(1 - e^{-(a+b)T}\right) - \frac{\sigma_2^2}{2b(b-a)}\left(1 - e^{-2bT}\right), \tag{2.29}$$

$$\mathrm{Cov}^{\mathbb{Q}}[r_T, \kappa_T] = \rho_2\xi\left[\left(\frac{\sigma_1}{a} + \frac{\rho_1\sigma_2}{(b-a)b}\right)\left(1 - e^{-aT}\right) - \frac{\rho_1\sigma_2}{(b-a)b}\left(1 - e^{-bT}\right)\right] \tag{2.30}$$

and

$$\mathrm{Cov}^{\mathbb{Q}}[u_T, \kappa_T] = \frac{\rho_1\rho_2\sigma_2\xi}{b}\left(1 - e^{-bT}\right). \tag{2.31}$$

2.4 Implementation

The Human Mortality Database's life table on Canadian males aged $x = 25, \ldots, 100$, from years 1970 to 2009, was utilised to fit the parameters a_x, b_x, and κ_t of the LC mortality model. It is assumed that Year 2009 is the current time $T = 0$ and the years thereafter are termed as the future; and 100 is the ultimate age in the life table. An ARIMA (0,1,0), i.e., a random walk with drift was fitted to produce parameter estimates of index κ_t, and the results are $\widehat{c} = -1.2785$ and $\widehat{\xi} = 0.4165$. The parameter specifications for the two-factor HW model are $a = 1, b = 0.1, \theta = 0.045, \rho_1 = 0.6, \sigma_1 = 0.01$ and $\sigma_2 = 0.01$, with $r_0 = 0.045$ and $u_0 = 0$. No further calibration is conducted for the HW model as we concentrate in showing the efficiency and accuracy of the proposed approximation. One may use a quasi-likelihood method to perform parameter estimation; see Mamon and Zhou []

2.4.1 Approximation of survival probability

We shall demonstrate the behaviour of the approximated quantiles of $S_x(n)$ using the comonotonic upper and lower bounds given by (2.18) and (2.21), respectively. The time t argument is suppressed from $S_x(t, t+n)$ to minimise clutter of notation. Figure 2.1 depicts the quantiles of the 10-year survival probability for a life aged 65 with a time horizon of $T = 15$. Equation (2.4), using 10,000 simulated sample paths under $\widetilde{\mathbb{Q}}$, gives the "true" quantiles. For a varying ρ, the quantiles of the comonotonic bounds are close to the simulated survival probability. Relatively small differences can be observed between the comonotonic approximations and simulated quantiles. Although the lower-bound approximations are slightly better, the calculation of the upper-bound approximations are more efficient because fewer terms are involved.

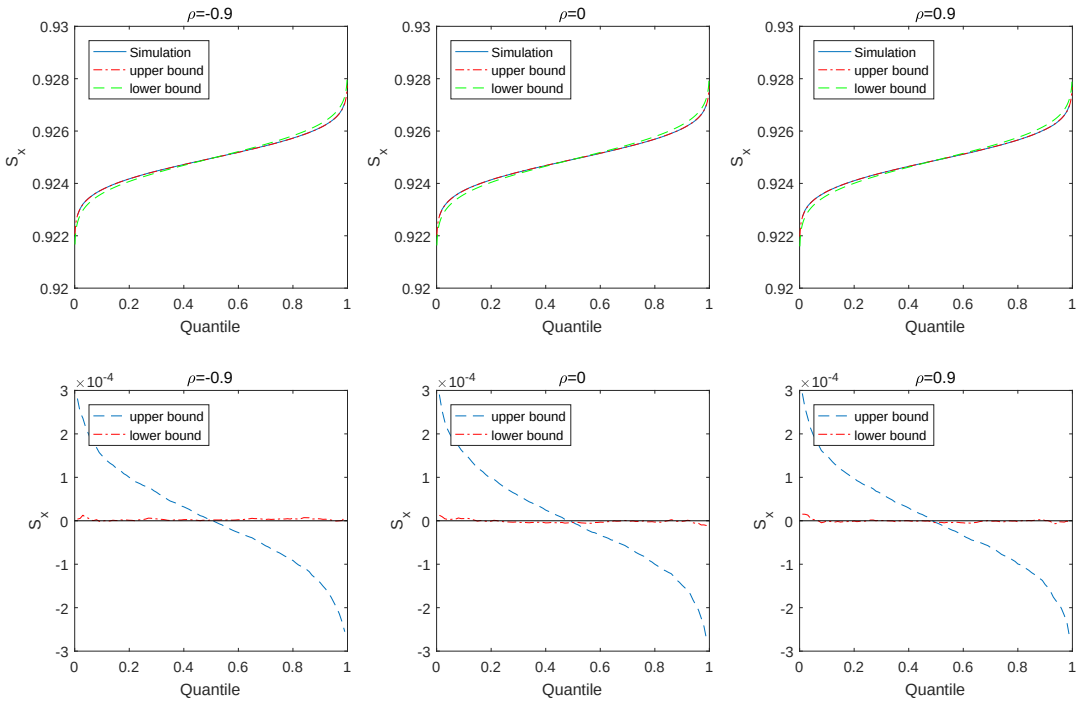

Figure 2.1: **Upper panel:** Quantile functions of $S_x(n)$, $S_x^u(n)$ and $S_x^l(n)$; **Lower panel:** Relative differences between the approximated quantiles and the simulated quantiles.

Equation (2.15) gives the expression for S_n, and the relation $S_n^l \preceq_{cx} S_n \preceq_{cx} S_n^u$ holds. Also, $S_x(n) = \exp(-S_n)$, and so $\exp(-S_n^l) \preceq_{sl} S_x(n) \preceq_{sl} \exp(-S_n^u)$. The approximations for the means of the 10-year survival probabilities are very accurate as shown in Table 2.1. The

correlation ρ_2 between mortality and interest rate risks has a small but noticeable effect on the survival probability. As ρ_2 increases, the survival probability decreases with $\rho_1 = 0.6$ fixed. For a 10-year survival probability, there is a small (i.e., 0.0123%) difference between the probability based on $\rho_2 = -0.9$ and the probability based on $\rho_2 = 0.9$, on average. However, this difference will grow the longer the duration is because sample paths will have greater variability. For instance, there is a 0.23% difference between the 40-year survival probability with $\rho_2 = -0.9$ and the 40-year survival probability with $\rho_2 = 0.9$. A more pronounced effect of ρ_2 to the annuity value is caused by the accumulation of these differences.

ρ_2	T=5			T=40		
	$S_{65}(10)$	$S^l_{65}(10)$	$S^u_{65}(10)$	$S_{65}(10)$	$S^l_{65}(10)$	$S^u_{65}(10)$
-0.9	0.811206	0.811159	0.811393	0.823134	0.823179	0.823405
-0.6	0.814421	0.814255	0.814486	0.825839	0.826105	0.826329
-0.3	0.817190	0.817296	0.817526	0.829053	0.828979	0.829200
0	0.820388	0.820284	0.820512	0.831948	0.831802	0.832021
0.3	0.822852	0.823220	0.823444	0.834731	0.834574	0.834790
0.6	0.826319	0.826103	0.826325	0.837409	0.837296	0.837510
0.9	0.828983	0.828935	0.829155	0.839612	0.839970	0.840182

Table 2.1: 10-year survival probability average value for a Canadian male aged 65 at future horizons T=5 and T=40.

2.4.2 Approximation of the annuity

We now investigate the approximation of $a_x(T)$ based on (2.3.4), whereby the conditional expectation is determined by the upper and lower bounds of the survival probabilities as well as equation (2.22). The triplet (r_T, u_T, κ_T), under $\mathbb{Q}$, are characterised by the moments given in (2.23) – (2.31). To calculate the "true" value of $a_x(T)$, we use equation (2.3.4) and apply the MC simulation method for the evaluation of the conditional expectation in each trial. Figure 2.2 shows that the quantiles of simulated $a_x(T)$ are closed to those of the comonotonic approximations. The relative differences, which are very small, are attributed to the "noise" due to survival probabilities' approximation and variations from simulation.

To examine the effect of ρ_2 on the annuity value, a sensitivity analysis is performed. In

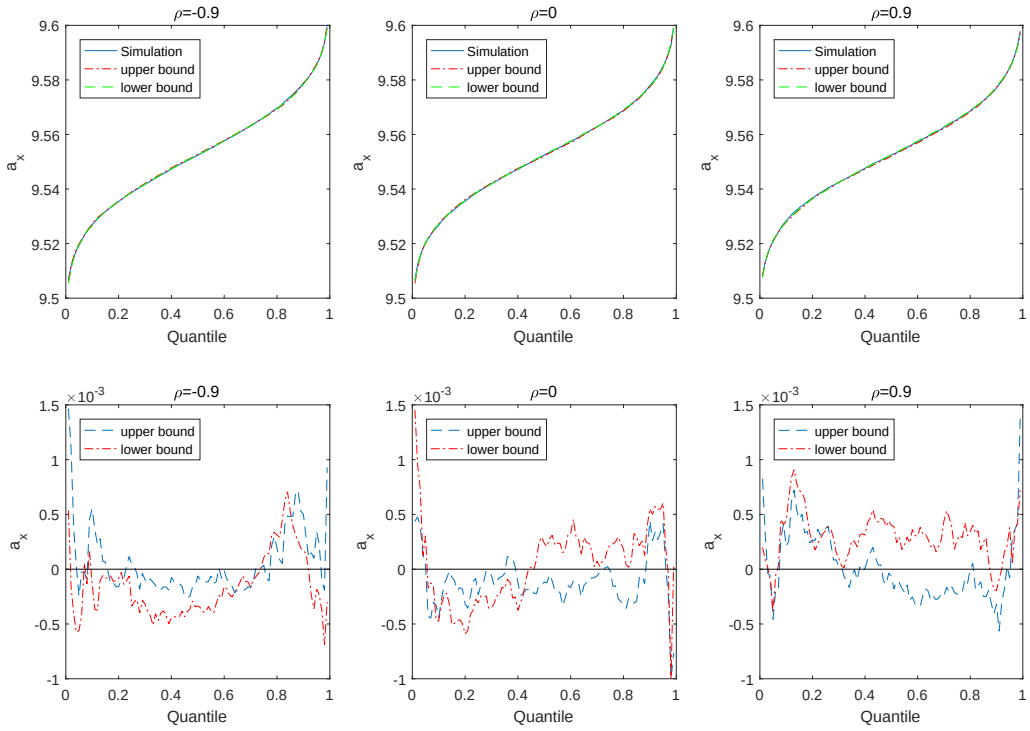

Figure 2.2: **Upper panel:** Quantile functions of a 10-year annuity immediate for time horizon T=15 based on values $a_{65}(5)$, $a^u_{65}(5)$ and $a^l_{65}(5)$. **Lower panel:** Relative differences between the approximated and simulated quantiles.

demonstrating a clear relation between ρ_2 and $a_x(T)$, the parameters σ_1 and σ_2 in the two-factor HW model, and ξ in the LC mortality model are magnified; these magnified parameters are $\sigma_1' = 0.35$, $\sigma_2' = 0.35$ and $\xi' = 30\xi$. They reflect an extreme scenario of a stressed financial environment and volatile health status of the cohort. We will consider a whole life annuity, and so with a maximum age of 100, a 35-year annuity immediate for an individual aged 65 is deemed a whole life annuity. The calculated annuities based on magnified parameter values are shown in Table 2.2 and 2.3 with 50,000 MC iterations. There is a discernible increasing trend in the annuity value as ρ_2 increases. On average, the difference between the annuity value corresponding to $\rho_2 = -0.9$ and the annuity corresponding to $\rho_2 = 0.9$ for $T = 5$ is 20%; whilst the difference is 22% for $T = 40$. This suggests that the correlation between interest and mortality risks could have a strong influence on annuity values under some extreme scenarios. The average relative difference between simulation results and approximations is 0.3%, which implies that our proposed method provides high

ρ_2	$a_{65}(5)$	$a^l_{65}(5)$	$a^u_{65}(5)$
-0.9	11.102878 (0.041781)	11.067061 (0.041571)	11.138986 (0.041792)
-0.6	11.542502 (0.042239)	11.505685 (0.042880)	11.586022 (0.042880)
-0.3	12.138739 (0.042480)	12.089327 (0.043299)	12.197056 (0.042937)
0	12.400552 (0.043584)	12.370652 (0.043436)	12.461776 (0.042851)
0.3	12.771842 (0.043521)	12.734359 (0.043650)	12.818750 (0.043998)
0.6	13.254950 (0.044504)	13.212704 (0.044099)	13.295973 (0.044711)
0.9	13.633704 (0.045391)	13.595405 (0.045716)	13.678474 (0.045943)
Computation Ave Time (hrs)	12.32	0.29	0.25

Table 2.2: 35-year annuity immediate average value for a Canadian male aged 65 at a future horizon T=5.

accuracy in pricing annuities.

Our approach also aims to reduce substantially computing time for annuity valuation. Upper and lower bound-approximations for $a_{65}(T)$ are displayed in Tables 2.2 and 2.3. For a given future time T and all values of ρ, the approximations for a 35-year annuity immediate are very close to their "true" values. Most notably, the difference between simulation and comonotonic-based approximation in terms of the average computing times to complete the annuity calculations is very highly significant (i.e., more than 12.5 hours for the former versus less than 16 minutes only for the latter). Ostensibly, the simulations involved in $a_{65}(T)$ took 12.5 hours because within each simulation an embedded simulation for the trivariate random variable (r_T, u_T, κ_T) is required; this is the so-called simulation-within-simulation, which presents a challenge in the brute-force MC method. The capacity for a huge computing-time saving is an important and gainful feature of our method in addition to its ability to give approximations with superb accuracy.

In Figure 2.3, we plot the annuity's 5th, 50th and 95th quantiles for horizons 1 to 40. These were obtained by the comonotonic upper and lower-bound approximations. The solid points are the quantiles of the true values for horizons 5, 20 and 40. Expectedly, as T goes bigger, the bound intervals also get wider. The increasing annuity trend is a direct result of the mortality index having a downward trend, pointing to the fact that indeed mortality improvement over time is happening. The quantiles with $n = 35$ are also presented as we are also particularly interested in life annuity. The bound intervals for the life annuity

ρ_2	$a_{65}(40)$	$a^l_{65}(40)$	$a^u_{65}(40)$
-0.9	18.169796 (0.044210)	18.124952 (0.044811)	18.210668 (0.044625)
-0.6	18.885663 (0.044323)	18.844803 (0.044931)	18.954663 (0.044320)
-0.3	19.871910 (0.045430)	19.296891 (0.045276)	19.313245 (0.045632)
0	20.537852 (0.045809)	20.474202 (0.045321)	20.592673 (0.045465)
0.3	21.120986 (0.046809)	21.079679 (0.046316)	21.164902 (0.046062)
0.6	22.057027 (0.046173)	22.002318 (0.046203)	22.114022 (0.046883)
0.9	22.738262 (0.047860)	22.686841 (0.047984)	22.793342 (0.047945)
Computation Ave Time (hrs)	12.41	0.29	0.26

Table 2.3: 35-year annuity immediate average value for a Canadian male aged 65 at a future horizon T=40.

are more significantly larger than those of the 10-year annuity and their increasing trend is more pronounced.

In Figure 2.4, we display the volatility pattern of the 10 year-annuity immediate at a future horizon $T = 40$ as a function of both ρ_1 and ρ_2. When ρ_1 is positive, ρ_2 has a strong influence on the volatility. But ρ_2 has less effect on the volatility when ρ_1 is negative. The correlation ρ_1 is estimated from the calibration of the term structure of interest rates. Different values of ρ_1 can reproduce various observed features of the bond prices. As Brigo and Mercurio [2] averred, a humped volatility structure of interest rate can be engendered by a negative ρ_1. Certainly, the volatility and distribution of the annuity rate are affected, to a greater extent, by both ρ_1 and ρ_2.

Life annuity prices are illustrated in Figure 2.5 at time horizon $T = 5$ under different values of σ_1, σ_2 and ξ. As σ_2 increases or ξ decreases, annuity value increases sharply. The annuity value has a small but visible decreasing pattern as σ_1 increases. It can be inferred that the annuity is more sensitive to σ_2 and ξ than σ_1. Thus, both σ_2 and ξ must be estimated accurately when using our proposed correlated interest and mortality framework to price an annuity.

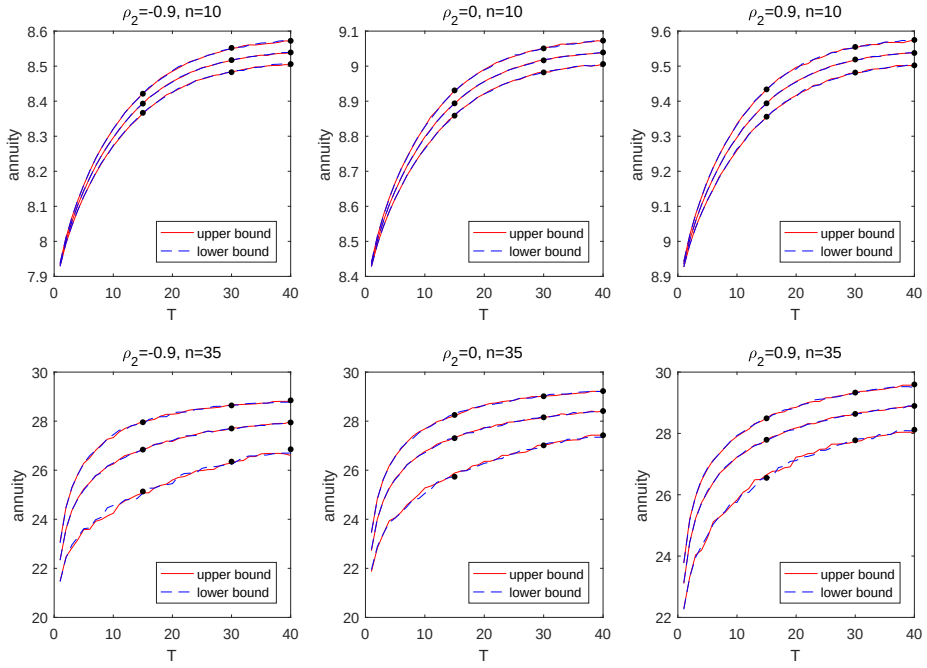

Figure 2.3: Prediction intervals for a 10-year annuity immediate and life annuity for forecasting horizons $T = 1, \ldots, 40$ years; solid points represent predicted quantiles based on Monte-Carlo simulations

2.5 Conclusion

This chapter put forward a computationally efficient approach with notable accuracy in determining the survival probability and pricing annuity via the combined power of the change-of-measure technique and comonotonic approximation. The comonotonic-based method resolves the issue of "simulation within simulation" in the evaluation of a future expected value dependent on a mortality risk with a stochastic evolution.

The analytic approximations for the survival probability's quantiles sidestep the impediment of not having a closed-form representation for the survival probability. The annuity pricing is accomplished straightforwardly by the change of measure method. Our numerical experiments and implementation established that the comonotonic approximation manifestly bore remarkable accuracy and patently shorter computational time when benchmarked to the MC simulation method. Our study verified the riskiness element of annuities at farther time horizons, and such riskiness could be measured by certain risk metrics mandated by insurance regulators. Likewise, the correlation between interest and

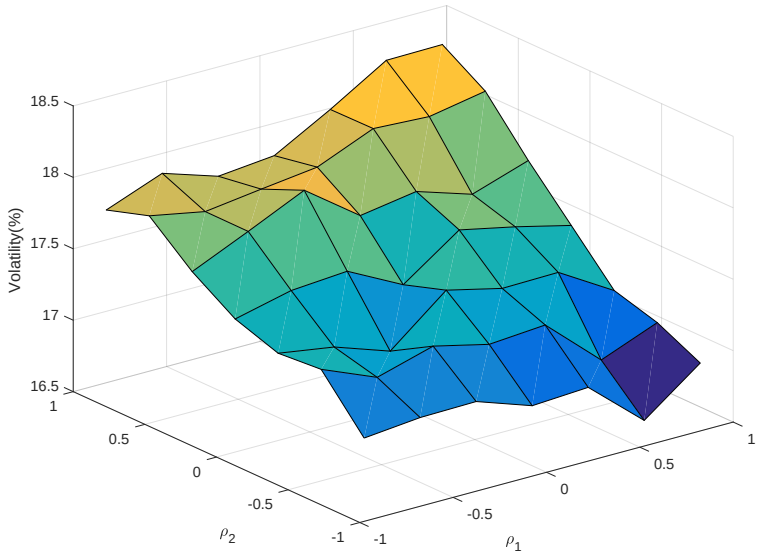

Figure 2.4: Volatility of annuity rate versus varying ρ_1 and ρ_2

mortality rates cogently influence annuity's distribution. The natural direction of this work, which will continue to be relevant and beneficial to investors, managers, and regulatory authorities, is the examination of longevity products, specifically the valuation and risk measurement, using the notions behind the development of computational schemes promoted in this research.

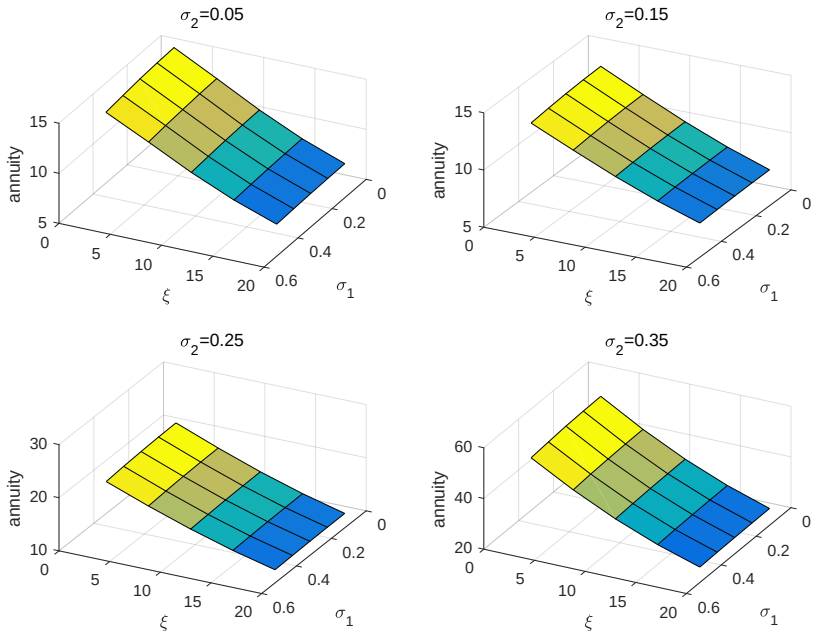

Figure 2.5: Life annuity values at time horizon $T = 40$ with varying σ_1, σ_2 and ξ

References

[1] E. Biffis, M. Denuit, and P. Devolder. Stochastic mortality under measure changes. *Scandinavian Actuarial Journal*, 2010(4):284–311, 2010.

[2] D. Brigo and F. Mercurio. *Interest Rate Models-Theory and Practice: With Smile, Inflation and Credit*. Springer, New York, 207.

[3] A. Cairns, D. Blake, and K. Dowd. Pricing deaths: Frameworks for the valuation and securitisation of mortality risk. *ASTIN Bulletin*, 36(1):79–120, 2006.

[4] M. Denuit. Comonotonic approximations to quantiles of life annuity conditional expected present value. *Insurance: Mathematics and Economics*, 42(2):831–838, 2008.

[5] M. Denuit and J. Dhaene. Comonotonic bounds on the survival probabilities in the lee–carter model for mortality projection. *Journal of Computational and Applied Mathematics*, 203(1):169–176, 2007.

[6] J. Dhaene, M. Denuit, M. Goovaerts, R. Kaas, and D. Vyncke. The concept of comonotonicity in actuarial science and finance: Applications. *Insurance: Mathematics and Economics*, 31(2):133–161, 2002.

[7] J. Dhaene, A. Kukush, E. Luciano, W. Schoutens, and B. Stassen. The concept of comonotonicity in actuarial science and finance: Applications. *Insurance: Mathematics and Economics*, 52(3):522–531, 2013.

[8] K. Dowd, D. Blake, and A. Cairns. A computationally efficient algorithm for estimating the distribution of future annuity values under interest-rate and longevity risks. *North American Actuarial Journal*, 15(2):237–247, 2011.

[9] H. Gao, R. Mamon, and X. Liu. Pricing a guaranteed annuity option under correlated and regime-switching risk factors. *European Actuarial Journal*, 5(2):309–326, 2015.

[10] M. Hardy. *Investment Guarantees: Modeling and Risk Management for Equity-Linked Life Insurance*. Wiley & Sons, New Jersey, 2003.

[11] J. Hull and A. White. Pricing interest rate derivative securities. *Review of Financial Studies*, 3(4):573–592, 1990.

[12] J. Hull and A. White. Numerical procedures for implementing term structure models I: Single-factor models. *Journal of Derivatives*, 2(1):7–16, 1994.

[13] L. Jalen and R. Mamon. Valuation of contingent claims with mortality and interest rate risks. *Mathematical and Computer Modelling*, 49(9):1893–1904, 2009.

[14] R. Lee and L. Carter. Modeling and forecasting us mortality. *Journal of the American Statistical Association*, 87:659–671, 1992.

[15] X. Liu, R. Mamon, and H. Gao. A comonotonicity-based valuation method for guaranteed annuity options. *Journal of Computational and Applied Mathematics*, pages 58–69, 2013.

[16] X. Liu, R. Mamon, and H. Gao. A generalised pricing framework addressing correlated mortality and interest risks: A change of probability measure approach. *Stochastics*, 86(4):594–608, 2014.

[17] A. Mahayni and D. Steuten. Deferred annuities - on the combined effect of stochastic mortality and interest rates. *Insurance: Mathematics and Economics*, 7(1):1–28, 2013.

[18] R. Mamon. Three ways to solve for bond prices in the Vasiček model. *Journal of Applied Mathematics and Decision Sciences*, 8(1):1–14, 2004.

[19] M. Rodrigo and R. Mamon. An alternative approach to the calibration of the Vasiček and CIR interest rate models via generating functions. *Quantitative Finance*, 14(11): 1961–1970, 2014.

[20] X. Vanduffel, S.and Chen, J. Dhaene, M. Goovaerts, L. Henrard, and R. Kaas. Optimal approximations for risk measures of sums of lognormals based on conditional expectations. *Journal of Computational and Applied Mathematics*, 221(1):202–218, 2008.

[21] A. Walker. Why use negative interest rates? URL `http://www.bbc.com/news/business-32284393`.

[22] X. Xi and R. Mamon. Capturing the regime-switching and memory properties of interest rates. *Computational Economics*, 44(3):307–337, 2014.

[23] Y. Zhao and R. Mamon. An efficient algorithm for the valuation of a guaranteed annuity option with correlated financial and mortality risks. *Insurance: Mathematics and Economics*, 78:1–12, 2018.

Chapter 3

An efficient algorithm for the valuation of a GAO with correlated financial and mortality risks

3.1 Introduction

Recent financial innovations in the market included the creation of many insurance products with option-embedded features such as guaranteed annuity options and equity-linked annuities; see Hardy [15]. These products depend on both mortality and interest rate risks. The previous methodology in evaluating this kind of products affected by these two risks is oversimplified. In the past literature, the interest rate is modelled as a stochastic process and the mortality rate is deemed deterministic; see Ballotta and Haberman [1, 2]. The underestimation of mortality risk could lead to huge losses for many insurance companies. Majority of research papers do not deal with the correlation between mortality and interest rate risks. It is more desirable to have a valuation setting that allows for the dependence between these two risk factors. In Liu, et al. [21], a valuation pricing framework covers the case of correlated mortality and interest risks, albeit the interest rate model is restricted to Vasiček to obtain analytic pricing solution of a guaranteed annuity option (GAO). Liu, et al. [20], on the other hand, proposed comonotonicity-based method to improve the efficiency of GAO pricing computation.

With the improvement of approaches in modelling mortality risks, more stochastic mortality models with greater flexibility, were put forward; see Cairns, et al. [6], Lee and Carter [17], and Lin and Liu [18], amongst others. The pricing of annuity products has become

more complicated as the complexity of the mortality model has also increased. We aim to construct a model with greater capability in fitting with the historical data very well, i.e., capturing ably the mortality evolution whilst attaining tractability for ease of implementation. However, building such a model that captures adequately both behavioural properties could be challenging. When a complicated mortality model is adopted, the computational burden is heavy and the "simulation-within-simulation" problem poses a difficulty in the implementation. Our goal is to develop a computationally efficient algorithm to evaluate the GAO price.

GAO valuation with regime-switching but under independent risk factors is put forward in [12]; the pricing under regime-switching with correlation structure involving Vasiček interest-rate dynamics and mortality rate is given in [11]; and the setting of GAO capital requirements using moment-based method is shown in [13]. This chapter could be viewed as an extension of the framework constructed in Liu, et al. [21] in which their model setting is limited only to Vasiček and Ornstein-Uhlenbeck-based models for the interest and mortality rates, respectively, due to the models' combined mathematical tractability. Nonetheless, we know that both risk processes have more complicated dynamics requiring a combined modelling framework with more capabilities. So, to bring further modelling development, we consider the CIR model for the interest rate process which is mean-reverting and its nonnegative feature provides a realistic description of the evolution of the interest rate. Also, the well-studied Lee-Carter mortality model is adopted in this investigation. As pointed out in Lee and Carter [17], their mortality model performs superbly in fitting the empirical data. However, the price of GAO for this choice of combined interest and mortality models, with correlation structure, does not yield a closed-form pricing solution so that the simulation technique must be used. To aid the price computation, the comonotonicity lower and upper bounds are calculated to give an approximation of the GAO value.

We note that our proposed research idea and that of Deelstra et al. [8] exhibit similarities in GAO pricing. These similarities include the (i) framework of correlated interest and mortality risks, (ii) examination of the influence brought about by the risks' dependence structure on GAO prices, (iii) employment of the change-of-measure technique, and (iv) short-term interest rate governed by the Cox-Ingersoll-Ross (CIR) model.

Nonetheless, this article also has certain features that depict distinctive differences from Deelstra et al. [8]. Such features justify our unique position relative to the current literature, and its contributions by all means complement those in [8]. We highlight the dif-

ferences as follows. (i) We assume the mortality rate evolves according to the Lee-Carter model whilst in [8], both mortality and short rates follow the multi-CIR or Wishart models. The Lee-Carter model arguably performs better in fitting mortality rates as this model was originally created to model mortality risks; in particular, it takes into account both the age and time factors. In contrast, the model in [8] considers only the time factor. (ii) In this chapter, the interest and mortality rates are governed by different models vis-à-vis the assumption in [8]. Thus, in our case, explicit solutions for the annuity rates and GAO prices are unattainable. But, with the aid of the concept of comonotonicity bounds, we get closed-form pricing approximations for annuity and GAO prices. (iii) The procedure to calculate our survival probability and price estimates is deemed efficient with the general Monte-Carlo simulation method as benchmark. Our numerical results are enhanced further by a systematic analysis that ascertains how sensitive the GAO prices are to the perturbations in various parameter values.

This chapter is organised as follows. Section 2.2 presents the formulation of the pricing framework along with the assumptions of the interest and mortality rate modelling set ups. In section 2.3, we describe the change of measure method and determine the dynamics of the interest and mortality rate processes under the forward measure. In section 2.4, the comonotonicity bounds are introduced and they are used in turn to evaluate the survival probability, annuity rate, and GAO price. Section 2.5 provides some numerical examples to illustrate the advantages of our proposed technique. Finally, we give some concluding remarks in section 2.6.

3.2 Valuation framework

3.2.1 Cox-Ingersoll-Ross (CIR) model

Under a risk-neutral measure Q, the short-term interest rate r_t is governed by the CIR model, i.e., r_t follows the dynamics

$$\mathrm{d}r_t = a(b - r_t)\,\mathrm{d}t + \sigma\sqrt{r_t}\,\mathrm{d}W_t^1, \tag{3.1}$$

where a, b and σ are positive constants and W_t^1 is a standard Brownian motion on some filtered probability space $(\Omega, \mathcal{R}_t, \{\mathcal{R}_t\}, Q)$. Here, $\{\mathcal{R}_t\}$ is the filtration generated by r_t. The square root term in the diffusion coefficient of equation (3.1) together with an appropriate choice of parameters imply that the interest rate is always positive and provided $2ab \geq \sigma^2$.

The respective mean and variance of r_t conditional on $\mathcal{R}_s$ are given by

$$\mathrm{E}[r_t|\mathcal{R}_s] = r_s e^{-a(t-s)} + b(1 - e^{-a(t-s)})$$

and

$$\mathrm{Var}[r_t|\mathcal{R}_s] = r_s \frac{\sigma^2}{a}\left(e^{-a(t-s)} - e^{-2a(t-s)}\right) + \frac{\sigma^2 b}{2a}\left(1 - e^{-a(t-s)}\right)^2.$$

Under the CIR setting, the price of a \$1 time-T zero-coupon bond at time t has an exponential affine representation given by

$$B(t,T) = \mathrm{E}^{Q}\left[e^{\int_t^T r_u du}\middle|\mathcal{R}_t\right] = e^{-A(t,T)r_t + D(t,T)}, \tag{3.2}$$

where

$$A(t,T) = \frac{2(e^{(T-t)h} - 1)}{2h + (a+h)(e^{(T-t)h} - 1)},$$
$$D(t,T) = \frac{2ab}{\sigma^2}\log\left(\frac{2he^{(a+h)(T-t)/2}}{2h + (a+h)(e^{(T-t)h} - 1)}\right)$$

and $h = \sqrt{a^2 + 2\sigma^2}$.

3.2.2 Lee-Carter model

We assume that the force of mortality $\mu_{x,t}$, for a life aged x at time t, follows the Lee-Carter model, which consists of two age-specific factors and a time-varying index. That is,

$$\log \mu_{x,t} = \alpha_x + \beta_x k_t + \epsilon_{x,t} \tag{3.3}$$

with constraints

$$\sum_t k_t = 0, \quad \sum_x \beta_x = 1,$$

where α_x and β_x are age-specific constants, k_t is a time-varying index, and $\epsilon_{x,t}$ is an error term. In equation (3.3), k_t satisfies the stochastic differential equation

$$\mathrm{d}k_t = c\,\mathrm{d}t + \xi\,\mathrm{d}Z_t, \tag{3.4}$$

where c and ξ are constants ($\xi > 0$) and $\{Z_t\}$ is a standard Brownian on $(\Omega, \mathcal{M}_t, \{\mathcal{M}_t\}, Q)$. Here, $\{\mathcal{M}_t\}$ is the filtration generated by μ_{xt} via k_t.

The Lee-Carter model parameters in equation (3.3) have intuitive interpretations: α_x is the average mortality rate that describes the differences between ages; k_t represents the changes

of mortality rate over time, which is a stochastic process; β_x explains at which ages mortality rate declines rapidly as influenced by k_t; and $\epsilon_{x,t}$ is a random disturbance.

Given the force of mortality $\mu_{x,t}$, we get the survival probability

$$S_x(t,T) = \exp\left(-\int_t^T u_{x+s,s}\,\mathrm{d}s\right).$$

Since $\mu_{x,t}$ is a stochastic process, the survival probability is also a random variable. To price an insurance product, we need to determine the conditional expectation of the survival probability, which is

$$P_x(t,T) := \mathrm{E}\left[\exp\left(-\int_t^T u_{x+s,s}\,\mathrm{d}s\right)\middle|\,\mathcal{M}_t\right]. \tag{3.5}$$

We assume that Z_t is correlated with W_t^1 with dependence structure

$$\mathrm{d}Z_t\,\mathrm{d}W_t^1 = \rho\,\mathrm{d}t,$$

where ρ is the correlation coefficient between the interest rate and mortality rate processes. Generating Z_t could be performed using the relation

$$Z_t = \rho W_t^1 + \sqrt{1-\rho^2}W_t^2,$$

where W_t^2 is a standard Brownian motion independent of W_t^1.

3.2.3 Valuation formula

We define the joint filtration $\{\mathcal{F}_t\}$ via $\mathcal{F}_t := \mathcal{R}_t \vee \mathcal{M}_t := \sigma(\mathcal{R}_t \cup \mathcal{M}_t)$. We develop a modelling framework based on the short interest rate r_t and the force of mortality u_t defined on $(\Omega, \mathcal{F}, \{\mathcal{F}_t\}, Q)$. Denote by $\tau(x,t)$ the future lifetime random variable of an individual aged x at current time t. The fair value of a survival benefit of \$1 payable at time T for a life aged x at time $t < T$ is

$$\begin{aligned}\boldsymbol{M}_x(t,T): &= \mathrm{E}^Q\left[e^{-\int_t^T r_u\,\mathrm{d}u}\mathrm{I}_{\{\tau>T\}}\middle|\,\mathcal{F}_t\right]\\ &= \mathrm{I}_{\{\tau>t\}}\mathrm{E}^Q\left[e^{-\int_t^T r_u\,\mathrm{d}u}e^{-\int_t^T \mu_{x+v,v}\,\mathrm{d}v}\middle|\,\mathcal{F}_t\right]\\ &= \mathrm{I}_{\{\tau>t\}}M_x(t,T),\end{aligned} \tag{3.6}$$

where I_A is the indicator function of a set A and $M_x(t,T) = \mathrm{E}^Q\left[e^{-\int_t^T r_u du}e^{-\int_t^T \mu_{x+v,v}\,\mathrm{d}v}\middle|\,\mathcal{F}_t\right]$.

Equation (3.6) provides the value of the pure endowment, which is conditional on the survival of x to time t. For a general contingent payoff conditional on the survival at time T, the fair value at time t is

$$\begin{aligned} \boldsymbol{C}_{x,t} &= \mathrm{E}^{Q}\left[e^{-\int_t^T r_u \,\mathrm{d}u} \mathrm{I}_{\{\tau>T\}} C_T \middle| \mathcal{F}_t \right] \\ &= \mathrm{I}_{\{\tau>t\}} \mathrm{E}^{Q}\left[e^{-\int_t^T r_u \,\mathrm{d}u} e^{-\int_t^T u_{x+v,v} \,\mathrm{d}v} C_T \middle| \mathcal{F}_t \right] \\ &= \mathrm{I}_{\{\tau>t\}} C_{x,t}, \end{aligned} \tag{3.7}$$

where $C_{x,t} = \mathrm{E}^{Q}\left[e^{-\int_t^T r_u \,\mathrm{d}u} e^{-\int_t^T u_{x+v,v} \,\mathrm{d}v} C_T \middle| \mathcal{F}_t \right]$.

In equation (3.7), C_T is a generalised contingent claim and may refer to a GAO or other type of insurance derivatives. We recall that a GAO is a contract that gives the policy holder the right to convert his survival benefit into an annuity at a pre-specified conversion rate at a certain future time. This kind of contract has been popular in UK pension policies since the late 70-80's. According to Bolton, et al. [3], the most commonly used guaranteed conversion rate for males aged 65 in the UK is $g = \frac{1}{9}$, which means a survival benefit of £1000 can be converted into an anuity of £111 per annum. If the annuity is sold at a price higher than $\frac{1}{g}$, the GAO is at a positive value; otherwise, it is worthless. The annuity is a series of survival benefits of \$1 conditional on a life aged x survive to time T.

The annuity rate $a_x(T)$, applicable at time T, for a life aged x at time t, is given by

$$a_x(T) = \sum_{n=1}^{\infty} M(T, T+n) = \sum_{n=1}^{\infty} \mathrm{E}^{Q}\left[e^{-\int_T^{T+n} r_u \,\mathrm{d}u} e^{-\int_T^{T+n} \mu_{x+v,v} \,\mathrm{d}v} \middle| \mathcal{F}_T \right]. \tag{3.8}$$

If we let $C_T = (g a_x(T) - 1)^+$, i.e., $C_T = g(a_x(T) - K)^+$ where $K = \frac{1}{g}$, then at time 0 the valuation formula for GAO is

$$P_{GAO} = \frac{1}{K} \mathrm{E}^{Q}\left[e^{-\int_0^T r_u \,\mathrm{d}u} e^{-\int_0^T u_{x+v,v} \,\mathrm{d}v} (a_x(T) - K)^+ \middle| \mathcal{F}_0 \right]. \tag{3.9}$$

It has to be noted that formula (3.9) requires simulation in two levels to evaluate the annuities and GAO values. This leads to a "simulation-within-simulation" problem. Consequently, this makes the valuation of GAO time-consuming and inefficient. We will introduce a method based on the theory of comonotonicity to improve valuation efficiency and substantially reduce the computing time for pricing GAOs.

3.3 Change of measure

One may observe that when generating the numerical results of the pure endowment in equation (3.6) under Q, trajectories of both the interest and mortality rates are needed. The change of numéraire technique will be applied to improve the efficiency of the calculations. Consider the bond price $B(t,T)$ as the new numéraire with associated measure $\widetilde{Q}$ equivalent to Q defined via the Radon-Nikodým derivative as per the Girsanov's theorem. With $\widetilde{Q}$ and the application of Bayes' theorem for conditional expectation, the pure endowment is essentially the discounted survival benefit of \$1. This could be written as

$$M_x(t,T) = B(t,T)\mathrm{E}^{\widetilde{Q}}\left[e^{-\int_t^T \mu_{x+v,v}\,\mathrm{d}v}\middle|\mathcal{F}_t\right]. \tag{3.10}$$

With the change of numéraire technique, we are able to split the pure endowment into the product of the bond price and the expectation of survival probability evaluated under the forward measure.

Consequently, we need to determine the dynamics of the interest rate and mortality rate processes under $\widetilde{Q}$. Following the results shown in Mamon [23], the standard Brownian motions under the forward measure $\widetilde{Q}$ have dynamics

$$\mathrm{d}\widetilde{W}_t^1 = \mathrm{d}W_t^1 + \sigma A(t,T)\sqrt{r_t}\,\mathrm{d}t \qquad \mathrm{d}\widetilde{W}_t^2 = \mathrm{d}W_t^2. \tag{3.11}$$

Hence,

$$\mathrm{d}\widetilde{Z}_t = \rho\,\mathrm{d}\widetilde{W}_t^1 + \sqrt{1-\rho^2}\,\mathrm{d}\widetilde{W}_t^2. \tag{3.12}$$

Plugging in equation (3.11) into equation (3.1), we obtain the dynamics of r_t under $\widetilde{Q}$ as illustrated by the succeeding calculations.

$$\begin{aligned}
\mathrm{d}r_t &= a(b-r_t)\,\mathrm{d}t + \sigma\sqrt{r_t}\,\mathrm{d}W_t^1 \\
&= a(b-r_t)\,\mathrm{d}t + \sigma\sqrt{r_t}(\mathrm{d}\widetilde{W}_t^1 - \sigma A(t,T)\sqrt{r_t}\,\mathrm{d}t) \\
&= a\left[b - \left(\frac{\sigma^2 A(t,T)}{a} + 1\right) r_t\right]\mathrm{d}t + \sigma\sqrt{r_t}\,\mathrm{d}\widetilde{W}_t^1.
\end{aligned}$$

We see that the short interest rate also follows the CIR model under $\widetilde{Q}$, i.e.,

$$\mathrm{d}r_t = \widetilde{a}\left[\widetilde{b} - r_t\right]\mathrm{d}t + \widetilde{\sigma}\sqrt{r_t}\,\mathrm{d}\widetilde{W}_t^1 \tag{3.13}$$

with new parameters $\widetilde{a} := a + \sigma^2 A(t,T)$, $\widetilde{b} := \dfrac{ab}{a + \sigma^2 A(t,T)}$ and $\widetilde{\sigma} := \sigma$.

Similarly, substituting equation (3.12) into equation (3.4), we obtain the dynamics of k_t under $\widetilde{Q}$ in accordance with the computation that follows.

$$\begin{aligned} \mathrm{d}k_t &= c\,\mathrm{d}t + \xi\,\mathrm{d}Z_t = c\,\mathrm{d}t + \xi[\rho dW_t^1 + \sqrt{1-\rho^2}\,\mathrm{d}W_t^2] \\ &= c\,\mathrm{d}t + \xi[\rho(\mathrm{d}\widetilde{W}_t^1 - \sigma A(t,T)\sqrt{r_t}\,\mathrm{d}t) + \sqrt{1-\rho^2}\,\mathrm{d}\widetilde{W}_t^2] \\ &= (c - \rho\xi\sigma A(t,T)\sqrt{r_t})\,\mathrm{d}t + \xi[\rho\,\mathrm{d}\widetilde{W}_t^1 + \sqrt{1-\rho^2}\,\mathrm{d}\widetilde{W}_t^2] \\ &= (c - \rho\xi\sigma A(t,T)\sqrt{r_t})\,\mathrm{d}t + \xi\,\mathrm{d}\widetilde{Z}_t. \end{aligned} \tag{3.14}$$

The integral representation of (3.14), given the initial value k_0, is

$$k_t = k_0 + ct - \rho\sigma\xi \int_0^t A(u,T)\sqrt{r_u}\,\mathrm{d}u + \xi\widetilde{Z}_t. \tag{3.15}$$

We aim to find the variance of k_t under $\widetilde{Q}$. Since ρ, σ, ξ and $\sqrt{r_u}$ are all less than 1 in general, $\rho\sigma\xi \int_0^t A(u,T)\sqrt{r_u}\,\mathrm{d}u$ is much smaller than $\xi\widetilde{Z}_t$. In fact, we verify numerically that the variation of the drift term is much smaller than that of the diffusion term. In particular, using a Monte-Carlo simulation method, we compare the standard deviations (SDs) of the drift and diffusion terms as we vary the parameters ρ, σ and ξ, with the other parameters taking the constant values displayed in Table 4.1. Indeed, we can observe from Tables 3.1-3.3 that the drift's SD is substantially smaller than the corresponding diffusion's SD. This shows that the diffusion term is the dominant random component of k_t under $\widetilde{Q}$.

Table 3.1: SDs of k_t's drift and diffusion terms under different values of ρ

ρ	-1.0	-0.5	0.0	0.5	1.0
drift	0.084107	0.039294	0.000000	0.042256	0.086062
diffusion	5.412869	5.24136	5.330050	5.212744	5.682106

Table 3.2: SDs of k_t's drift and diffusion terms under different values of ξ

ξ	0.25	0.50	0.75	1.00
drift	0.013783	0.027282	0.040481	0.054616
diffusion	1.742354	3.517697	5.419593	7.216929

Table 3.3: SDs of k_t's drift and diffusion terms under different values of σ

σ	0.010	0.025	0.050	0.075
drift	0.004843	0.029818	0.103759	0.203865
diffusion	5.294222	5.368703	5.371906	5.471100

It is not easy to determine the distribution of $\rho\sigma\xi \int_0^t A(u,T)\sqrt{r_u}\,\mathrm{d}u$. However, the term $\xi\widetilde{Z}_t$ follows the normal distribution and as noted above, it is the dominating source of randomness for k_t. For tractability, k_t will be treated as a normally distributed random variable, at least approximately. Such an assumption will be justified empirically further in section 3.5 via normality tests.

A closed-form solution to the survival probability driven by k_t does not exist. Therefore, we provide an approximate solution through comonotonicity theory. We shall now determine the expectation of $\sqrt{r_t}$ and variance of r_t under $\widetilde{Q}$; they are needed in section 4.

Write

$$c_t := \frac{4a}{\sigma^2(1-\exp(-at))}. \tag{3.16}$$

In Brigo and Mecurio [4], r_t governed by the CIR model could be expressed as $r_t = \dfrac{Y}{c_t}$ where c_t is the parameter defined in (3.16) and Y is a random variable that follows the non-central chi-square distribution with v_t degrees of freedom and non-centrality parameter λ_t. Then $Y = c_t r_t$ follows the non-central chi-square distribution with parameters

$$v_t = \frac{4ab}{\sigma^2}, \tag{3.17}$$

and

$$\lambda_t = c_t r_0 \exp(-at), \tag{3.18}$$

where a, b and σ are constants appearing in the short-term interest rate process of equation (3.1).

A general non-central chi-square random variable with degrees of freedom v ($v > 0$) and non-centrality parameter λ ($\lambda > 0$) has the density function (see Brigo and Mercurio [4])

$$p_{\chi^2(v,\lambda)}(z) = \sum_{i=0}^{\infty} \frac{e^{-\lambda/2}(\lambda/2)^i}{i!} p_{\Gamma(i+v/2,1/2)}(z) \tag{3.19}$$

with

$$p_{\Gamma(i+v/2,1/2)}(z) = \frac{(1/2)^{i+v/2} z^{i+v/2-1}}{\Gamma(i+v/2)} e^{-z/2}, \tag{3.20}$$

where $i = 0, 1, \ldots,$.

Equations (3.16)-(3.20) are under Q, and under this measure, the parameters a, b and σ are replaced by $\widetilde{a}$, $\widetilde{b}$ and $\widetilde{\sigma}$, which are the parameters in the interest rate model (see equation (3.13)). Considering that $\widetilde{a}$ and $\widetilde{b}$ are time-dependent functions under $\widetilde{Q}$, we invoke Maghsoodi [22] to obtain the distribution of r_t. To do this, write

$$\widetilde{c}_t := \left[\frac{1}{4}\int_0^t e^{-\int_0^s \widetilde{a}(u)\,\mathrm{d}u}\widetilde{\sigma}^2\,\mathrm{d}s\right]^{-1} \quad \text{and} \quad \widetilde{\lambda}_t := \widetilde{c}_t r_0 \exp\left(-\int_0^t \widetilde{a}(s)\,\mathrm{d}s\right),$$

where $\widetilde{a}(s) := a + \sigma^2 A(s,T)$ and $\widetilde{\sigma}^2 = \sigma^2$.

From the description involving equation (3.13), it turns out that $\widetilde{\nu}_t$ is a constant; specifically,

$$\widetilde{\nu}_t := \frac{4\widetilde{a}\widetilde{b}}{\widetilde{\sigma}^2} = \frac{4ab}{\sigma^2}.$$

So, by Maghsoodi [22], the argument justifying the derivation of the distribution of r_t still holds under the $\widetilde{Q}$ measure here. Thus, the expectation of the square root of r_t under $\widetilde{Q}$ can be calculated by evaluating the pertinent integral, i.e.,

$$\mathrm{E}^{\widetilde{Q}}[\sqrt{r_t}] = \frac{1}{\sqrt{\widetilde{c}_t}}\int_0^\infty \sqrt{z}\sum_{i=0}^{\infty}\frac{e^{-\widetilde{\lambda}_t/2}(\widetilde{\lambda}_t/2)^i}{i!}p_{\Gamma(i+\widetilde{\nu}_t/2,1/2)}(z)\,\mathrm{d}z.$$

After simplification (see Appendix for details of the succeeding result), we have

$$\mathrm{E}^{\widetilde{Q}}[\sqrt{r_t}] = \sqrt{\frac{2}{\widetilde{c}_t}}\sum_{i=0}^{\infty}\frac{e^{-\widetilde{\lambda}_t/2}(\widetilde{\lambda}_t/2)^i}{i!}\frac{\Gamma(i+\widetilde{\nu}_t/2+1/2)}{\Gamma(i+\widetilde{\nu}_t/2)}. \tag{3.21}$$

The expectation in (3.21) is written as a series. Based on the parameter values used in the implementation section of this chapter, our numerical experiment shows that 25 terms are required for an approximating partial sum to give a precision of 0.001, and 30 terms for a precision of 0.0001. Employing equations (3.21) and (3.15), we get the respective expectation and variance of k_t under measure $\widetilde{Q}$ as

$$\mathrm{E}^{\widetilde{Q}}[k_t] = k_0 + ct - \rho\sigma\xi\int_0^t A(u,T)\mathrm{E}^{\widetilde{Q}}[\sqrt{r_u}]\,\mathrm{d}u, \tag{3.22}$$

$$\begin{aligned}\mathrm{Var}^{\widetilde{Q}}[k_t] = (\rho\sigma\xi)^2\int_0^t A(u,T)^2(\mathrm{E}^{\widetilde{Q}}[r_u] - \mathrm{E}^{\widetilde{Q}}[\sqrt{r_u}]^2)\,\mathrm{d}u + \xi^2 t \\ + \rho\sigma\xi^2\int_0^t A(u,T)\mathrm{Cov}^{\widetilde{Q}}[\sqrt{r_u}, \widetilde{Z}_u]\,\mathrm{d}u.\end{aligned} \tag{3.23}$$

Since we do not have a closed-form solution to the survival probability, we propose an approximation method in obtaining their numerical results. Our approximation, with the aid of the moments of k_t, will be shown to be more efficient than the Monte-Carlo simulation method. It must be noted that this section contains characterisations of the moments of the CIR process with time-dependent parameters under the forward measure $\widetilde{Q}$. These results enhance the developments in the study of CIR processes with time-varying coefficients that were previously examined in Deelstra [7], Maghsoodi [22] and Shirakawa [24].

3.4 Comonotonicity bounds

3.4.1 Comonotonicity theory

The random variables $X_1, X_2, \ldots, X_n$ are said to be comonotonic if there exists a random variable V and monotonic functions $g_1, g_2, \ldots, g_n$ such that $(X_1, X_2, \ldots, X_n)$ is distributed as $(g_1(V), g_2(V), \ldots, g_n(V))$. If the random vector $X = (X_1, X_2, \ldots, X_n)$ has comonotonic distribution, two possible outcomes $(x_1, x_2, \ldots, x_n)$ and $(y_1, y_2, \ldots, y_n)$ of $(X_1, X_2, \ldots, X_n)$ are ordered componentwise. It means that all the elements of the vector move in the same direction.

We consider a random variable X with cumulative distribution function F_X. Its p^{th} quantile is defined as

$$F_X^{-1}(p) = \inf\{x \in R;\ F_X(x) \geq p\}.$$

This is also referred to as the inverse function of F_X. For a random variable and a continuous function $g(x)$, we have

$$F_{g(X)}^{-1}(p) = g(F_X^{-1}(p))$$

for a non-decreasing function $g(x)$ and

$$F_{g(X)}^{-1}(p) = g(F_X^{-1}(1-p))$$

for a non-increasing function $g(x)$.

We follow the development in Liu, et al. [19] in the succeeding discussion of the distribution of $\sum_{i=1}^{n} X_i$. If $X_1, X_2, \ldots, X_n$ are comonotonic random variables and $(X_1, X_2, \ldots, X_n)$

is distributed as $(g_1(V), g_2(V), \ldots, g_n(V))$, where $g_1, g_2, \ldots, g_n$ are non-decreasing (or non-increasing) functions, the quantile additive property states

$$F^{-1}_{X_1+\cdots+X_n}(p) = \sum_{i=1}^{n} g_i(F_V^{-1}(p)).$$

Consider two random variables X and Y. X is said to be smaller than Y in the convex order, which is denoted by $X \preceq_{cx} Y$, if and only if

$$\mathrm{E}[X] = \mathrm{E}[Y] \text{ and } \mathrm{E}[(X-d)^+] \leq \mathrm{E}[(Y-d)^+], \text{ for all } d \in R.$$

The convex-order relation $X \preceq_{cx} Y$ also implies that Y has a heavier lower and upper tails than that of X. The probability that Y has an extreme value is higher than that of X; therefore, $\mathrm{Var}[X] \leq \mathrm{Var}[Y]$.

In the remaining part of this section, we utilise the concept of comonotonicity to approximate the random variable of the form

$$S = \sum_{i=1}^{n} X_i,$$

where $X_1, X_2, \ldots, X_n$ are dependent and their marginal distributions F_{X_i} are known but their joint distribution is unspecified and is typically hard to determine. Furthermore, the distribution of the sum of S is difficult to derive. The idea to find the comonotonic approximation is to replace the dependent random variables $X_1, X_2, \ldots, X_n$ with comonotonic random variables $Y_1, Y_2, \ldots, Y_n$. Then S can be approximated by $\widetilde{S} = \sum_{i=1}^{n} Y_i$. Applying the quantile additive property, the distribution of $\widetilde{S}$ can be derived in a more efficient way. The idea of utilising the comonotonicity theory to approximate the sum of dependent random variables was initiated by Dhaene, et al. [9]. Such technique was implemented in a stochastic life annuity framework by Liu, et al. [19]. We consider the upper and lower bounds of S in a convex order, which are denoted by S^u and S^l, respectively; S^u and S^l must satisfy $S^l \preceq_{cx} S \preceq_{cx} S^u$.

One approach to find the convex-order upper bound S^u is by setting $S^u = \sum_{i=1}^{n} F^{-1}_{X_i}(U)$, where U is a uniform random variable between 0 and 1. Note that the components in S^u are comonotonic and they have the same distribution as $X_i's$. Hence, S^u has the convex-largest sum of S. In order to determine the lower bound S^l, we shall use the conditional

expectation $E[X_i|\Lambda]$ to set up the lower bound $S^l = \sum_{i=1}^{n} E[X_i|\Lambda]$, where Λ is some conditioning random variable. The lower bound is a function of Λ and it is desired to choose a Λ that can approximate S accurately. In Dhaene, et al. [10], it is suggested to choose Λ as the first-order Taylor approximation of S.

3.4.2 Comonotonicity bounds of survival probabilities

We assume that the force of mortality within each band of age and time remains constant, i.e, $\mu_{x+\epsilon}(t+\tau) = \mu_x(t)$ for $0 \leq \epsilon, \tau < 1$. The survival probability of a life aged x at time t reaching time $t+n$ can be written as

$$S_x(t, t+n) = \exp\left(-\sum_{j=0}^{n-1} \mu_{x+j,t+j}\right) = \exp\left(-\sum_{j=0}^{n-1} \exp(\alpha_{x+j} + \beta_{x+j} k_{t+j})\right).$$

As previously indicated in section 3, k_t is approximately normally distributed, so that μ_t is log-normally distributed. In the LC model, the k_{t+j}'s are independent random variables. The exponent in $S_x(t, t+n)$ is the sum of correlated log-normal random variables. Therefore, we could obtain the comonotonic bounds to approximate $S_x(t, t+n)$. Write

$$S_n := \sum_{j=0}^{n-1} \exp(\alpha_{x+j} + \beta_{x+j} k_{t+j}) = \sum_{j=0}^{n-1} \delta_j e^{X_j},$$

where $\delta_j = e^{\alpha_{x+j}}$ and $X_j = \beta_{x+j} k_{t+j}$.

Consequently, $S_x(t, t+n) = \exp(-S_n)$. Recall that with the survival probability evaluated under $\widetilde{Q}$, the dynamics of k_t is given by equation (3.14). Therefore, we have $X_j \sim N(\mu_j, \sigma_j^2)$, where u_j and σ_j^2

$$\mu_j = \beta_{x+j} \mathrm{E}^{\widetilde{Q}}[k_{t+j}]$$

and

$$\sigma_j^2 = \beta_{x+j}^2 \mathrm{Var}^{\widetilde{Q}}[k_{t+j}].$$

Note that $\mathrm{E}^{\widetilde{Q}}[k_{t+j}]$ and $\mathrm{Var}^{\widetilde{Q}}[k_{t+j}]$ are determined employing equations (3.22) and (3.23), respectively.

We then obtain the convex-order upper bound for S_n as

$$S_n^u = \sum_{j=0}^{n-1} \delta_j e^{\mu_j + \sigma_j Z},$$

where $Z \sim N(0,1)$. The relation $S_n \preceq_{cx} S_n^u$ implies $P_x(t,t+n) \preceq_{cx} \exp(-S_n^u)$. The quantile for S_n^u is given by

$$F^{-1}_{S_n^u}(\epsilon) = \sum_{j=0}^{n-1} \delta_j e^{\mu_j + \sigma_j \Phi^{-1}(\epsilon)}, \tag{3.24}$$

where Φ^{-1} is the quantile function of the standard normal distribution.
In order to find the convex-order lower bound, we require the conditioning random variable Λ_n. Here, we choose the first-order Taylor approximation of S as Λ_n, that is,

$$\Lambda_n = \sum_{j=0}^{n-1} \delta_j X_j, \tag{3.25}$$

and Λ_n is normally distributed with parameters

$$\mu_\Lambda = \mathrm{E}^{\widetilde{Q}}[\Lambda_n] = \sum_{j=0}^{n-1} \delta_j \mu_j \tag{3.26}$$

and

$$\sigma_\Lambda^2 = \mathrm{Var}^{\widetilde{Q}}[\Lambda_n] = \sum_{i=0}^{n-1}\sum_{j=0}^{n-1} \delta_i \delta_j \sigma_{ij}, \tag{3.27}$$

where σ_{ij} is the covariance of X_i and X_j. Moreover, the covariance between X_i and Λ_n is

$$\mathrm{Cov}^{\widetilde{Q}}[X_i, \Lambda_n] = \sum_{j=0}^{n-1} \delta_j \sigma_{ij}. \tag{3.28}$$

We define the correlation coefficient between X_i and Λ_n as

$$\psi_i = \frac{\mathrm{Cov}^{\widetilde{Q}}[X_i, \Lambda_n]}{\sigma_i \sigma_\Lambda}. \tag{3.29}$$

This means that $X_i|\Lambda_n \sim N\left(\mu_i + \psi_i \frac{\sigma_i}{\sigma_\Lambda}(\Lambda_n - \mu_\Lambda), (1-\psi_i^2)\sigma_i^2\right)$. Note that $\frac{\Lambda - \mu_\Lambda}{\sigma_\Lambda}$ is a standard normal random variables, and so

$$\mathrm{E}^{\widetilde{Q}}\left[e^{X_i}\middle|\Lambda_n\right] = e^{\mu_i + \psi_i \sigma_i Z + \frac{1}{2}(1-\psi_i^2)\sigma_i^2},$$

where Z is the standard normal random variable. Hence, the convex-order lower bound is

$$S_n^l = \sum_{i=0}^{n-1} \delta_i \mathrm{E}^{\widetilde{Q}}\left[e^{X_i}\middle|\Lambda_n\right] = \sum_{i=0}^{n-1} \delta_i e^{\mu_i + \psi_i \sigma_i Z + \frac{1}{2}(1-\psi_i^2)\sigma_i^2}.$$

The relation $S_n^l \preceq_{cx} S_n$ implies that $\exp(-S_n^u) \preceq_{cx} P_x(t, t+n)$, and the quantile function of S_n^l is

$$F^{-1}_{S_n^l}(\epsilon) = \sum_{i=0}^{n-1} \delta_i e^{\mu_i + \psi_i \sigma_i \Phi^{-1}(\epsilon) + \frac{1}{2}(1-\psi_i^2)\sigma_i^2}. \tag{3.30}$$

3.4.3 Comonotonicity bounds of annuity rate

The annuity rate in equation (3.8) is the sum of dependent random variables and finding its analytical solution is not easy. So, we shall approximate the annuity rate by using the comonotonicity bounds of survival probabilities. Plugging in equations (3.2) and (3.10) into equation (3.8), we have the annuity rate

$$\begin{aligned} a_x(T) &= \sum_{i=1}^{n} B(T, T+i) \mathrm{E}^{\widetilde{Q}} \left[e^{-\int_T^{T+i} \mu_{x+v,v} \, \mathrm{d}v} \middle| \mathcal{F}_T \right] \\ &= \sum_{i=1}^{n} e^{-A(T,T+i) r_T + D(T,T+i)} \mathrm{E}^{\widetilde{Q}} \left[e^{-\int_T^{T+i} \mu_{x+v,v} \, \mathrm{d}v} \middle| \mathcal{F}_T \right]. \end{aligned} \tag{3.31}$$

Note that the annuity rate is the sum of the products of bond price and expectation of survival probability evaluated under the forward measure. The bond price has a closed-form solution and it is determined by r_T. The expectation term does not have a closed-form expression but we may approximate it using comonotonicity bounds. The expectation of the n-year survival probability of an individual aged x at time T can be efficiently obtained by numerical method via the quantile function of the comonotonic bounds. In particular, we have

$$\mathrm{E}^{\widetilde{Q}} \left[e^{-\int_T^{T+i} \mu_{x+v,v} \, \mathrm{d}v} \middle| \mathcal{F}_T \right] = \int_0^1 F_p^{-1}(p) \, \mathrm{d}p, \tag{3.32}$$

where $F_p^{-1}(p)$ can be either the lower or upper bound of the survival probability $P_x(T, T+n)$, which is obtained in the last subsection. The annuity rate $a_x(T)$ at time T depends on r_T and k_T. Hence, given the values of r_T and k_T, we are able to compute annuity rate efficiently by using comonotonicity bounds. Since (r_T, k_T) is a pair of random variables, $a_x(T)$ is also a random variable. We intend to determine the distribution and the mean of annuity rate at time T. This can be achieved by the Monte-Carlo simulation. We generate samples of (r_T, k_T) and compute $a_x(T)$ for each trail. Then we are able to obtain the approximation of the distribution of $a_x(T)$.

3.4.4 GAO estimation

The value of a GAO is provided by the pricing formula

$$P_{GAO} = g\mathrm{E}^{Q}\left[e^{\int_0^T r_v \,\mathrm{d}v} e^{\int_0^T \mu_{x+v,v}\,\mathrm{d}v}\left(a_x(T) - \frac{1}{g}\right)^{+}\right]. \tag{3.33}$$

As mentioned in section 3.2, for the general implementation of the simulation method, equation (3.33) requires simulations within a set of simulations as we have to know the annuity rate $a_x(T)$ for each simulation. In section 3.3, we stated that there is no closed-form solution to the survival probability under $\widetilde{Q}$. Hence, there is no closed-form solution to the pure endowment $M(T, T+n)$ or the annuity rate $a_x(T)$.

In this section, we utilise the comonotonic method to obtain the convex-order upper and lower bounds for the annuity rate $a_x(T)$. Then we are able to approximate the annuity rate by using comonotonic bounds and circumvent the tedious simulations within each simulation. Therefore, the evaluation procedure reduces to a one-level simulation only, which substantially improves both the computing time and calculation efficiency.

3.5 Numerical illustration

3.5.1 Lee-Carter model estimation

To implement our proposed modelling approach, we consider the data from the Human Mortality Database (HMD). We shall examine the data for the Canadian males aged $x = 25, \ldots, 100$ from 1970 to 2009. We select the year 2009 as the current time. The maximum likelihood estimation method in Brouhns, et al. [5] will be employed in estimating the parameters of the LC model. The parameter estimates, as they vary through age (year), are shown in Figure 3.1. We have $\widehat{c} = -1.2210$ and $\widehat{\xi} = 0.7646$ for the time-varying index k_t described in equation (3.4).

3.5.2 Survival probability approximations

We investigate the behaviour of the comonotonic bounds for the survival probability $S_x(t, t+n)$. The approximated quantile function of $S_x(t, t+n)$ is evaluated using equations (3.24)

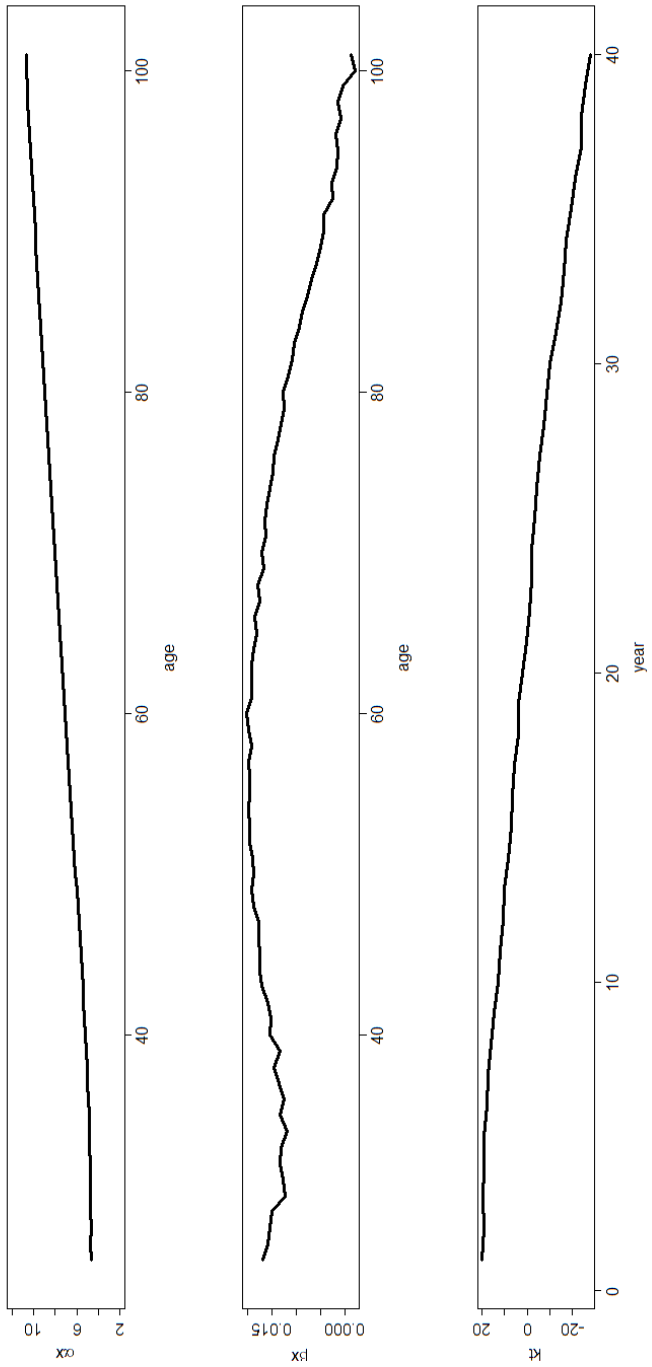

Figure 3.1: Estimated parameters as specified in equation (3.3) of the LC model versus age (year)

and (3.30). The simulated quantile function is obtained by simulating 1,000 sample paths for r_t and k_t using equation (3.5). The results will show that pricing values are already within a narrow bandwith of the lower and upper comonotonic bounds, implying robustness even for this small number of sample paths.

The parameter values used for the numerical computation in this section are shown in Table 4.1. The numerical results are produced by varying the value of one parameter whilst holding the other parameters fixed.

Our simulations in the numerical implementation of the correlated models make use of the Euler discretisation scheme given in Glasserman [14]. However, in order to avoid generating negative interest rates arising from the discretisation of the CIR model, we employ the discretisation modifications proposed by Labbé, et al. [16].

Contract specification			
$g = 11.1\%$	$T = 15$	$n = 35$	
Interest rate model			
$a = 0.15$	$b = 0.045$	$\sigma = 0.03$	$r_0 = 0.045$
Mortality model			
$c = -1.2210$	$\xi = 0.7646$	$k_0 = -27.65504$	$\rho = 0.3$

Table 3.4: Parameter values

Before approximating the survival probability, we first test if indeed k_t follows the normal distribution approximately. We generate 5,000 sample paths to form the distribution of k_t at time $t = T + n$. We also vary the parameters within a reasonable range. The Shapiro test is used to check formally the normality of k_t. From the results shown in Table 3.5, we see large p-values so that we do not reject the null hypothesis, i.e., we do not have enough evidence to refute that k_t follows the normal distribution. We complement the statistical tests with the QQ plots and the results are shown in Figure 3.2. The plots in the upper panel are for different values of ρ and those in the lower panel are for different values of n. From these results, we can conclude that k_t follows the normal distribution.

In Figure 3.3, we display the comonotonicity-based quantile functions for $\rho = -0.9$, 0 and 0.9. These quantile functions are very close to those obtained from simulation and all absolute differences are smaller than 0.001. Thus, it is not straightforward to determine which

Table 3.5: p-values for the Shapiro test associated with different values of parameters

n	5	15	20	35	45		
p-value	0.082644207	0.378690903	0.939415845	0.474067433	0.65368055		
ρ	-0.9	-0.6	-0.3	0	0.3	0.6	0.9
p-value	0.52854673	0.15152869	0.81366067	0.13107350	0.67794200	0.75626646	0.23700257
a	0.05	0.10	0.15	0.20	0.25	0.30	0.35
p-value	0.39848631	0.68066950	0.99698376	0.24584751	0.11577257	0.69668452	0.58837425
b	0.030	0.035	0.040	0.045	0.050	0.055	0.060
p-value	0.12394266	0.16926209	0.49796616	0.42103821	0.82749761	0.25970541	0.93997943
σ	0.01	0.03	0.05	0.10	0.15	0.30	
p-value	0.79761570	0.14426807	0.13299200	0.69133551	0.10743794	0.372396912	
c	-1.5	-1.4	-1.3	-1.2	-1.1	-1.0	-0.9
p-value	0.5725514	0.3170961	0.7082644	0.3470099	0.6283086	0.6293595	0.6456897
ξ	0.5	0.6	0.7	0.8	0.9	1.0	1.1
p-value	0.6698388	0.2157423	0.2129757	0.2729455	0.2822947	0.9231017	0.8329281

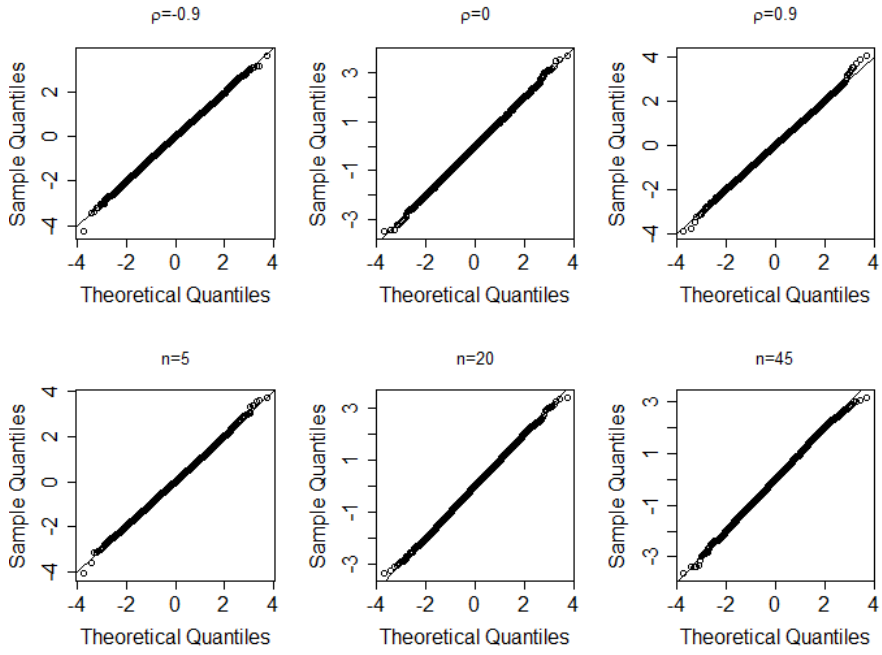

Figure 3.2: QQ plot for k_t

bound is better as their accuracies are quite similar. However, the upper bound is more efficient than the lower bound when the computation complexity is considered because the conditioning random variable Λ is still needed when calculating convex-lower bound.

We choose different values of parameters within a reasonable range and perform the simulation for the expected survival probability $P_{65}(15, 15+n)$. Tables 3.6–3.11 display the expectation of the survival probabilities using different approximation methods. Standard errors (SEs) for the estimated survival probabilities by simulation are given in parentheses. At a significance level of say 5%, confidence intervals for the estimated values by simulation overlap with the corresponding intervals spanned by the lower and upper bonds. This statistically provides support that our comonotonic approximations are accurate, with the simulated values serving as benchmarks. We carry a 4-decimal accuracy for the comonotonic approximations. The parameters of the interest model has a small but visible influence on the survival probability. As ρ increases, the survival probability increases, and vice-versa. The parameter c has a significant influence on the results. The survival probability decreases as c increases.

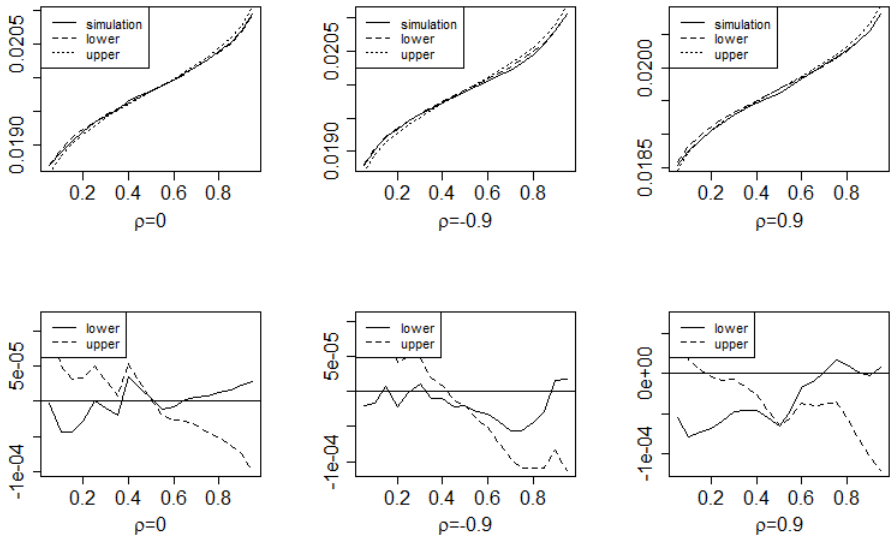

Figure 3.3: Quantiles to demonstrate the differences in the approximation of $S_{65}(15, 15 + 35)$

3.5.3 Annuity rate approximation

In this subsection, we assess the performance of the approximation that evaluates the annuity rate $a_x(T)$. Similar to the survival probability, we obtain the quantiles of the comonotonic approximations for $a_x(T)$ using equations (3.31) and (3.32). The simulated quantiles are obtained by equation (3.8), and we generated 2,000 sample paths for r_t and k_t. From Figure 3.4, we see that the quantiles of the comonotonic bounds closely approximate the simulated value. The upper panel shows the quantile functions and the lower panel shows the relative differences between the approximated and simulated quantiles. All differences in absolute value are less than 0.2.

The means of annuity rates are displayed in Table 3.12-3.17. We observe that the comonotonic bounds still exhibit good performance in approximating $a_x(T)$; the absolute values of the differences are less than 0.1. As n increases, the annuity also increases. A fivefold magnification of the original σ and ξ estimates was introduced in order to illustrate perspicuously the influence of ρ on annuity rates as illustrated in Table 3.12; the annuity rate increases as ρ increases. The annuity rate decreases significantly as parameters a, b, σ, c or ξ increases, and vice-versa.

When $n = 15$, the computing time for our approximation is only 4% of that required for the

Table 3.6: Valuation of $P_{65}(15, 15+n)$ with different values of ρ

	n=10			n=35		
ρ	simulation	lower	upper	simulation	lower	upper
-0.9	0.869956 (2.8×10^{-5})	0.869946	0.869947	0.019684 (7×10^{-6})	0.019685	0.019688
-0.6	0.870048 (2.8×10^{-5})	0.870005	0.870006	0.019722 (7×10^{-6})	0.019724	0.019726
-0.3	0.870108 (2.8×10^{-5})	0.870063	0.870065	0.019760 (7×10^{-6})	0.019762	0.019765
0	0.870164 (2.8×10^{-5})	0.870122	0.870123	0.019799 (7×10^{-6})	0.019800	0.019803
0.3	0.870217 (2.8×10^{-5})	0.870181	0.870182	0.019833 (7×10^{-6})	0.019839	0.019842
0.6	0.870239 (2.8×10^{-5})	0.870239	0.870241	0.019880 (7×10^{-6})	0.019877	0.019880
0.9	0.870308 (2.8×10^{-5})	0.870298	0.870299	0.019919 (7×10^{-6})	0.019916	0.019919

Table 3.7: Valuation of $P_{65}(15, 15+n)$ with different values of a

	n=10			n=35		
a	simulation	lower	upper	simulation	lower	upper
0.05	0.870211 (2.8×10^{-5})	0.870202	0.870203	0.019876 (7.0×10^{-6})	0.019878	0.019881
0.10	0.870201 (2.8×10^{-5})	0.870190	0.870191	0.019847 (7.0×10^{-6})	0.019853	0.019856
0.15	0.870199 (2.8×10^{-5})	0.870181	0.870182	0.019840 (7.0×10^{-6})	0.019839	0.019842
0.20	0.870186 (2.8×10^{-5})	0.870173	0.870174	0.019830 (7.0×10^{-6})	0.019830	0.019833
0.25	0.870179 (2.8×10^{-5})	0.870167	0.870168	0.019824 (7.0×10^{-6})	0.019825	0.019827
0.30	0.870167 (2.8×10^{-5})	0.870162	0.870163	0.019820 (7.0×10^{-6})	0.019821	0.019824
0.35	0.870156 (2.8×10^{-5})	0.870158	0.870159	0.019817 (7.0×10^{-6})	0.019818	0.019821
0.40	0.870153 (2.8×10^{-5})	0.870154	0.870156	0.019813 (7.0×10^{-6})	0.019816	0.019819

Monte-Carlo method in average. When $n = 35$ the computing time for the approximation is only 2% of that required for the Monte-Carlo method in average. Ostensibly, the approach via the comonotonic bounds provides a more efficient method to approximate the annuity rate.

Table 3.8: Valuation of $P_{65}(15, 15+n)$ with different values of b

	n=10			n=35		
b	simulation	lower	upper	simulation	lower	upper
0.030	0.870171 (2.8×10^{-5})	0.870177	0.870179	0.019832 (7.0×10^{-6})	0.019834	0.019837
0.035	0.870176 (2.8×10^{-5})	0.870179	0.870180	0.019831 (7.0×10^{-6})	0.019836	0.019838
0.040	0.870180 (2.8×10^{-5})	0.870180	0.870181	0.019836 (7.0×10^{-6})	0.019837	0.019840
0.045	0.870182 (2.8×10^{-5})	0.870181	0.870182	0.019835 (7.0×10^{-6})	0.019839	0.019842
0.050	0.870186 (2.8×10^{-5})	0.870182	0.870183	0.019837 (7.0×10^{-6})	0.019840	0.019843
0.055	0.870193 (2.8×10^{-5})	0.870183	0.870184	0.019844 (7.0×10^{-6})	0.019842	0.019844
0.060	0.870195 (2.8×10^{-5})	0.870184	0.870185	0.019839 (7.0×10^{-6})	0.019842	0.019846

Table 3.9: Valuation of $P_{65}(15, 15+n)$ with different values of σ

	n=10			n=35		
σ	simulation	lower	upper	simulation	lower	upper
0.01	0.870136 (2.8×10^{-5})	0.870142	0.870143	0.019812 (7.0×10^{-6})	0.019814	0.019816
0.03	0.870173 (2.8×10^{-5})	0.870181	0.870182	0.019843 (7.0×10^{-6})	0.019839	0.019842
0.05	0.870223 (2.8×10^{-5})	0.870218	0.870219	0.019861 (7.0×10^{-6})	0.019861	0.019863
0.10	0.870287 (2.8×10^{-5})	0.870294	0.870295	0.019894 (7.0×10^{-6})	0.019895	0.019898
0.15	0.870334 (2.8×10^{-5})	0.870340	0.870341	0.019916 (7.0×10^{-6})	0.019902	0.019905
0.30	0.870365 (2.8×10^{-5})	0.870334	0.870336	0.019988 (7.0×10^{-6})	0.019873	0.019877

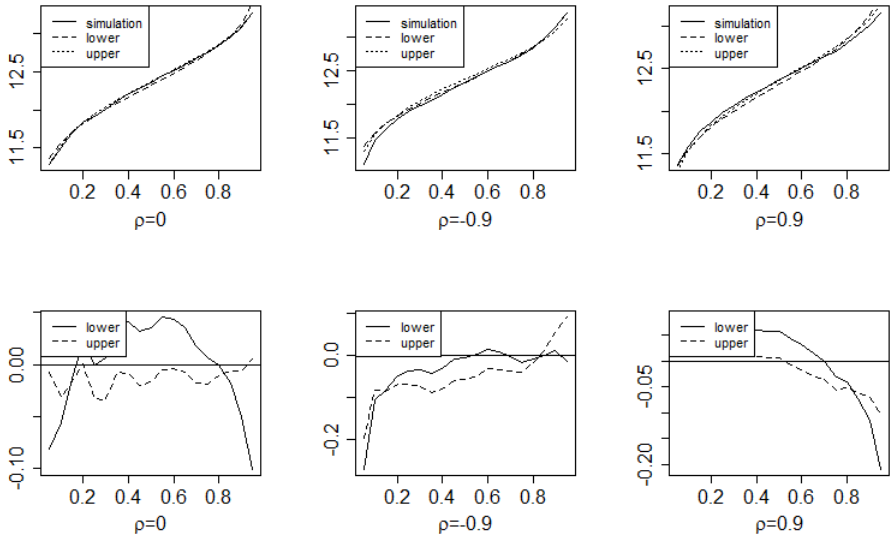

Figure 3.4: Quantiles and differences in the approximation of $a_{65}(15)$ for $n = 35$

Table 3.10: Valuation of $P_{65}(15, 15+n)$ with different values of c

	n=10			n=35		
c	simulation	lower	upper	simulation	lower	upper
-1.5	0.872939 (2.8×10^{-5})	0.872938	0.872940	0.021037 (7.0×10^{-6})	0.021038	0.021040
-1.4	0.871956 (2.8×10^{-5})	0.871958	0.871960	0.020605 (7.0×10^{-6})	0.020605	0.020608
-1.3	0.871967 (2.8×10^{-5})	0.870969	0.870970	0.020177 (7.0×10^{-6})	0.020176	0.020179
-1.2	0.870978 (2.8×10^{-5})	0.869971	0.869972	0.019749 (7.0×10^{-6})	0.019750	0.019753
-1.1	0.869966 (2.8×10^{-5})	0.868963	0.868967	0.019326 (7.0×10^{-6})	0.019327	0.019330
-1.0	0.867950 (2.8×10^{-5})	0.867946	0.867947	0.018903 (7.0×10^{-6})	0.018907	0.018910
-0.9	0.866931 (2.8×10^{-5})	0.866920	0.866921	0.018485 (7.0×10^{-6})	0.018491	0.018494

Table 3.11: Valuation of $P_{65}(15, 15+n)$ with different values of ξ

	n=10			n=35		
ξ	simulation	lower	upper	simulation	lower	upper
0.5	0.870200 (1.8×10^{-5})	0.870194	0.870195	0.019823 (4.0×10^{-6})	0.019824	0.019825
0.6	0.870214 (2.2×10^{-5})	0.870204	0.870205	0.019832 (5.0×10^{-6})	0.019830	0.019832
0.7	0.870212 (2.6×10^{-5})	0.870212	0.870214	0.019838 (6.0×10^{-6})	0.019835	0.019838
0.8	0.870224 (3.0×10^{-5})	0.870229	0.870231	0.019836 (7.0×10^{-6})	0.019841	0.019844
0.9	0.870236 (3.3×10^{-5})	0.870235	0.870237	0.019844 (8.0×10^{-6})	0.019846	0.019850
1.0	0.870253 (3.6×10^{-5})	0.870249	0.870241	0.019851 (9.0×10^{-6})	0.019852	0.019857
1.1	0.870217 (3.9×10^{-5})	0.870252	0.870255	0.019853 (1.0×10^{-5})	0.019858	0.019864
1.2	0.870262 (4.4×10^{-5})	0.870263	0.870267	0.019862 (1.1×10^{-5})	0.019864	0.019870

Table 3.12: aluation of annuity with different values of ρ

	n=10			n=35		
ρ	simulation	lower	upper	simulation	lower	upper
-0.9	7.377389	7.377197	7.378049	12.26755	12.26709	12.26942
-0.6	7.398602	7.395779	7.408123	12.29378	12.29059	12.29691
-0.3	7.416339	7.413593	7.418294	12.32284	12.32028	12.32534
0	7.424933	7.422534	7.428741	12.33934	12.33572	12.34245
0.3	7.436314	7.431407	7.438583	12.35322	12.34982	12.35635
0.6	7.451433	7.449221	7.452682	12.38246	12.37941	12.38236
0.9	7.467994	7.467035	7.469789	12.41030	12.40901	12.41217
computing time	1184.26 secs	52.72 secs		12043.34 secs	262.87 secs	

Table 3.13: Valuation of annuity with different values of a. All SEs for simulated values are less than 9.5×10^{-4}.

	n=10			n=35		
a	simulation	lower	upper	simulation	lower	upper
0.05	7.440523	7.441846	7.458045	12.52017	12.48421	12.52668
0.10	7.421565	7.428505	7.437837	12.41622	12.37775	12.40001
0.15	7.429408	7.422686	7.428543	12.34290	12.33722	12.35015
0.20	7.422491	7.419634	7.423604	12.32006	12.31772	12.32600
0.25	7.416134	7.417810	7.420668	12.28791	12.30683	12.31254
0.30	7.415625	7.416618	7.418772	12.30592	12.30012	12.30428
0.35	7.417167	7.415790	7.417471	12.29519	12.29568	12.29885
0.40	7.413073	7.415188	7.417471	12.29084	12.29258	12.29508
computing time	1257.41 secs	54.85 secs		13780.91 secs	296.04 secs	

Table 3.14: Valuation of annuity with different values of b. All SEs for simulated values are less than 9.5×10^{-4}.

	n=10			n=35		
b	simulation	lower	upper	simulation	lower	upper
0.030	7.972695	7.965416	7.971999	14.26360	14.25534	14.27131
0.035	7.780771	7.778834	7.785152	13.61697	13.56855	13.58339
0.040	7.596806	7.597992	7.604069	12.95986	12.93058	12.94442
0.045	7.422507	7.422686	7.428543	12.36373	12.33722	12.35015
0.050	7.251678	7.252724	7.258376	11.78635	11.78466	11.79679
0.055	7.087846	7.087919	7.093380	11.27769	11.26948	11.28087
0.060	6.917590	6.928092	6.933372	10.78459	10.78856	10.79928
computing time	1102.36 secs	49.08 secs		12082.57 secs	270.15 secs	

Table 3.15: Valuation of annuity with different values of σ. All SEs for simulated values are less than 9.5×10^{-4}.

	n=10			n=35		
σ	simulation	lower	upper	simulation	lower	upper
0.01	7.410818	7.413585	7.414247	12.28469	12.28699	12.28846
0.03	7.423400	7.422686	7.428543	12.33366	12.33722	12.35015
0.05	7.446104	7.440506	7.456197	12.44000	12.43283	12.46717
0.07	7.454350	7.466471	7.495548	12.54979	12.56807	12.63091
0.09	7.499653	7.499792	7.544276	12.71330	12.73576	12.83038
computing time	831.94 secs	57.68 secs		10243.30 secs	314.94 secs	

Table 3.16: Valuation of annuity with different values of c. All SEs for simulated values are less than 9.5×10^{-4}.

	n=10			n=35		
c	simulation	lower	upper	simulation	lower	upper
-1.5	7.452310	7.459493	7.465387	12.56111	12.56444	12.57770
-1.4	7.453556	7.446639	7.452520	12.49959	12.48411	12.49726
-1.3	7.444359	7.433413	7.439280	12.40151	12.40255	12.41558
-1.2	7.431990	7.419803	7.425656	12.33854	12.31977	12.33269
-1.1	7.402086	7.405799	7.411639	12.22570	12.23577	12.24857
-1.0	7.383719	7.391393	7.397218	12.16437	12.15056	12.16323
-0.9	7.373812	7.376573	7.382383	12.04440	12.06415	12.07670
computing time	1108.76 secs	50.35 secs		12115.92 secs	270.20 secs	

Table 3.17: Valuation of annuity with different values of ξ. All SEs for simulated values are less than 9.5×10^{-4}.

	n=10			n=35		
ξ	simulation	lower	upper	simulation	lower	upper
0.5	7.428001	7.422682	7.428539	12.34633	12.33657	12.34950
0.6	7.431360	7.422686	7.428542	12.31695	12.33682	12.34976
0.7	7.429945	7.422687	7.428543	12.31162	12.33707	12.35000
0.8	7.424207	7.422686	7.428542	12.34886	12.33730	12.35024
0.9	7.422763	7.422682	7.428539	12.33217	12.33752	12.35046
1.0	7.432457	7.422676	7.428533	12.33108	12.33773	12.35067
1.1	7.423462	7.422668	7.428525	12.35035	12.33794	12.35087
1.2	7.417140	7.422658	7.428515	12.34545	12.33813	12.35106
computing time	1167.48 secs	55.84 secs		13289.06 secs	303.38 secs	

3.5.4 GAO evaluation

We now compare the comonotonic approximations and the simulated values for GAO. The comonotonic approximations are obtained using equations (3.31) and (3.33). The simulated values are obtained through equations (3.8) and (3.9). Both methods make use of 5,000 sample paths. However, for a simulated value, we have to generate 5,000 sample paths to calculate $a_x(T)$ for each simulation.

Tables 3.18-3.20 present the numerical results for different values of parameters. Almost all approximations are precise to the third decimal place and the average of relative differences is smaller than 1%. Our estimated σ and ξ were also quintupled to clearly the impact of ρ on GAO prices, which are displayed in Table 3.18. We can see that GAO values exhibit variation as ρ changes. Also, we observe that the GAO value decreases as a , b or c increases. The computational time takes only 0.36% of that for the crude Monte-Carlo simulations, which clearly suggests that the comonotonic method provides a much more efficient way to estimate GAO prices.

ρ	simulation (SE)	approximation
-0.9	0.1730782 (0.0005562)	0.1730448
-0.6	0.1747384 (0.0005932)	0.1747469
-0.3	0.1768427 (0.0006263)	0.1764492
0	0.1773337 (0.0006410)	0.1773474
0.3	0.1785088 (0.0006722)	0.1781523
0.6	0.1794514 (0.0006887)	0.1798531
0.9	0.1806418 (0.0007126)	0.1811562
computing time	76782.23 secs	278.45 secs

Table 3.18: Valuation of GAO with different values of ρ

a	simulation (SE)	approximation
0.05	0.196577 (1.5×10^{-4})	0.201189
0.10	0.184769 (9.3×10^{-4})	0.185583
0.15	0.177708 (6.7×10^{-4})	0.182774
0.20	0.175712 (5.1×10^{-4})	0.176002
0.25	0.175032 (4.1×10^{-4})	0.174719
0.30	0.173473 (3.3×10^{-4})	0.172924
0.35	0.173397 (2.9×10^{-4})	0.173910
computing time	77937.82 secs	289.14 secs

Table 3.19: Valuation of GAO with different values of a

b	simulation (SE)	approximation
0.030	0.321141 (8.7×10^{-4})	0.322056
0.035	0.266019 (8.1×10^{-4})	0.266583
0.040	0.219750 (7.4×10^{-4})	0.217499
0.045	0.178533 (6.7×10^{-4})	0.177478
0.050	0.142920 (6.1×10^{-4})	0.139237
0.055	0.111113 (5.4×10^{-4})	0.110972
0.060	0.084868 (4.9×10^{-4})	0.082836
computing time	84610.26 secs	268.15 secs

Table 3.20: Valuation of GAO with different values of b

c	simulation (SE)	approximation
-1.5	0.191594 (6.9×10^{-4})	0.190959
-1.4	0.186615 (6.9×10^{-4})	0.186058
-1.3	0.181677 (6.9×10^{-4})	0.182320
-1.2	0.178045 (6.7×10^{-4})	0.175953
-1.1	0.171942 (6.4×10^{-4})	0.171123
-1.0	0.166786 (6.4×10^{-4})	0.168111
-0.9	0.164060 (6.4×10^{-4})	0.161401
computing time	74167.97 secs	267.55 secs

Table 3.21: Valuation of GAO with different values of c

ξ	simulation (SE)	approximation
0.5	0.176827 (6.6×10^{-4})	0.177805
0.6	0.178300 (6.6×10^{-4})	0.177412
0.7	0.179225 (6.6×10^{-4})	0.177938
0.8	0.177798 (6.8×10^{-4})	0.181160
0.9	0.177917 (6.7×10^{-4})	0.175302
1.0	0.178547 (6.8×10^{-4})	0.179936
1.1	0.176970 (6.8×10^{-4})	0.177625
1.2	0.178705 (6.9×10^{-4})	0.174075
computing time	82925.64 secs	305.44 secs

Table 3.22: Valuation of GAO with different values of ξ

3.6 Conclusion

We presented an important application of the comonotonicity-based methodology. The comonotonic approximations of survival probabilities and annuities provide a powerful way to improve the computation of prices with greater efficiency and excellent precision. It avoids the "simulation-within-simulation" problem in GAO valuation. Although the short-term interest rate r_t and force of mortality μ_t are dependent and as such, there is no closed-form solution to the pure endowment and annuity rate, we are still able to provide high-performance approximations for them.

In particular, we employed the change of measure technique to simplify the endowment formula and make the comonotonic method accessible. Numerical illustrations show that

the comonotonic approximation indeed provide an efficient method to estimate the survival probability, annuity rate and GAO price. They also demonstrate that the comonotonic bounds provide superb accuracy and laid down the mechanics on how this method could be implemented with ease.

Further research works could use stochastic parameters in the model. For instance, we may apply the Markov regime-switching methodology to develop a much more flexible modelling set up. We certainly could also utilise the ideas behind our proposed efficient algorithm here to price other contingent products whose values depend on both the short rate and force of mortality with a given correlation.

References

[1] L. Ballotta and S. Haberman. Valuation of guaranteed annuity conversion options. *Insurance: Mathematics and Economics*, 33(1):87–108, 2003.

[2] L. Ballotta and S. Haberman. The fair valuation problem of guaranteed annuity options: The stochastic mortality environment case. *Insurance: Mathematics and Economics*, 38(1):195–214, 2006.

[3] M. Bolton, D Carr, P. Collis, C. George, V. Knowles, and A. Whitehouse. Reserving for annuity guarantees. *Report of the Annuity Guarantees Working Party*, 1997.

[4] D. Brigo and F. Mercurio. *Interest Rate Models-Theory and Practice: With Smile, Inflation and Credit*. Springer Science & Business Media, New York, 2007.

[5] N. Brouhns, M. Denuit, and J. Vermunt. A Poisson log-bilinear regression approach to the construction of projected lifetables. *Insurance: Mathematics and economics*, 31(3):373–393, 2002.

[6] A. Cairns, D. Blake, K. Dowd, G. Coughlan, D. Epstein, A. Ong, and I. Balevich. A quantitative comparison of stochastic mortality models using data from England and Wales and the United States. *North American Actuarial Journal*, 13(1):1–35, 2009.

[7] G. Deelstra. Yield option pricing in the generalized Cox-Ingersoll-Ross model, 1999. URL `http://homepages.ulb.ac.be/~grdeelst/yield.pdf`.

[8] G. Deelstra, M. Grasselli, and C. Van Weverberg. The role of the dependence between mortality and interest rates when pricing guaranteed annuity options. *Insurance: Mathematics and Economics*, 71:205–219, 2016.

[9] J. Dhaene, M. Denuit, M. Goovaerts, R. Kaas, and D. Vyncke. The concept of comonotonicity in actuarial science and finance: Theory. *Insurance: Mathematics and Economics*, 31(1):3–33, 2002.

[10] J. Dhaene, M. Denuit, M. Goovaerts, R. Kaas, and D. Vyncke. The concept of comonotonicity in actuarial science and finance: Applications. *Insurance: Mathematics and Economics*, 31(2):133–161, 2002.

[11] H. Gao, R. Mamon, and X. Liu. Pricing a guaranteed annuity option under correlated and regime-switching risk factors. *European Actuarial Journal*, 5(2):309–326, 2015.

[12] H. Gao, R. Mamon, X. Liu, and A. Tenyakov. Mortality modelling with regime-switching for the valuation of a guaranteed annuity option. *Insurance: Mathematics and Economics*, 63:108–120, 2015.

[13] H. Gao, R. Mamon, and X. Liu. Risk measurement of a guaranteed annuity option under a stochastic modelling framework. *Mathematics and Computers in Simulation*, 132:100–119, 2017.

[14] P.l Glasserman. *Monte Carlo Methods in Financial Engineering*, volume 53. Springer Science & Business Media, New York, 2013.

[15] M. Hardy. *Investment Guarantees: Modeling and Risk Management for Equity-Linked Life Insurance*, volume 215. John Wiley & Sons, New Jersey, 2003.

[16] C. Labbé, B. Rémillard, and J. Renaud. A simple discretization scheme for non-negative diffusion processes with applications to option pricing. *arXiv e-prints*, page arXiv:1011.3247, 2010. URL `https://ui.adsabs.harvard.edu/\#abs/2010arXiv1011.3247L`.

[17] R. Lee and L. Carter. Modeling and forecasting US mortality. *Journal of the American Statistical Association*, 87(419):659–671, 1992.

[18] X.S. Lin and X. Liu. Markov aging process and phase-type law of mortality. *North American Actuarial Journal*, 11(4):92–109, 2007.

[19] X. Liu, J. Jang, and S.M. Kim. An application of comonotonicity theory in a stochastic life annuity framework. *Insurance: Mathematics and Economics*, 48(2):271–279, 2011.

[20] X. Liu, R. Mamon, and H. Gao. A comonotonicity-based valuation method for guaranteed annuity options. *Journal of Computational and Applied Mathematics*, 250: 58–69, 2013.

[21] X. Liu, R. Mamon, and H. Gao. A generalized pricing framework addressing correlated mortality and interest risks: A change of probability measure approach. *Stochastics: An International Journal of Probability and Stochastic Processes*, 86(4):594–608, 2014.

[22] Y. Maghsoodi. Solution of the extended CIR term structure and bond option valuation. *Mathematical Finance*, 6(1):89–109, 1996.

[23] R. Mamon. Three ways to solve for bond prices in the Vasiček model. *Advances in Decision Sciences*, 8(1):1–14, 2004.

[24] H. Shirakawa. Squared Bessel processes and their applications to the square root interest rate model. *Asia-Pacific Financial Markets*, 9(3):169–190, 2002.

Chapter 4

A two-decrement model for the valuation and risk measurement of a GAO

4.1 Introduction

Financial innovations, created to respond to the needs of clients amidst increased longevity and an ageing population, have made the insurance market an investment hub. A wider range of products that both act as income security and investment protection is now available. This kind of products typically has option-embedded features and requires the accurate modelling of the uncertainty akin to various risk factors along with the correlation amongst them. Interest and mortality risks are deemed to be the two most important factors in the valuation and risk management of longevity products; they have been extensively examined altogether for several decades. Nonetheless, lapse risk is another essential factor in pricing insurance products; such a risk refers to the possibility that policyholders terminate their policies early for various reasons. Policy's lapse risk could then lead to huge losses and liquidity problem for insurance companies, and therefore, is an important consideration given economic and financial uncertainties.

Some theoretical and empirical studies were carried out in an attempt to explain the lapses' determinants and eventually incorporate them in actuarial pricing and risk management. For instance, Kim [15] and Zians et al. [27] developed lapse-rate models with explanatory variables dependent mainly on (i) unemployment rate and (ii) the difference between market interest and credit rates, whilst Albizzati and Geman [3] and Bacinello [5] considered the surrender option embedded in a life insurance. An alternative way is to consider the lapse or surrender risk with a rational surrendering model by formulation an optimal sur-

rendering problem as an optimal stopping problem; see Siu [**?**]. As a related point, such an optimal stopping problem with factors targetting the risk characteristics of the policyholders (e.g., financial and economic factors). For a comprehensive review of lapse-rate modelling in life insurance, one may refer to Eling and Kochanski [8].

In current practice, lapse rate is assumed constant in actuarial valuation as research advances on its modelling are rather slow and not sustaining as those of interest and mortality dynamics. Such a lack of research progress is attributed primarily to the absence of reliable data and inability to access copyrighted data owned by a company or professional organisation. One may use, however, insights on certain longevity product (e.g., variable annuity (VA)) in probing the very nature of lapse risk. Recall that a VA is a tax-deferred investment that allows the holder to choose from a suite of investments paying retirement income at a level dependent on the over all performance of the selected investments. A penalty is levied when a VA contract is terminated, and this mechanism somehow mitigates policy surrender, thereby lowering the lapse rate. Nonetheless, the surrender of a VA is most likely if there are investment alternatives that have better returns outweighing surrender losses.

Also, we note that policyholder's decision to surrender is directly affected by economic circumstances. For instance, when interest rate falls, which in turn stimulates borrowing, a low lapse rate is expected because the policy holder can obtain a loan at a lower interest rate instead of incurring a heavy surrender penalty. Although there are papers that deal with the dynamic behaviour of lapse rates (e.g., Xue [26]; De Giovanni [6]; and Loisel and Milhaud [19]), their aims are not aligned to actuarial applications. Furthermore, their frameworks do not take into consideration the interaction amongst lapse risk, interest rate and mortality risk.

Pertinent developments in recent years, covering the valuation of GAO with closely related objectives and setting to this chapter, are given in Gao et al. [10] and Gao et al. [11]. A pricing method for GAO utilising comonotonic bounds is demonstrated as well in Liu et al. [17]. The specific intent of this article is to extend Liu et al. [18] and Gao et al. [12], thereby enabling modelling advances over one-decrement actuarial models with correlated mortality and financial risk factors. Our proposed modelling framework distinctly presents lapse rate as one of the three major contributing risk factors. Our model exploits the results of Duffie and Kan [7] and Mamon [20] showing that affine dynamics for multiple factors yield exponential bond prices and vice versa. We employ the change of measure technique and bypass the "simulation-within-simulation" problem associated in the evaluation of GAO

liabilities. Numerical results show that our method outperforms the classical Monte-Carlo (MC) method, and these led to the efficient computations of GAO's capital requirements under several risk measures emphasised by regulatory authorities (e.g., Canada's OSFI). Concentrating on the challenge of efficiently characterising the GAO's loss function for risk measurement, we make use of the moment-based density approximation popularised in Provost [22], and update the results under this alternative technique in the context of Gao et al. [12].

This chapter is organised as follows. The combined modelling framework of the dependent risk factors is constructed in Section 4.2, which also details the formulation of the pricing set up and the loss function of a GAO. In Section 4.3, we determine the value of a GAO with the aid of certain numèraires corresponding to the sequence of probability measure changes involving forward, survival, and risk-endowment probability measures. Some risk measures are evaluated using the moment-based density approximation method in Section 4.4, and the results are benchmarked with those from the MC simulation and forward-measure methods . We present a numerical implementation in Section 4.5 illustrating the advantages of our proposed method and quantifying the impact of lapse rate on GAO prices and risk measures. Finally, Section 4.6 concludes.

4.2 Modelling framework

Our valuation of insurance and annuity products relies on three kinds of interrelated uncertainty risks represented by the short-rate process r_t for financial risk, force of mortality μ_t for mortality risk, and lapse rate l_t for lapse risk. We assume that these processes are defined on a filtered probability space $(\Omega, \mathcal{F}, \{\mathcal{F}_t\}, Q)$, where Q is a risk-neutral probability and $\mathcal{F}_t$ is the joint filtration generated by r_t, μ_t and l_t.

4.2.1 Interest rate model

Under Q, r_t follows the Vasiček model dynamics given by

$$\mathrm{d}r_t = a(b - r_t)\,\mathrm{d}t + \sigma\,\mathrm{d}X_t, \tag{4.1}$$

where a, b and σ are positive constants, and X_t is a standard Brownian motion (BM). The price $B(t,T)$ of a T-maturity zero-coupon bond at time $t < T$ is known to be

$$B(t,T) = \mathbb{E}^Q\left[e^{-\int_t^T r_u\,\mathrm{d}u}\middle|\mathcal{F}_t\right] = e^{-A(t,T)r_t + D(t,T)}, \tag{4.2}$$

where

$$A(t,T) = \frac{1 - e^{-a(T-t)}}{a}$$

and

$$D(t,T) = \left(b - \frac{\sigma^2}{2a^2}\right)[A(t,T) - (T-t)] - \frac{\sigma^2 A(t,T)^2}{4a}.$$

4.2.2 Mortality model

The dynamics of the force of mortality process μ_t is given by

$$\mathrm{d}\mu_t = c\mu_t\,\mathrm{d}t + \xi\,\mathrm{d}Y_t, \tag{4.3}$$

where c and ξ are positive constants, and Y_t is a standard BM under Q. We suppose that X_t and Y_t are correlated and their dependence is modelled as

$$\mathrm{d}X_t\,\mathrm{d}Y_t = \rho_{12}\,\mathrm{d}t.$$

The survival probability for an individual aged (x) at time t surviving to time T is $e^{-\int_t^T \mu_u\,\mathrm{d}u}$. Note that this is a random variable; and so we define the survival function

$$S(t,T) = \mathbb{E}^Q\left[e^{-\int_t^T \mu_u\,\mathrm{d}u}\middle|\mathcal{F}_t\right],$$

which is the expectation of the survival probability. This expectation is under Q because our purpose is to price a financial contract.

4.2.3 Lapse rate model

As mentioned in Kim [15] and Zians et al. [27], lapse rate is driven by many factors including the policyholder's behavioural characteristics, product's specificities, financial market and macro-economic environments. Thus, there is no denying that building an appropriate model for the lapse rate is a challenging endeavour. For pricing tractability, we shall propose a simplified model yet capable enough to incorporate the stylised facts presently observed in the risk process. As per the findings in Kuo et al. [16], lapse rate is hugely influenced by the interest rate and somehow by the unemployment rate and GDP. Since these

intervening factors are also largely driven by the economic cycle, lapse must also exhibit a mean-reverting feature. Therefore, for the process l_t, we adopt the dynamics

$$\mathrm{d}l_t = h(m - l_t)\,\mathrm{d}t + \zeta\,\mathrm{d}Z_t, \tag{4.4}$$

where h, m and ζ are positive constants and Z_t is a standard BM correlated with both X_t and Y_t; in particular,

$$\mathrm{d}X_t\,\mathrm{d}Z_t = \rho_{13}\,\mathrm{d}t \quad \text{and} \quad \mathrm{d}Y_t\,\mathrm{d}Z_t = \rho_{23}\,\mathrm{d}t.$$

Remark 4.1 *The mean-reverting model for the lapse rate could be thought of as a macroeconomic approach for the lapse rate's description; this is considering the premise that the lapse rate is related to certain macro-economic factors such as interest rate, unemployment rate, GDP, and economic cycles.*

In order to implement a consistent correlation matrix when generating X_t, Y_t and Z_t for simulation and other financial-modelling objectives, these BMs' dynamics are specified as follows:

$$\begin{aligned}
\mathrm{d}X_t &= \mathrm{d}W_t^1, \\
\mathrm{d}Y_t &= \rho_{12}\,\mathrm{d}W_t^1 + \sqrt{1-\rho_{12}^2}\,\mathrm{d}W_t^2, \\
\mathrm{d}Z_t &= \rho_{13}\,\mathrm{d}W_t^1 + \rho'_{23}\,\mathrm{d}W_t^2 + \sqrt{1-\rho_{13}^2-\rho_{23}'^2}\,\mathrm{d}W_t^3,
\end{aligned}$$

where W_t^1, W_t^2 and W_t^3 are independent standard BMs and

$$\rho'_{23} = \frac{\rho_{23} - \rho_{12}\rho_{13}}{\sqrt{1-\rho_{12}^2}}. \tag{4.5}$$

Note that equation (4.5) does not apply to any values of ρ_{12}, ρ_{13} and ρ_{23}. We should choose appropriate values for ρ_{12}, ρ_{13} and ρ_{23} such that $|\rho'_{23}| \leq 1$. In general, if we have to systematically come up with n correlated samples from normal distributions with the correlation between sample i and sample j, where ρ_{ij} is the desired correlation, a Cholesky decomposition could be applied; see Hull [13], for example.

4.2.4 Valuation framework

Let $M^d(t,T)$ be the fair value at time t of a pure endowment of \$1 at maturity T when mortality is the only decrement. From the risk-neutral pricing principle, $M^d(t,T)$ is given by

$$M^d(t,T) = \mathbb{E}^Q\left[e^{-\int_t^T r_u\,\mathrm{d}u}e^{-\int_t^T \mu_u\,\mathrm{d}u}\middle|\mathcal{F}_t\right]. \tag{4.6}$$

Similarly, let $M^\tau(t,T)$ be the fair value at time t of a \$1 pure endowment at maturity T under a two-decrement model (both mortality and lapse rates are considered). From the risk-neutral pricing principle,

$$M^\tau(t,T) = \mathbb{E}^Q\left[e^{-\int_t^T r_u\,\mathrm{d}u}e^{-\int_t^T \mu_u\,\mathrm{d}u}e^{-\int_t^T l_u\,\mathrm{d}u}\middle|\mathcal{F}_t\right]. \tag{4.7}$$

Define $a_x(T)$ as the annuity rate, which is the risk-neutral value evaluated at time T, of a life annuity paying \$1 to an insured annually conditional on his/her survival at the moment of payments, and given that the insured is alive at the time of valuation. Note that $a_x(T)$ is a sequence of pure endowment contracts of \$1 paying at the beginning of each year so that

$$a_x(T) = \sum_{n=0}^{\infty}\mathbb{E}^Q\left[e^{-\int_T^{T+n} r_u\,\mathrm{d}u}e^{-\int_T^{T+n}\mu_u\,\mathrm{d}u}\middle|\mathcal{F}_T\right] = \sum_{n=0}^{\infty}M^d(T,T+n). \tag{4.8}$$

Let us now focus on the guaranteed annuity option (GAO), which is a contract that gives the policyholder the right to convert the survival benefit into an annuity at a pre-specified guaranteed conversion rate g (quoted as an annuity/cash value ratio). For example, a survival benefit with a cash value of \$1000 can be converted into an annuity of \$1000g per annum. If g is higher than the prevailing market rate which is determined by $a_x(T)$, the value of the GAO contract is positive; this is because the policyholder will exercise the contract to receive the annuity instead of the cash. On the other hand if g is lower than the prevailing market rate, then the the GAO contract is valueless; in this case, the policyholder will opt to receive the cash and use it to buy an annuity contract at a prevailing conversion rate in the market.

Thus, the GAO's payoff function, per dollar cash amount, time T is $C_T = g(a_x(T) - K)^+$, where $K = 1/g$. The loss L is the payoff 'discounted' by mortality and lapse factors, i.e.,

$$L = ge^{-\int_0^T \mu_u\,\mathrm{d}u}e^{-\int_0^T l_u\,\mathrm{d}u}(a_x(T) - K)^+. \tag{4.9}$$

Consequently, the fair value of GAO at time 0, by risk-neutral pricing, is

$$P_{GAO} = g\mathbb{E}^Q\left[e^{-\int_0^T r_u\,\mathrm{d}u}e^{-\int_0^T \mu_u\,\mathrm{d}u}e^{-\int_0^T l_u\,\mathrm{d}u}(a_x(T) - K)^+\middle|\mathcal{F}_0\right]. \tag{4.10}$$

4.3 Derivation of GAO prices

4.3.1 The forward measure

The change of measure technique is employed to facilitate our pricing calculation. The bond price $B(t,T)$ is chosen as a numéraire associated with the forward measure $\widetilde{Q}$, which is equivalent to the risk-neutral measure Q on $\mathcal{F}_T$. The corresponding Radon-Nikodým derivative is given by

$$\left.\frac{\mathrm{d}\widetilde{Q}}{\mathrm{d}Q}\right|_{\mathcal{F}_T} = \Lambda_T^1 := \frac{e^{-\int_0^T r_u \,\mathrm{d}u} B(T,T)}{B(0,T)}.$$

Under measure Q, Λ_T^1 is a martingale. So, for $t \le T$,

$$\Lambda_t^1 = \mathbb{E}^Q[\Lambda_T^1|\mathcal{F}_t] = \frac{e^{-\int_0^t r_u \,\mathrm{d}u} B(t,T)}{B(0,T)}.$$

By the Bayes' rule for conditional expectation, for any $\mathcal{F}_t$-integrable random variable H,

$$\mathbb{E}^{\widetilde{Q}}[H|\mathcal{F}_t] = \frac{\mathbb{E}^Q[\Lambda_T^1 H|\mathcal{F}_t]}{\mathbb{E}^Q[\Lambda_T^1|\mathcal{F}_t]}.$$

This implies

$$\mathbb{E}^{\widetilde{Q}}[H|\mathcal{F}_t] = \frac{\mathbb{E}^Q\left[e^{-\int_t^T r_u \,\mathrm{d}u} H\middle|\mathcal{F}_t\right]}{B(t,T)}.$$

Hence,

$$\mathbb{E}^Q\left[e^{-\int_t^T r_u \,\mathrm{d}u} H\middle|\mathcal{F}_t\right] = B(t,T)\mathbb{E}^{\widetilde{Q}}[H|\mathcal{F}_t].$$

Therefore, equation (4.6) can be expressed as

$$M^d(t,T) = B(t,T)\mathbb{E}^{\widetilde{Q}}\left[e^{-\int_t^T \mu_u \,\mathrm{d}u}\middle|\mathcal{F}_t\right], \tag{4.11}$$

whilst 4.7 can be represented as

$$M^\tau(t,T) = B(t,T)\mathbb{E}^{\widetilde{Q}}\left[e^{-\int_t^T \mu_u \,\mathrm{d}u} e^{-\int_t^T l_u \,\mathrm{d}u}\middle|\mathcal{F}_t\right]. \tag{4.12}$$

Note that the conditional expectations in equations (4.11) and (4.12) are under $\widetilde{Q}$. Once the $\widetilde{Q}$ dynamics of μ_t and l_t are available, explicit solutions for such conditional expectations follow. With the aid of the generalised result in Mamon [21], we have

$$\mathrm{d}\widetilde{W}_t^1 = \mathrm{d}W_t^1 + A(t,T)\sigma\,\mathrm{d}t, \quad \mathrm{d}\widetilde{W}_t^2 = \mathrm{d}W_t^2 \quad \text{and} \quad \mathrm{d}\widetilde{W}_t^3 = \mathrm{d}W_t^3,$$

where $\{\widetilde{W}_t^1\}$, $\{\widetilde{W}_t^2\}$ and $\{\widetilde{W}_t^3\}$ are standard BMs under $\widetilde{Q}$. Therefore, the respective $\widetilde{Q}$ dynamics of r_t, μ_t and l_t are

$$\mathrm{d}r_t = [ab - \sigma^2 A(t,T) - ar_t]\,\mathrm{d}t + \sigma\,\mathrm{d}\widetilde{X}_t,$$

$$\mathrm{d}\mu_t = [-\rho_{12}\sigma\xi A(t,T) + c\mu_t]\,\mathrm{d}t + \xi\,\mathrm{d}\widetilde{Y}_t,$$

and

$$\mathrm{d}l_t = [hm - \rho_{13}\sigma\zeta A(t,T) - hl_t]\,\mathrm{d}t + \zeta\,\mathrm{d}\widetilde{Z}_t,$$

where $\mathrm{d}\widetilde{X}_t = \mathrm{d}\widetilde{W}_t^1$, $\mathrm{d}\widetilde{Y}_t = \rho_{12}\,\mathrm{d}\widetilde{W}_t^1 + \sqrt{1-\rho_{12}^2}\,\mathrm{d}\widetilde{W}_t^2$ and $\mathrm{d}\widetilde{Z}_t = \rho_{13}\,\mathrm{d}\widetilde{W}_t^1 + \rho'_{23}\,\mathrm{d}\widetilde{W}_t^2 + \sqrt{1-\rho_{13}^2-\rho_{23}'^2}\,\mathrm{d}\widetilde{W}_t^3$.

Following the results given in Liu et al. [18], we have

$$S(t,T) = \mathbb{E}^{\widetilde{Q}}\left[e^{-\int_t^T \mu_u\,\mathrm{d}u}\middle|\mathcal{F}_t\right] = e^{-\mu_t\widetilde{G}(t,T)+\widetilde{H}(t,T)}. \tag{4.13}$$

where

$$\widetilde{G}(t,T) = \frac{e^{c(T-t)}-1}{c}$$

and

$$\widetilde{H}(t,T) = \left(\frac{\rho_{12}\sigma\xi}{ac} - \frac{\xi^2}{2c^2}\right)[\widetilde{G}(t,T) - (T-t)] + \frac{\rho_{12}\sigma\xi}{ac}[A(t,T) - \phi(t,T)] + \frac{\xi^2}{4c}\widetilde{G}(t,T)^2$$

with

$$\phi(t,T) = \frac{1-e^{-(a-c)(T-t)}}{a-c}.$$

Using equations (5.6), (4.11) and (4.13), we have

$$M^d(t,T) = e^{-(A(t,T)r_t+\widetilde{G}(t,T)\mu_t)+D(t,T)+\widetilde{H}(t,T)} = \beta^d(t,T)e^{-V^d(t,T)}, \tag{4.14}$$

where

$$\beta^d(t,T) = e^{D(t,T)+\widetilde{H}(t,T)}$$

and

$$V^d(t,T) = A(t,T)r_t + \widetilde{G}(t,T)\mu_t.$$

With equations (4.8) and (4.14) combined together, we get

$$a_x(T) = \sum_{n=0}^{\infty} M^d(T,T+n) = \sum_{n=0}^{\infty}\beta^d(T,T+n)e^{-V^d(T,T+n)}. \tag{4.15}$$

Thus, upon substitution of (4.15) into (4.10),

$$P_{GAO} = g\mathbb{E}^{Q}\left[e^{-\int_0^T r_u\,\mathrm{d}u}e^{-\int_0^T \mu_u\,\mathrm{d}u}e^{-\int_0^T l_u\,\mathrm{d}u}\left(\sum_{n=0}^{\infty}\beta^d(T,T+n)e^{-V^d(T,T+n)}-K\right)^{+}\middle|\mathcal{F}_0\right]. \tag{4.16}$$

4.3.2 The survival measure

In an effort to obtain an explicit solution to equation (4.12), we construct a new measure utilising the survival function $S(t,T)$. We define a measure $\bar{Q}$ equivalent to the forward measure $\widetilde{Q}$ via the Radon-Nikodým derivative

$$\left.\frac{\mathrm{d}\bar{Q}}{\mathrm{d}\widetilde{Q}}\right|_{\mathcal{F}_T} = \Lambda_T^2 := \frac{e^{-\int_0^T \mu_u\,\mathrm{d}u}S(T,T)}{S(0,T)}.$$

Since Λ_t^2 is a martingale, then for $t \le T$ we have

$$\Lambda_t^2 = \mathbb{E}^{\widetilde{Q}}[\Lambda_T^2|\mathcal{F}_t] = \frac{e^{-\int_0^t \mu_u\,\mathrm{d}u}S(t,T)}{S(0,T)}.$$

Thus,

$$\mathbb{E}^{\bar{Q}}\left[e^{-\int_t^T \mu_u\,\mathrm{d}u}e^{-\int_t^T l_u\,\mathrm{d}u}\middle|\mathcal{F}_t\right] = S(t,T)\mathbb{E}^{\bar{Q}}\left[e^{-\int_t^T l_u\,\mathrm{d}u}\middle|\mathcal{F}_t\right]. \tag{4.17}$$

Linking equations (4.12) and (4.17), we have

$$M^{\tau}(t,T) = \mathbb{E}^{Q}\left[e^{-\int_t^T r_u\,\mathrm{d}u}e^{-\int_t^T \mu_u\,\mathrm{d}u}e^{-\int_t^T l_u\,\mathrm{d}u}\middle|\mathcal{F}_t\right] = B(t,T)S(t,T)\mathbb{E}^{\bar{Q}}\left[e^{-\int_t^T l_u\,\mathrm{d}u}\middle|\mathcal{F}_t\right]. \tag{4.18}$$

To further obtain a closed-form solution to (4.18), the dynamics of l_t under $\bar{Q}$ are needed. It may be verified that

$$\mathrm{d}l_t = (hm - \rho_{13}\sigma\zeta A(t,T) - \rho_{23}\xi\zeta\widetilde{G}(t,T) - hl_t)\,\mathrm{d}t + \zeta\,\mathrm{d}\overline{Z}_t,$$

where $\mathrm{d}\overline{Z}_t = \rho_{13}\,\mathrm{d}\overline{W}_t^1 + \rho'_{23}\,\mathrm{d}\overline{W}_t^2 + \sqrt{1-\rho_{13}^2-\rho_{23}'^2}\,\mathrm{d}\overline{W}_t^3$; $\overline{W}_t^1, \overline{W}_t^2$ and $\overline{W}_t^3$ are standard BMs under $\overline{Q}$. Write

$$\overline{a}(t) := hm - \rho_{13}\sigma\zeta A(t,T) - \rho_{23}\xi\zeta\widetilde{G}(t,T), \quad \overline{b}(t) := \int_0^t h\,\mathrm{d}u = ht$$

and

$$\overline{\gamma}(t) := \int_t^T e^{-\overline{b}(u)}\,\mathrm{d}u = \frac{e^{-ht}-e^{-hT}}{h} = \frac{e^{-ht}}{h}(1-e^{-h(T-t)}).$$

Invoking the result in Elliott and Kopp [9] for Vasiček dynamics with time-varying coefficients, we have

$$\mathbb{E}^{\overline{Q}}[e^{-\int_t^T l_u \,\mathrm{d}u}|\mathcal{F}_t] = e^{-l_t\overline{I}(t,T)+\overline{J}(t,T)} \tag{4.19}$$

where

$$\overline{I}(t,T) = e^{\bar{b}(t)}\int_t^T e^{-\bar{b}(u)}\,\mathrm{d}u = e^{\bar{b}(t)}\overline{\gamma}(t) = \frac{1-e^{-h(T-t)}}{h},$$

and

$$\begin{aligned}\overline{I}(t,T) &= -\int_t^T\left(e^{\bar{b}(u)}\overline{a}(u)\overline{\gamma}(u) - \frac{1}{2}e^{2\bar{b}(u)}\xi^2\overline{\gamma}^2(u)\right)\mathrm{d}u \\ &= \left(\frac{\rho_{23}\xi\zeta}{ch} - \frac{\rho_{13}\sigma\zeta}{ah} - \frac{\zeta^2}{2h^2} + m\right)[\overline{I}(t,T)-(T-t)] + \frac{\rho_{13}\sigma\zeta}{ah}[A(t,T) - \\ &\quad \vartheta(t,T)] + \frac{\rho_{23}\xi\zeta}{ch}[\widetilde{G}(t,T)-\psi(t,T)] - \frac{\zeta^2}{4h}\overline{I}(t,T)^2\end{aligned}$$

with

$$\psi(t,T) = \frac{1-e^{-(h-c)(T-t)}}{h-c} \quad \text{and} \quad \vartheta(t,T) = \frac{1-e^{-(a+h)(T-t)}}{a+h}.$$

From equations (5.6), (4.13), (4.18) and (4.19), we have the analytic solution

$$M^\tau(t,T) = e^{-(A(t,T)r_t+\widetilde{G}(t,T)\mu_t+\overline{I}(t,T)l_t)+D(t,T)+\widetilde{H}(t,T)+\overline{J}(t,T)} = \beta^\tau(t,T)e^{-V^\tau(t,T)},$$

where

$$\beta^\tau(t,T) = e^{D(t,T)+\widetilde{H}(t,T)+\overline{J}(t,T)}$$

and

$$V^\tau(t,T) = A(t,T)r_t + \widetilde{G}(t,T)\mu_t + \overline{I}(t,T)l_t.$$

4.3.3 The endowment-risk-adjusted measure

The final objective of this section is to determine efficiently the P_{GAO} value. To this end, a new measure $\widehat{Q}$, called the endowment-risk-adjusted measure, is introduced with $M^\tau(t,T)$ as the associated numéraire. The measure $\widehat{Q}$ is equivalent to Q defined by

$$\left.\frac{\mathrm{d}\widehat{Q}}{\mathrm{d}Q}\right|_{\mathcal{F}_T} = \Lambda_T^3 := \frac{e^{-\int_0^T r_u\,\mathrm{d}u}e^{-\int_0^T \mu_u\,\mathrm{d}u}e^{-\int_0^T l_u\,\mathrm{d}u}M^\tau(T,T)}{M^\tau(0,T)}.$$

Since Λ_t^3 is a martingale under Q, we have

$$\Lambda_t^3 = \mathbb{E}^Q[\Lambda_T^3|\mathcal{F}_t] = \frac{e^{-\int_0^t r_u\,\mathrm{d}u}e^{-\int_0^t \mu_u\,\mathrm{d}u}e^{-\int_0^t l_u\,\mathrm{d}u}M^\tau(t,T)}{M^\tau(0,T)}$$

for any $t \leq T$. Then, equation (4.10) can be rewritten as

$$\begin{aligned} P_{GAO} &= gM^{\tau}(0,T)\mathbb{E}^{\widehat{Q}}[(a_x(T)-K)^+|\mathcal{F}_0] \\ &= gM^{\tau}(0,T)\mathbb{E}^{\widehat{Q}}\left[\left(\sum_{n=0}^{\infty}\beta^d(T,T+n)e^{-V^d(T,T+n)}-K\right)^+\middle|\mathcal{F}_0\right]. \end{aligned} \tag{4.20}$$

To evaluate equation (4.20), we must have the dynamics of r_t and μ_t under $\widehat{Q}$. To have them, we first consider the dynamics of

$$\Lambda_t^3 := \frac{V_t^1 V_t^2 V_t^3}{M^{\tau}(0,T)},$$

where

$$\begin{aligned} V_t^1 &= e^{-\int_0^t r_u\,\mathrm{d}u}e^{-A(t,T)r_t+D(t,T)}, \\ V_t^2 &= e^{-\int_0^t \mu_u\,\mathrm{d}u}e^{-\widetilde{G}(t,T)\mu_t+\widetilde{H}(t,T)} \end{aligned}$$

and

$$V_t^3 = e^{-\int_0^t l_u\,\mathrm{d}u}e^{-\overline{I}(t,T)l_t+\overline{J}(t,T)}.$$

Our calculations show that

$$\mathrm{d}V_t^1 = -\sigma A(t,T)V_t^1\,\mathrm{d}X_t^1 = -\sigma A(t,T)V_t^1\,\mathrm{d}W_t^1,$$

$$\begin{aligned} \mathrm{d}V_t^2 &= -\xi\widetilde{G}(t,T)V_t^2\,\mathrm{d}\widetilde{Y}_t \\ &= -\xi\widetilde{G}(t,T)V_t^2\left(\rho_{12}\,\mathrm{d}\widetilde{W}_t^1+\sqrt{1-\rho_{12}^2}\,\mathrm{d}\widetilde{W}_t^2\right) \end{aligned}$$

and

$$\begin{aligned} \mathrm{d}V_t^3 &= -\zeta\overline{I}(t,T)V_t^3\,\mathrm{d}\overline{Z}_t \\ &= -\zeta\overline{I}(t,T)V_t^3\left(\rho_{13}\,\mathrm{d}\overline{W}_t^1+\rho'_{23}\,\mathrm{d}\overline{W}_t^2+\sqrt{1-\rho_{13}-\rho'_{23}}\,\mathrm{d}\overline{W}_t^3\right). \end{aligned}$$

Hence,

$$\begin{aligned} \mathrm{d}V_t^1V_t^2 &= V_t^2\,\mathrm{d}V_t^1+V_t^1\,\mathrm{d}V_t^2+\mathrm{d}V_t^1\,\mathrm{d}V_t^2 \\ &= -\sigma A(t,T)V_t^1V_t^2\,\mathrm{d}W_t^1-\xi\widetilde{G}(t,T)V_t^1V_t^2\left[\rho_{12}\,\mathrm{d}\widetilde{W}_t^1+\sqrt{1-\rho_{12}^2}\,\mathrm{d}\widetilde{W}_t^2\right] \\ &\quad+\rho_{12}\sigma\xi A(t,T)\widetilde{G}(t,T)V_t^2V_t^1\,\mathrm{d}t \\ &= -V_t^1V_t^2\left[\left(\sigma A(t,T)+\rho_{12}\xi\widetilde{G}(t,T)\right)\mathrm{d}W_t^1+\xi\widetilde{G}(t,T)\sqrt{1-\rho_{12}^2}\,\mathrm{d}W_t^2\right]. \end{aligned}$$

Furthermore,

$$\begin{aligned}
\mathrm{d}V_t^1V_t^2V_t^3 &= V_t^3\,\mathrm{d}V_t^1V_t^2 + V_t^1V_t^2\,\mathrm{d}V_t^3 + \mathrm{d}V_t^1V_t^2\,\mathrm{d}V_t^3\\
&= -V_t^1V_t^2V_t^3\left[\left(\sigma A(t,T)+\rho_{12}\xi\widetilde{G}(t,T)\right)\mathrm{d}W_t^1 + \xi\widetilde{G}(t,T)\sqrt{1-\rho_{12}^2}\,\mathrm{d}W_t^2\right]\\
&\quad - \zeta\bar{I}(t,T)V_t^1V_t^2V_t^3\left[\rho_{13}\,\mathrm{d}\overline{W}_t^1 + \rho'_{23}\,\mathrm{d}\overline{W}_t^2 + \sqrt{1-\rho_{13}-\rho'_{23}}\,\mathrm{d}\overline{W}_t^3\right]\\
&\quad + V_t^1V_t^2V_t^3\left[\rho_{13}\zeta\bar{I}(t,T)\left(\sigma A(t,T)+\rho_{12}\xi\widetilde{G}(t,T)\right) + \rho'_{23}\xi\zeta\bar{I}(t,T)\widetilde{G}(t,T)\sqrt{1-\rho_{12}^2}\right]\mathrm{d}t\\
&= -V_t^1V_t^2V_t^3\Big[\left(\sigma A(t,T)+\rho_{12}\xi\widetilde{G}(t,T)+\rho_{13}\zeta\bar{I}(t,T)\right)\mathrm{d}W_t^1\\
&\quad + \left(\xi\widetilde{G}(t,T)\sqrt{1-\rho_{12}^2}+\rho'_{23}\zeta\bar{I}(t,T)\right)\mathrm{d}W_t^2 + \zeta\bar{I}(t,T)\sqrt{1-\rho_{13}-\rho'_{23}}\,\mathrm{d}W_t^3\Big].
\end{aligned}$$

Thus, the dynamics of Λ_t^3 under Q is given by

$$\begin{aligned}
\mathrm{d}\Lambda_t^3 &= -\Lambda_t^3\Big[\left(\sigma A(t,T)+\rho_{12}\xi\widetilde{G}(t,T)+\rho_{13}\zeta\bar{I}(t,T)\right)\mathrm{d}W_t^1\\
&\quad + \left(\xi\widetilde{G}(t,T)\sqrt{1-\rho_{12}^2}+\rho'_{23}\zeta\bar{I}(t,T)\right)\mathrm{d}W_t^2 + \zeta\bar{I}(t,T)\sqrt{1-\rho_{13}-\rho'_{23}}\,\mathrm{d}W_t^3\Big].
\end{aligned}$$

By the Girsanov's theorem,

$$\mathrm{d}\widehat{W}_t^1 = \mathrm{d}W_t^1 + \left(\sigma A(t,T)+\rho_{12}\xi\widetilde{G}(t,T)+\rho_{13}\zeta\bar{I}(t,T)\right)\mathrm{d}t,$$

$$\mathrm{d}\widehat{W}_t^2 = \mathrm{d}W_t^2 + \left(\xi\widetilde{G}(t,T)\sqrt{1-\rho_{12}^2}+\rho'_{23}\zeta\bar{I}(t,T)\right)\mathrm{d}t$$

and

$$\mathrm{d}\widehat{W}_t^3 = \mathrm{d}W_t^3 + \zeta\bar{I}(t,T)\sqrt{1-\rho_{13}-\rho'_{23}}\,\mathrm{d}t,$$

where $\widehat{W}_t^1$, $\widehat{W}_2^1$ and $\widehat{W}_t^3$ are $\widehat{Q}-$standard BMs.

So, the respective stochastic dynamics of r_t, μ_t and l_t are

$$\mathrm{d}r_t = (ab - \sigma^2A(t,T) - \rho_{12}\sigma\xi\widetilde{G}(t,T) - \rho_{13}\sigma\zeta\bar{I}(t,T) - ar_t)\,\mathrm{d}t + \sigma\,\mathrm{d}\widehat{X}_t, \tag{4.21}$$

$$\mathrm{d}\mu_t = (c\mu_t - \rho_{12}\sigma\xi A(t,T) - \xi^2\widetilde{G}(t,T) - \rho_{23}\xi\zeta\bar{I}(t,T))\,\mathrm{d}t + \xi\,\mathrm{d}\widehat{Y}_t \tag{4.22}$$

and

$$\mathrm{d}l_t = (hm - \rho_{13}\sigma\zeta A(t,T) - \zeta^2\bar{I}(t,T) - \rho_{23}\xi\zeta\widetilde{G}(t,T))\,\mathrm{d}t + \xi\,\mathrm{d}\widehat{Z}_t.$$

From equations (4.21) and (4.22), both r_t and μ_t follow the extended Vasiček model, and therefore by Elliott and Kopp [9], they are each normally distributed under $\widehat{Q}$. The pair (r_t, μ_t) is a bivariate normal random variable, under $\widehat{Q}$, with the following moments:

$$\begin{aligned}\mathbb{E}^{\widehat{Q}}[r_t] = e^{-at}r_0 + b\left(a - e^{-at}\right) - \frac{\sigma^2}{a}\left[\frac{1-e^{-at}}{a} - \frac{e^{-aT+at} - e^{-aT-at}}{2a}\right] \\ - \frac{\rho_{12}\sigma\xi}{c}\left[\frac{e^{cT-ct} - e^{cT-at}}{a-c} - \frac{1-e^{-at}}{a}\right] \\ - \frac{\rho_{13}\sigma\zeta}{h}\left[\frac{1-e^{-at}}{a} - \frac{e^{-hT+ht} - e^{-hT-at}}{a+h}\right],\end{aligned}$$

$$\mathbb{V}\mathrm{ar}^{\widehat{Q}}[r_t] = \frac{\sigma^2}{2a}\left[1 - e^{-2at}\right], \tag{4.23}$$

$$\begin{aligned}\mathbb{E}^{\widehat{Q}}[\mu_t] = e^{ct}\mu_0 - \frac{\rho_{12}\sigma\xi}{a}\left[\frac{e^{ct}-1}{c} - \frac{e^{-aT+at} - e^{-aT+ct}}{a-c}\right] \\ - \frac{\xi^2}{c}\left[\frac{e^{cT+ct} - e^{cT-ct}}{2c} - \frac{e^{ct}-1}{c}\right] - \frac{\rho_{23}\xi\zeta}{h}\left[\frac{e^{ct}-1}{c} - \frac{e^{-hT+ht} - e^{-hT+ct}}{h-c}\right],\end{aligned} \tag{4.24}$$

$$\mathbb{V}\mathrm{ar}^{\widehat{Q}}[\mu_t] = \frac{\xi^2}{2c}\left[e^{2ct} - 1\right] \tag{4.25}$$

and

$$\mathbb{C}\mathrm{ov}^{\widehat{Q}}[r_t, \mu_t] = \frac{\rho_{12}\sigma\xi}{a-c}\left[1 - e^{-(a-c)t}\right]. \tag{4.26}$$

4.4 Risk measurement of GAO

4.4.1 Description of risk measures

As stated by Artzner et al. [4], a risk measure ϕ is a mapping from a loss random variables to the real numbers, i.e., $\phi : \mathcal{L} \to \mathbb{R} \cup \{+\infty\}$, and satisfies the following properties:

Normalisation $\phi(0) = 0$;

Translation-invariance If $Z \in \mathcal{L}$ and $b \in \mathbb{R}$, then $\phi(Z + b) = \phi(Z) + b$;

Monotonicity If $Z_1, Z_2 \in \mathcal{L}$ and $P(Z_1 \leq Z_2) = 1$, then $\phi(Z_1) \leq \phi(Z_2)$.

Moreover, if a risk measure is coherent, then it satisfies:

Sub-additivity If $Z_1, Z_2 \in \mathcal{L}$, then $\phi(Z_1 + Z_2) \leq \phi(Z_1) + \phi(Z_2)$;

Positive homogeneity If $Z \in \mathcal{L}$ and $b > 0$, then $\phi(bZ) = b\phi(Z)$.

VaR has been used widely and it is the most popular risk measure. It is defined as the value which the loss random variable exceeds with a probability of at most $1 - \alpha$, where α is the confidence level. Given $Z \in \mathcal{L}$ and $0 < \alpha < 1$, the $100\alpha\%$ VaR is

$$\text{VaR}_\alpha(Z) = \inf\{z : P(Z \leq z) \geq \alpha\}.$$

A major drawback of VaR is that it ignores the profile of the potential loss beyond the confidence level. In addition, it is not a coherent risk measure. This limitation leads to the introduction of an alternative risk measure called conditional tail expectation (CTE), which is the expected value of the loss given that the loss is greater than $\text{VaR}_a(Z)$. Formally,

$$\text{CTE}_\alpha(Z) = \mathbb{E}[Z|Z > \text{VaR}_\alpha(Z)].$$

Both VaR and CTE only consider though the tail of the loss distribution and do not make full use of information in the entire loss distribution. So, to put risk-related matters in perspective, we also consider another kind of coherent measure ζ proposed by Wang [24]. More specifically, we are referring to the distortion risk measure defined as

$$\zeta_\chi(z) = \int_0^\infty \chi(S_Z(z))\,\mathrm{d}z, \tag{4.27}$$

where $S_Z(z)$ is the survival function of the loss random variable Z and $\chi(x)$ is the distortion function $\chi\colon [0,1] \to [0,1]$, which is a non-decreasing function with $\chi(0) = 0$ and $\chi(1) = 1$. The distortion function allows adjustment in the true probability measure to give more weights to higher risk events. The well-known distortion risk measures are the proportional hazard (PH), Wang, and lookback (LB) transforms. Wang [23] developed the PH transform, which can be applied to risk-adjusted premium calculations. The distortion function $\chi(x)$ for the PH transform is given by

$$\chi(x) = x^\gamma,$$

where $\gamma \in (0, 1]$ is the risk-aversion parameter; higher γ means less aversion towards risk. The distortion function $\chi(x)$ for the Wang transform (WT) described in Wang [25] is

$$\chi(x) = \Phi(\Phi^{-1}(x) + \Phi^{-1}(\iota)),$$

where Φ is the cumulative distribution function (CDF) of a standard normal random variable and $\iota \in [0, 1]$, whilst for the LB transform proposed in Hürlimann [14],

$$\chi(x) = x^{\eta}(1 - \eta \log(x)),$$

where $\eta \in (0, 1]$.

We also consider the spectral risk measure, also a coherent measure, which represents the weighted average of the quantiles of a loss function. The spectral risk measure has been discussed in Acerbi [1] and Adam et al. [2] and it can be used for capital requirement calculations. Individual's risk aversion is reflected by the weights of certain outcomes; and bad outcomes are typically assigned higher weights. In this chapter, the spectral risk measure φ is given by

$$\varphi_{\omega} = \int_0^1 \omega(\upsilon) q(\upsilon) \, \mathrm{d}\upsilon,$$

where $\omega(\upsilon)$ is a weighting function such that $\int_0^1 \omega(\upsilon) d\upsilon = 1$ and $q(\upsilon)$ is a quantile function of a loss random variable. The choice of weighting function is based on individual's risk tolerance. Two commonly-used weighting functions, the power and exponential functions $\omega_E(\upsilon)$ and $\omega_P(\upsilon)$ are highlighted in this chapter and defined by

$$\omega_E(\upsilon) = \frac{\kappa e^{-\kappa(1-\upsilon)}}{1 - e^{-\kappa}} \quad \text{and} \quad \omega_P(\upsilon) = \delta \nu^{\delta - 1}.$$

They correspond to the computations of the exponential and the power weighted quantile risk measures (EWQRM and PWQRM, respectively).

4.4.2 Moment-based density approximation

The usual way to estimate risk measures is through the MC method, which gives the empirical distribution of the loss random variable. Alternatively, an analytical approximation of the loss random variable could be used. We adopt the moment-based density approximation method introduced by Provost [22]. The underlying idea of this method is the fact that the exact density function with known first n moments can be approximated by the product of (i) a base density, whose tail behavior is congruent to that of distribution to be approximated, and (ii) a polynomial of degree q. The parameters of the base density can be determined by matching the moments of the loss random variable and the approximated density.

Combining equations (4.9) and (4.15), the loss random variable can be expressed as

$$L = ge^{-\int_0^T \mu_u \,\mathrm{d}u} e^{-\int_0^T l_u \,\mathrm{d}u} \left(\sum_{n=0}^{\infty} \beta^d(T, T+n) e^{-V^d(T,T+n)} - K \right)^+ .$$

Since L is truncated at 0, it is not straightforward to find an appropriate base function in estimating the exact distribution. Thus, we need to reflect this truncation by re-formulating L as L_p given by

$$L_p = ge^{-\int_0^T \mu_u \,\mathrm{d}u} e^{-\int_0^T l_u \,\mathrm{d}u} \left(\sum_{n=0}^{\infty} \beta^d(T, T+n) e^{-V^d(T,T+n)} - K \right).$$

Write

$$L := \begin{cases} 0 & \text{if } L_p \leq 0, \\ L_p & \text{if } L_p > 0. \end{cases}$$

The distribution of L_p can be estimated by the moment-based approximation method. Then the CDF of L can be determined through the CDF of L_p by

$$F_L(l) = \begin{cases} F_{L_P}(0) & \text{if } l \leq 0, \\ F_{L_P}(l) & \text{if } l > 0. \end{cases} \tag{4.28}$$

On the other hand, the probability density function (PDF) of L is given by

$$f_L(l) = \begin{cases} F_{L_P}(0) & \text{if } l \leq 0, \\ f_{L_P}(l) & \text{if } l > 0. \end{cases} \tag{4.29}$$

The choice of the base function depends on the loss distribution. Gao et al. [12] suggested the use of the Student's t and normal distributions as base functions in estimating the loss distribution. We observe that the loss random variable has an asymmetric distribution, and so we choose the gamma distribution as the base function. Since a gamma random variable is nonnegative, we make the transformation $Z := L_p - u$, where u is a relatively small value. Let the moments of the random variable Z be $\mu_Z(i)$ for $i = 0, 1, \ldots, q$. Since it is not possible to obtain the theoretical moments of Z, we can use the sample moments obtained from the MC method. Let the theoretical moments of the base function $\Psi(z)$ be $m_Z(i)$ for $i = 0, 1, \ldots, 2q$. The parameters α and θ of $\Psi(z)$ can be determined by setting $\mu_Z(i) = m_Z(i)$ for $i = 1, 2$. Hence, we have

$$\widehat{\alpha} = \frac{\mu_Z^2(1)}{\mu_Z(2) - \mu_Z^2(1)} \quad \text{and} \quad \widehat{\theta} = \frac{\mu_Z(2) - \mu_Z^2(1)}{\mu_Z(1)}.$$

The PDF of Z is approximated as

$$f_Z(z) = \Psi(z) \sum_{i=0}^{q} y_i z^i,$$

where y_i's, $i = 0, \ldots, n$, are polynomial coefficients and they are determined via

$$(k_0, k_1, \ldots, k_n)^\top = \mathbf{M}^{-1}(\mu_Z(0), \mu_Z(1), \ldots, \mu_Z(q))^\top,$$

where $\top$ is the transpose of a vector and $\mathbf{M}$ is a $(q+1) \times (q+1)$ symmetric matrix whose $(i+1)^{\text{th}}$ row is $(m_Z(i), m_Z(i+1), \ldots, m_Z(i+q))$.

Consequently, the approximated density of L_p is given by

$$f_{L_p}(l) = \frac{(l-u)^{\alpha-1}}{\Gamma(\alpha)\theta^\alpha} e^{-(l-u)/\theta} \sum_{i=0}^{q} k_i (l-u)^i. \tag{4.30}$$

4.5 Numerical illustration

4.5.1 GAO pricing

We calculate the GAO prices using both equations (4.16) and (4.20) via the MC simulation method. The approach using equation (4.16) is a brute-force implementation of the MC method under the risk-neutral measure; this approach is doable but time-consuming. In (4.20), the pure endowment $M^{\mathrm{r}}(t, T)$ is explicitly determined one r_0, μ_0 and l_0 are set. Thus, we only require the simulation of the pair (r_T, μ_T) and do not need to know the trajectory of the risk processes from time 0 and T. The pair (r_T, μ_T) is bivariate normal and can be generated through equations (4.23)-(4.26).

The simulations of r_t, μ_t and l_t between times 0 and T are needed in applying (4.16) to calculate the GAO prices. We subdivide the time interval $[0, T]$ into k subintervals of same length $\Delta t = T/k$, and let $t_i = i\Delta t$ for $i = 0, \ldots, k$. Based on the evolutions described in equations (4.1), (4.3) and (4.4), the respective sample paths of r_t, μ_t and l_t are generated by the discretisations

$$r_{t_i} = r_{t_{i-1}} + a(b - r_{t_{i-1}})\Delta t + \sigma \sqrt{\Delta t} \varepsilon^1_{t_i},$$

$$\mu_{t_i} = \mu_{t_{i-1}} + c\mu_{t_{i-1}}\Delta t + \xi\sqrt{\Delta t}\left(\rho_{12}\varepsilon^1_{t_i} + \sqrt{1-\rho^2_{12}}\varepsilon^2_{t_i}\right)$$

and

$$l_{t_i} = l_{t_{i-1}} + h(m - l_{t_{i-1}})\Delta t + \zeta\sqrt{\Delta t}\left(\rho_{13}\varepsilon^1_{t_i} + \rho'_{23}\varepsilon^2_{t_i} + \sqrt{1-\rho^2_{13}-\rho'^2_{23}}\varepsilon^3_{t_i}\right),$$

where $\{\varepsilon^1_{t_i}\}_{i=1,\ldots,m}$, $\{\varepsilon^2_{t_i}\}_{i=1,\ldots,m}$ and $\{\varepsilon^3_{t_i}\}_{i=1,\ldots,m}$ are three independent sequences of standard normal random variables.

The integral in (4.16), via the trapezoidal rule, has the approximate solution

$$\int_0^T r(u)\,\mathrm{d}u \approx \frac{\Delta t}{2}\left[r_0 + r_m + 2\sum_{k=1}^{m-1} r_k\right].$$

Consequently, numerical values for the product $e^{-\int_0^T r_u\,\mathrm{d}u}e^{-\int_0^T \mu_u\,\mathrm{d}u}e^{-\int_0^T l_u\,\mathrm{d}u}$ is obtained, and the generated results for r_T and μ_T are then used to evaluate $a_x(T)$.

Our MC implementation involves 100,000 sample paths in conjunction with model parameter values for equations (4.1), (4.3) and (4.4) being shown in Table 4.1; the results are reported in Table 4.2. A wide range of correlation values ρ_{12}, ρ_{13} and ρ_{23} are tested to see their influences on GAO prices. The the maximum age of an individual is assumed 100 and the GAO contract matures at age 65 (i.e., $T = 15$ for a person buying the GAO at age 50).

In Table 4.2, the prices calculated under the direct approach and the endowment-risk-adjusted measure method are displayed in the second and third columns, respectively. The numbers enclosed in the parentheses are standard errors (SEs). The SEs in the third column are lower than those in the second column. This tells us that the results based on endowment-risk-adjusted method is more accurate than those based on the direct method. The total computing time using equation (4.20) is only 0.07% of the computation time using equation (4.16). Thus, the endowment-risk-adjusted method is way more efficient than the direct application of the MC method. It is worth noting that the GAO prices significantly change as correlations vary. Prices increase as the number of negative correlations decreases. On a component-wise basis of the correlation vector $(\rho_{12}, \rho_{13}, \rho_{23})$, GAO prices also tend to increase as the magnitude in absolute value of the correlation decreases.

We compare the GAO prices under stochastic lapse rates with prices under a constant lapse rate. We vary ρ_{12} and ρ_{13} and set $\rho_{23} = \rho_{12}\rho_{13}$. The results are shown in Table 4.3. Prices increase as ρ_{13} increases with ρ_{12} fixed. Price values vary from 12% less to 18% more than the prices with the constant lapse rate. It can be observed that the GAO prices assuming

Table 4.1: Parameter values

Contract specification			
$g = 11.1\%$	$T = 15$	$n = 35$	
Interest rate model			
$a = 0.15$	$b = 0.045$	$\sigma = 0.03$	$r_0 = 0.045$
Mortality model			
$c = 0.1$	$\xi = 0.0003$	$\mu_0 = -0.006$	
Lapse rate model			
$h = 0.12$	$m = 0.02$	$\zeta = 0.01$	$l_0 = 0.02$

constant lapse rate are lower or higher than those obtained under the stochastic lapse rate assumption, and the absolute price differences could be relatively substantial (as high as 25%).

In order to assess the impact of lapse-model parameters on the GAO price, we perform price-sensitivity analyses with respect to h, m, ξ and ρ_{13}. The results are displayed in Figure 4.1. The first plot in the upper panel demonstrates that m is negatively related to the GAO price. The parameter m is the lapse rate's mean-reverting level; so, such a result is consistent with the view that the GAO price decreases as lapse rate increases. The inverse relation between GAO price and lapse rate is analogous to the relation between bond price and the interest rate level. High lapse rate implies that there is more risk that the policy holder will terminate the contract. Therefore, the price of the pre-existing contract would have to decrease enough to compensate for the possibility of lapsation and must match the same return yielded by prevailing interest rates adjusted for the 'lapse risk premium'.

The parameter h produces GAO prices forming a similar pattern to those produced by m but its resulting curve is not as smooth as that resulting from m. The last two plots in the lower panel show that each ξ and ρ_{13} moves in the same direction of the GAO prices. As the lapse rate's volatility increases, the GAO price increases. We also examine the impact of the maturity length T on the GAO price. Figure 4.2 depicts the GAO prices with T changing from 1 to 20 years, demonstrating that as T gets larger, the lapse rate has more impact on GAO prices.

Table 4.2: GAO prices calculated based on equations (4.16) and (4.20)

$(\rho_{12},\ \rho_{13},\ \rho_{23})$	Using eq (4.16)	Using eq (4.20)
$(-0.9, -0.9, 0.81)$	0.06012 (0.00024)	0.05942 (0.00019)
$(-0.6, -0.6, 0.36)$	0.06682 (0.00030)	0.06608 (0.00021)
$(-0.3, -0.3, 0.09)$	0.07407 (0.00036)	0.07414 (0.00023)
$(0.0, 0.0, 0.0)$	0.08270 (0.00045)	0.08272 (0.00025)
$(0.3, 0.3, 0.3)$	0.09444 (0.00054)	0.09396 (0.00028)
$(0.6, 0.6, 0.6)$	0.10758 (0.00069)	0.10650 (0.00032)
$(0.9, 0.9, 0.9)$	0.11993 (0.00081)	0.11954 (0.00035)
$(-0.9, 0.81, -0.9)$	0.07866 (0.00043)	0.07868 (0.00023)
$(-0.6, 0.36, -0.6)$	0.07773 (0.00041)	0.07710 (0.00023)
$(-0.3, 0.09, -0.3)$	0.07941 (0.00042)	0.07880 (0.00024)
$(0.81, -0.9, -0.9)$	0.07947 (0.00038)	0.07865 (0.00026)
$(0.36, -0.6, -0.6)$	0.07875 (0.00038)	0.07772 (0.00025)
$(0.09, -0.3, -0.3)$	0.07957 (0.00040)	0.07972 (0.00025)
average computing time	213.82 secs	0.14 secs

4.5.2 Valuation of risk measures

We employ both the MC and moment-based density approximation methods to evaluate the risk measures of GAO. In the MC method, we generate N replicates of the loss random variable using equation (4.9). We then re-arrange these replicates to get an ascending ordered sequence $\{L_{(1)}, L_{(2)}, \ldots, L_{(N)}\}$. The VaR_α is estimated as

$$\widehat{\text{VaR}}_\alpha(L) = L_{(\lfloor N\alpha \rfloor + 1)}$$

and the estimate of CTE_α is

$$\widehat{\text{CTE}}_a(L) = \frac{\sum_{\lfloor N\alpha \rfloor + 1}^{N} L_{(j)}}{N(1-\alpha)},$$

where $\lfloor \cdot \rfloor$ denotes the greatest integer function and $j = 1, 2, \ldots, N$.

To estimate the distortion risk measures, we may use the empirical decumulative function, which is given by

$$S_L(L_{(j)}) = 1 - \frac{j}{N}.$$

Consequently, the distortion function can be obtained as $\chi(S_L(L_{(j)}))$. Hence, the distortion

Table 4.3: GAO prices under constant and stochastic lapse rates

ρ_{12}	Constant	ρ_{13}				
		-0.9	-0.5	0	0.5	0.9
-0.9	0.0679	0.0595	0.0635	0.0689	0.0747	0.0800
-0.8	0.0693	0.0603	0.0651	0.0704	0.0762	0.0817
-0.7	0.0712	0.0615	0.0660	0.0721	0.0777	0.0835
-0.6	0.0717	0.0631	0.0675	0.0731	0.0800	0.0859
-0.5	0.0738	0.0639	0.0685	0.0751	0.0819	0.0880
-0.4	0.0750	0.0652	0.0698	0.0768	0.0838	0.0899
-0.3	0.0765	0.0662	0.0712	0.0782	0.0854	0.0919
-0.2	0.0780	0.0677	0.0727	0.0800	0.0876	0.0944
-0.1	0.0808	0.0685	0.0739	0.0814	0.0892	0.0961
0.0	0.0810	0.0700	0.0754	0.0831	0.0911	0.0985
0.1	0.0836	0.0711	0.0769	0.0843	0.0933	0.1001
0.2	0.0842	0.0718	0.0780	0.0859	0.0948	0.1029
0.3	0.0863	0.0731	0.0799	0.0881	0.0975	0.1049
0.4	0.0883	0.0749	0.0812	0.0898	0.0993	0.1071
0.5	0.0896	0.0757	0.0823	0.0911	0.1013	0.1097
0.6	0.0913	0.0770	0.0839	0.0929	0.1035	0.1121
0.7	0.0930	0.0776	0.0854	0.0949	0.1057	0.1145
0.8	0.0948	0.0793	0.0865	0.0964	0.1074	0.1168
0.9	0.0964	0.0812	0.0884	0.0980	0.1094	0.1192

risk measures is then approximated, using (4.27), as

$$\zeta_\chi(z) = \int_0^\infty \chi(S_L(l))\,\mathrm{d}l \approx \sum_{j=0}^{N-1} \chi(S_L(L_{(j)}))(L_{(j+1)} - L_{(j)}), \tag{4.31}$$

where $L_{(0)} = 0$. Plugging the distortion functions given in Subsection 4.4.1 into equation (4.31), we get the estimate of the distortion risk measure. For the spectral risk measures, they can be approximated by the empirical quantiles of L.

For the moment-based density approximation method described in subsection 4.4.2, we first approximate the density function of L_p given in 6.7 by generating N replicates of L_p, which in turn gives the approximated CDF of L_p. Thus, the distribution of L may be determined by equations (4.28) and (4.29). The approximated distributions of L_p are displayed in Figure 4.3 and the approximated distributions of L are shown in Figure 4.4. The results

Figure 4.1: GAO prices under different parameter values

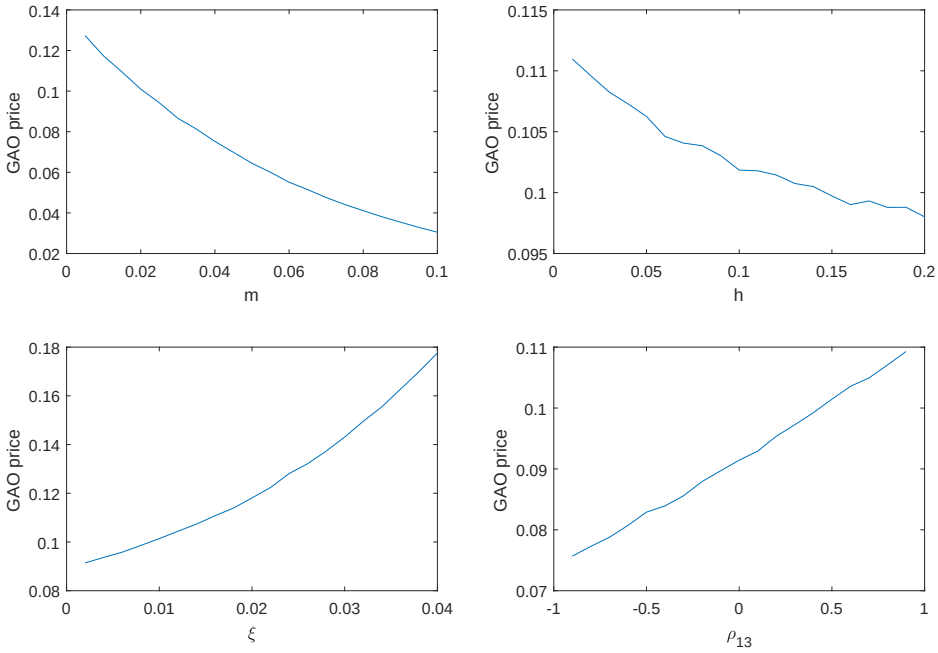

are calculated under three different sample sizes of 10,000, 100,000 and 1,000,000. The moment-based density approximation performs very well in approximating the distribution of L_p and L. The Kolmogorov-Smirnov (KS) test is used to validate the goodness of fit of our approximations. The KS p-values corresponding to the three different sample sizes are 0.2367, 0.6735 and 0.9120. This implies that the approximations have excellent fitting with the simulated distributions.

To strengthen our simulation analysis, we employ the bootstrap method; the L_p's are resampled 1,000 times in order to generate the approximated density functions. We then analyse the distribution of the p-values arising from the test of equality between the moment- and simulated-based densities of the loss random variable. The results are shown in Figure 4.5 illustrating that there are only a few cases of p-values falling below the significance level. These imply that the moment-based density approximation fits the distribution of L very well.

Table 4.4 shows the calculated values of risk measures under both the empirical CDF (ECDF) and moment-based CDF (MCDF) approximation methods with different number of replicates. Note that there is no significant difference between the numerical results of these two methods. It can also be observed that each difference is becoming smaller as the

Figure 4.2: GAO prices under varying maturities

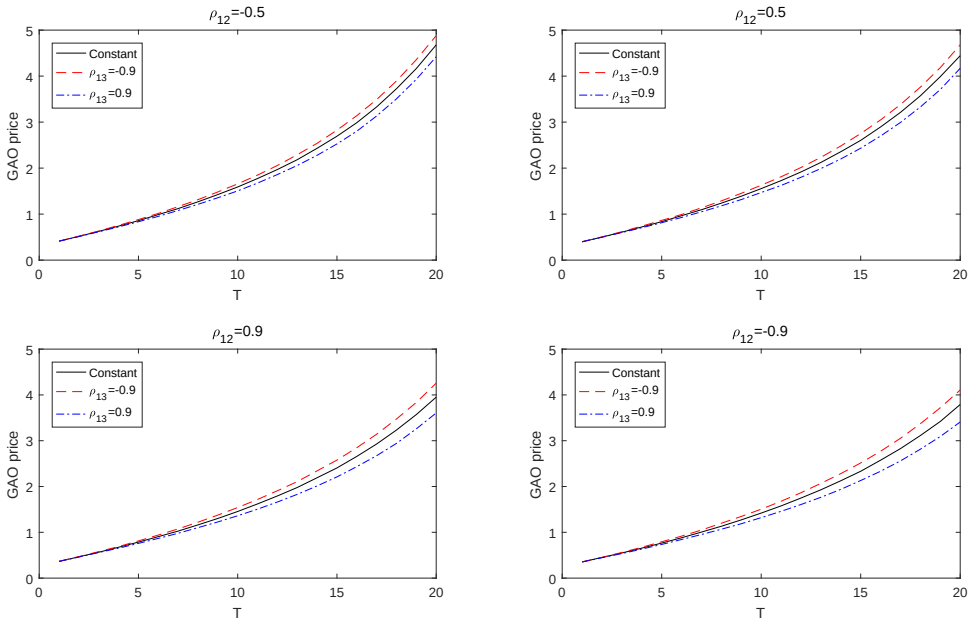

number of replicates increases. This implies that the accuracy can be improved by increasing the sample size.

We vary the values of the correlation coefficient ρ_{13} to ascertain the impact of the correlation between the interest and lapse rates upon the risk measures. The results are depicted in Figure 4.6. The estimated values of the risk measures have a slightly decreasing trend as ρ_{13} goes down. This is in agreement with the fact that as correlation between interest and lapse rates is getting more negative, the risk is reduced (hence, GAO risk measure is getting lower) as one factor serves as a hedge for the other. The impact of other parameters (i.e., m, h, ξ and ρ_{13}) on the GAO price is further explored; see Figure 4.7. The mean-reverting level m of the lapse rate has an inverse relation with the GAO price as pointed out in Subsection 4.5.1. The lapse rate's speed of mean reversion h also has a similar effect to that of m on the GAO price albeit a slightly less impact. The two plots in the lower panel of Figure 4.7 show that the GAO price goes in the same direction with the movements of ξ and ρ_{13}. Apparently, the higher the lapse rate's volatility, the riskier the profile of the GAO, and therefore, the higher its price.

Figure 4.3: Approximating the distribution of L_p

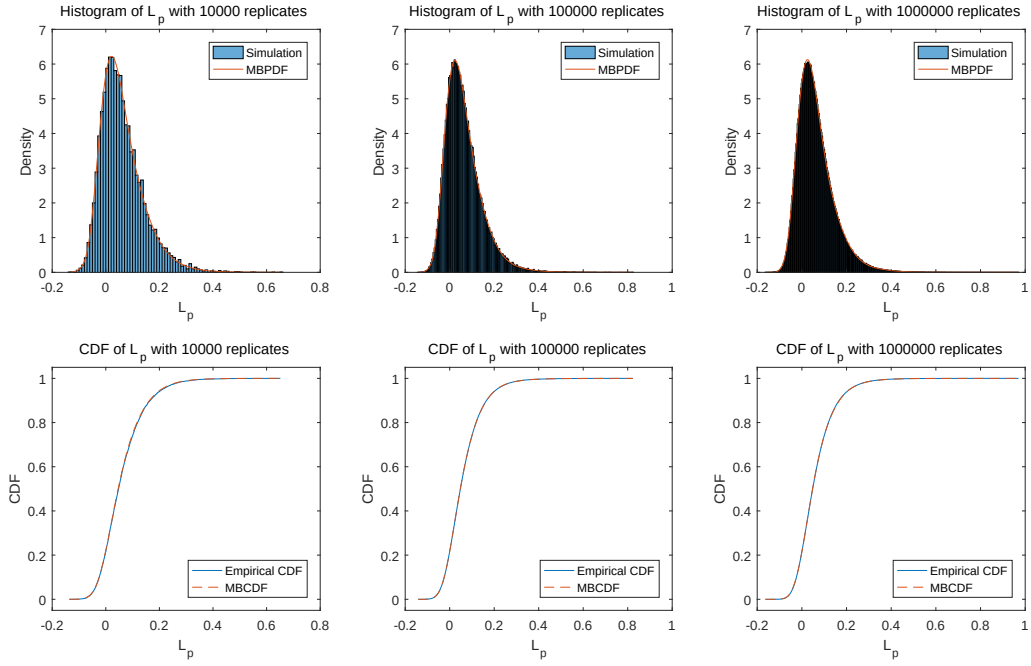

4.6 Conclusion

The main contribution of this chapter is the development of a closely integrated modelling framework for GAO pricing and capital requirement determination. The lapse risk was given the same level of importance as with mortality and interest rate risks. Each of our three risk factors has an affine structure specification and their correlations with one another is fully described. The modelling philosophy of this research is consistent with the goal of regulatory authority, such as Canada's OSFI, in ensuring that a synthesised modelling approach for pricing and risk management must be an integral part of planning, monitoring and controlling of the insurance company's risk-taking capability.

We employed iteratively the change of probability measure technique to evaluate GAO prices efficiently and accurately. The forward, survival, and risk-endowment measures were introduced facilitating the derivation of a simplified expression for the GAO price. This method can be extended to other option-embedded contingent claims in which correlated risk factors of any dimension are assumed to follow affine dynamics. We further evaluate seven different risk measures for GAO through the empirical CDF and moment-based density approximation methods. The appropriateness of the gamma distribution for the latter method was highlighted in the context and uniqueness of the GAO's risk profile

Figure 4.4: Approximating the distribution of L

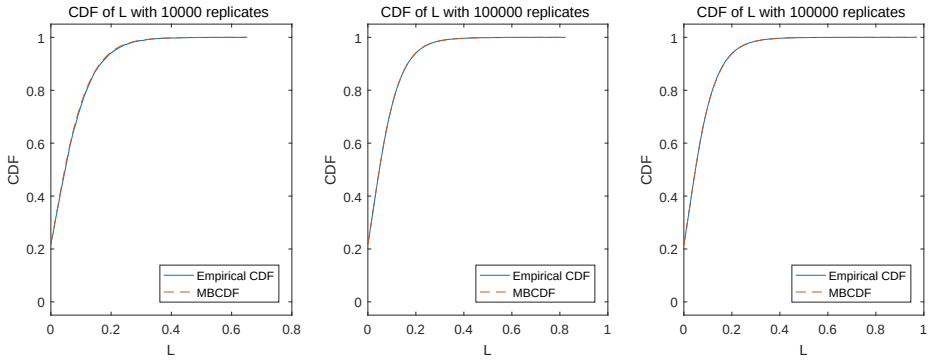

Figure 4.5: Distribution of the p-values in testing the fitness of moment-based approximated density with the simulated density

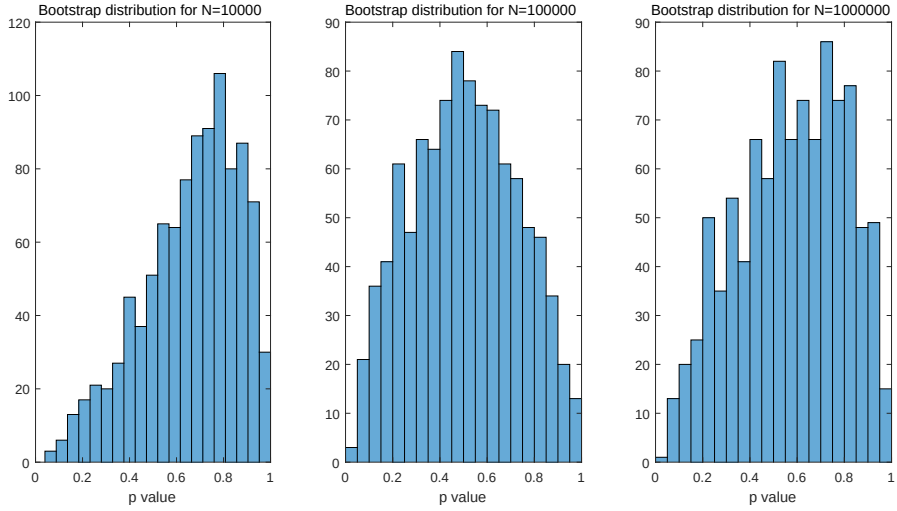

studied here. This is a step ahead relative to the current risk measurement literature that so far only features the normal and $t-$ distributions as base densities in the applications of the moment-based techniques.

Our numerical results confirmed the efficiency and accuracy of our proposed methods in the valuation of GAO and in its risk measurement. Compared to the general MC simulation method, our approach cuts down the average computing time by 99%, whilst the obtained estimates' standard errors are also less than those of MC simulation. The results provided strong support in using the moment-based approximation method to accurately approximate GAO's risk measures. The extent of the influence of various lapse risk model's parameters on GAO's prices and risk measures was investigated as well. We found that some small perturbations in the values of parameters could lead to substantial changes in

Table 4.4: Risk measures of gross loss for GAO under different sample sizes

Risk measures	$N = 10,000$		$N = 100,000$		$N = 1,000,000$	
	ECDF	MCDF	ECDF	MCDF	ECDF	MCDF
VaR ($\alpha = 0.90$)	0.1659	0.1631	0.1655	0.1658	0.1669	0.1681
VaR ($\alpha = 0.95$)	0.2115	0.2068	0.2114	0.2104	0.2139	0.2143
VaR ($\alpha = 0.99$)	0.3127	0.3042	0.3190	0.3211	0.3237	0.3271
CTE ($\alpha = 0.90$)	0.2300	0.2243	0.2328	0.2321	0.2353	0.2364
CTE ($\alpha = 0.95$)	0.2739	0.2664	0.2798	0.2787	0.2830	0.2842
CTE ($\alpha = 0.99$)	0.3757	0.3658	0.3964	0.3935	0.3970	0.4016
WT ($\gamma = 0.90$)	0.1872	0.1818	0.1920	0.1922	0.1935	0.1938
WT ($\gamma = 0.50$)	0.2340	0.2254	0.2426	0.2430	0.2444	0.2443
WT ($\gamma = 0.10$)	0.3356	0.3156	0.3574	0.3586	0.3614	0.3570
PH ($\iota = 0.10$)	0.0752	0.0736	0.0760	0.0760	0.0765	0.0767
PH ($\iota = 0.05$)	0.1361	0.1317	0.1401	0.1402	0.1413	0.1411
PH ($\iota = 0.01$)	0.4199	0.4076	0.4895	0.4908	0.5332	0.5345
LB ($\eta = 0.90$)	0.1549	0.1496	0.1575	0.1576	0.1587	0.1593
LB ($\eta = 0.50$)	0.2668	0.2500	0.2816	0.2826	0.2853	0.2822
LB ($\eta = 0.10$)	0.5885	0.5670	0.7190	0.7215	0.8148	0.8186
EWQRM ($\kappa = 1$)	0.0867	0.0852	0.0875	0.0875	0.0881	0.0884
EWQRM ($\kappa = 20$)	0.2469	0.2444	0.2517	0.2517	0.2542	0.2557
EWQRM ($\kappa = 100$)	0.3512	0.3564	0.3660	0.3664	0.3673	0.3714
PWRM ($\delta = 1$)	0.0672	0.0659	0.0678	0.0678	0.0683	0.0684
PWRM ($\delta = 20$)	0.2485	0.2460	0.2534	0.2534	0.2559	0.2574
PWRM ($\delta = 100$)	0.3515	0.3567	0.3664	0.3668	0.3676	0.3718

the prices and risk measures. This suggests that the stochastic behaviour of the lapse rate must be captured accurately and taken into account when designing, pricing and monitoring insurance products given its potentially huge effect as per our empirical work demonstrated.

Figure 4.6: Variation of risk measures as a function of ρ_{13} with a given ρ_{12} and $\rho_{23} = \rho_{12}\rho_{13}$

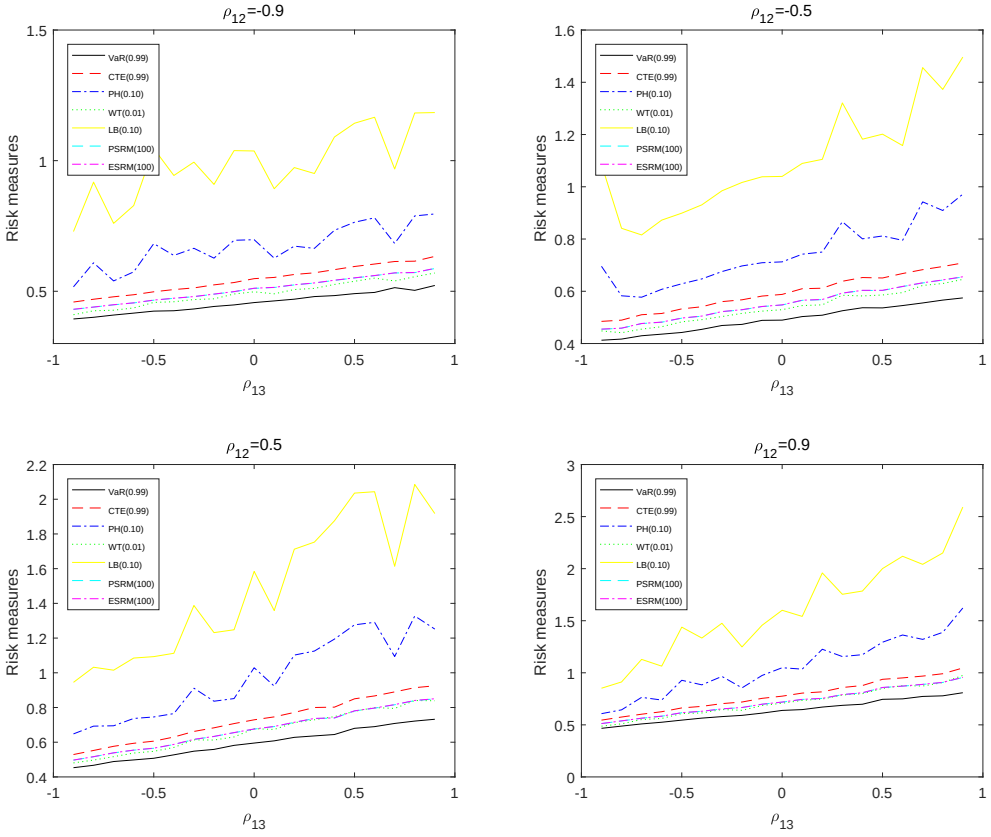

Figure 4.7: Sensitivity of risk measures to various parameters

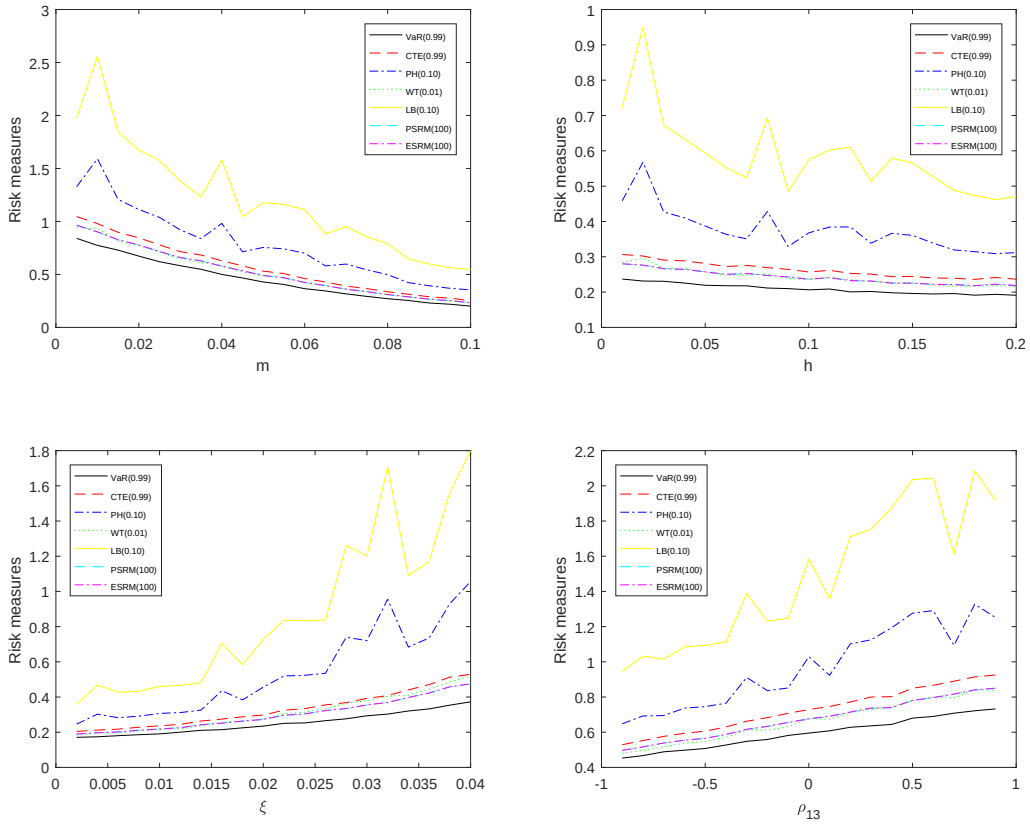

References

[1] C. Acerbi. Spectral measures of risk: A coherent representation of subjective risk aversion. *Journal of Banking & Finance*, 26(7):1505–1518, 2002.

[2] A. Adam, M. Houkari, and J. Laurent. Spectral risk measures and portfolio selection. *Journal of Banking & Finance*, 32(9):1870–1882, 2008.

[3] M. Albizzati and H. Geman. Interest rate risk management and valuation of the surrender option in life insurance policies. *Journal of Risk and Insurance*, 61(4):616–637, 1994.

[4] P. Artzner, F. Delbaen, J. Eber, and D. Heath. Coherent measures of risk. *Mathematical Finance*, 9(3):203–228, 1999.

[5] A.R. Bacinello. Fair valuation of a guaranteed life insurance participating contract embedding a surrender option. *Journal of Risk and Insurance*, 70(3):461–487, 2003.

[6] D. De Giovanni. Lapse rate modeling: A rational expectation approach. *Scandinavian Actuarial Journal*, 2010(1):56–67, 2010.

[7] D. Duffie and R. Kan. A yield-factor model of interest rates. *Mathematical Finance*, 6(4):379–406, 1996.

[8] M. Eling and M. Kochanski. Research on lapse in life insurance: What has been done and what needs to be done? *Journal of Risk Finance*, 14(4):392–413, 2013.

[9] R. Elliott and P.E. Kopp. *Mathematics of Financial Markets*. Springer Finance, New York, 2005.

[10] H. Gao, R. Mamon, and X. Liu. Pricing a guaranteed annuity option under correlated and regime-switching risk factors. *European Actuarial Journal*, 5(2):309–326, 2015.

[11] H. Gao, R. Mamon, X. Liu, and A. Tenyakov. Mortality modelling with regime-switching for the valuation of a guaranteed annuity option. *Insurance: Mathematics and Economics*, 63:108–120, 2015.

[12] H. Gao, R. Mamon, and X. Liu. Risk measurement of a guaranteed annuity option under a stochastic modelling framework. *Mathematics and Computers in Simulation*, 132:100–119, 2017.

[13] J. Hull. *Options, Futures, and Other Derivatives*. Pearson Education, Inc, New Jersey, 2015.

[14] W. Hürlimann. Inequalities for lookback option strategies and exchange risk modelling. In *Proceedings of the 1st Euro-Japanese Workshop on Stochastic Modelling for Finance, Insurance, Production and Reliability, Brussels*, 1998.

[15] C. Kim. Modeling surrender and lapse rates with economic variables. *North American Actuarial Journal*, 9(4):56–70, 2005.

[16] W. Kuo, C. Tsai, and W. Chen. An empirical study on the lapse rate: The cointegration approach. *Journal of Risk and Insurance*, 70(3):489–508, 2003.

[17] X. Liu, R. Mamon, and H. Gao. Mortality modelling with regime-switching for the valuation of a guaranteed annuity option. *Insurance: Mathematics and Economics*, 250:58–69, 2013.

[18] X. Liu, R. Mamon, and H. Gao. A generalized pricing framework addressing correlated mortality and interest risks: A change of probability measure approach. *Stochastics: An International Journal of Probability and Stochastic Processes*, 86(4):594–608, 2014.

[19] S. Loisel and X. Milhaud. From deterministic to stochastic surrender risk models: Impact of correlation crises on economic capital. *European Journal of Operational Research*, 214(2):348–357, 2011.

[20] R. Mamon. On the interface of probabilistic and pde methods in a multifactor term structure theory. *International Journal of Mathematical Education in Science and Technology*, 35(5):661–668, 2004.

[21] R. Mamon. Three ways to solve for bond prices in the Vasiček model. *Advances in Decision Sciences*, 8(1):1–14, 2004.

[22] S. Provost. Moment-based density approximants. *Mathematica Journal*, 9(4):727–756, 2005.

[23] S. Wang. Insurance pricing and increased limits ratemaking by proportional hazards transforms. *Insurance: Mathematics and Economics*, 17(1):43–54, 1995.

[24] S. Wang. A class of distortion operators for pricing financial and insurance risks. *Journal of Risk and Insurance*, pages 15–36, 2000.

[25] S. Wang. A universal framework for pricing financial and insurance risks. *ASTIN Bulletin: The Journal of the IAA*, 32(2):213–234, 2002.

[26] Y. Xue. Interactions between dynamic lapses and interest rates in stochastic modeling. *Product Matters!*, 77:8–12, 2010.

[27] J. Zians, A. Miller, and F. Ducuroir. Lapse rate models in life insurance and a practical method to foresee interest rates dependencies, 2016. URL https://www.reacfin.com/wp-content/uploads/2016/12/160799-Reacfin-White-Paper-Lapse-rate-models-in-life-insurance-and-a-practical-method-to-foresee-Interest-Rates-dependencies-v1.1.pdf.

Chapter 5

The valuation of a guaranteed minimum maturity benefit under a regime-switching framework

5.1 Introduction

Product development in the insurance markets all over the world has changed dramatically in the past few decades. Policyholders are getting more aware of investment opportunities outside the insurance sector; they want to benefit simultaneously from both equity investments and mortality protection. In order to meet this dual demand for insurance and investment, insurers issue various types of equity-linked insurance contracts. Examples include segregated fund contracts in Canada; unit-linked insurance in the UK; and variable annuities and equity-indexed annuities in the USA; see Hardy [16] for a comprehensive survey. Equity-linked insurance is a contract in which the policyholder's fund level depends on the performance of a stock market indicator. Insurers offer guarantees embedded in equity-linked contracts to provide downside protection. Such guarantees pass the risks from policy holders to insurers, making the contracts more attractive. There are several classifications of a guaranteed minimum benefit (GMB). A guaranteed minimum maturity benefit (GMMB) is a guarantee that provides the policyholder with a minimum benefit on maturity date. A guaranteed minimum death benefit (GMDB) is a guarantee that pays out a minimum benefit upon death during the term of the contract. A guaranteed minimum accumulation benefit (GMAB) allows the policy holder to renew the contract at a guaranteed level. A guaranteed minimum income benefit (GMIB) gives the policy holder the right to convert at maturity the account value to an annuity at a guaranteed rate.

The pricing of GMBs entails the modelling of risk factors such as interest rate, mortality rate and the underlying stock index. Various frameworks for GMB valuation have been put forward previously. In Fung et al. [14] and Da Fonseca and Ziveyi [5], independence between mortality rates and financial markets are assumed. Peng et al. [25], Dai et al. [6], Chen et al. [4] and Marshall et al. [22] ignored mortality affects whilst Fung et al. [14] set mortality rate as constant. Some authors endorsed the GBM as a suitable model for the underlying fund dynamics (e.g. Brennan and Schwartz [2], Milevsky and Salisbury [23], Feng and Vecer [13] , Bauer et al. [1] and Piscopo and Haberman [26]). A GMMB embedded in a segregated fund contract is the focus of this article. We construct a framework for pricing a GMMB under a combined regime-switching models for three risk factors whose parameters are driven by a hidden Markov model (HMM). The application of HMM to the pricing of certain GMBs were carried out before (e.g., Gao et al. [15] and Ignatieva et al. [17]). However, Gao et al. [15] assumed that only the volatilities are governed by an HMM; whilst Ignatieva et al. [17] supposed the force of interest is constant with different states. Those assumptions are relaxed in this chapter. The HMMs are also found applications in the valuation of other insurance products, such as longevity bonds and options e.g., Shen and Siu [27] and Fan et al. [12]). Interest and mortality rates are governed by an HMM in Shen and Siu [27] whilst in Fan et al. [12], interest rate and stock index are regime-switching.

For the valuation of GMMB, we utilise the change of measure technique and the Fourier transform method. Fourier transform was first introduced by Carr and Madan [3] for option pricing. It was then applied to value an option under a regime-switching set up in Liu et al. [19] and Fan et al. [12]. The method is also used for GMBs in Da Fonseca and Ziveyi [5] and Ignatieva et al. [17]. To estimate the model parameters under our framework, we adopt the recursive filtering technique following the method originally introduced by Elliott [8]. Filtering of signals in the financial markets is utilised to estimate parameters in an interest rate model (e.g., Erlwein and Mamon [11]) and commodity futures price model (e.g., Date et al. [7]).

The remaining parts of this chapter are organised as follows. Section 5.2 presents the development of a regime-switching framework that covers the interconnectedness of models for interest rate, mortality rate and stock index. A detailed derivation of the semi-closed form pricing formula for GMMB and the corresponding numerical calculation are discussed in Section 5.3. Changing probability measures in conjunction with the Fourier transform is

applied for the valuation of GMMB. In Section 5.4, we show the derivation of the recursive formulae for the pertinent functions of a Markov chain that will be used in turn for the estimation of model parameters. We feature a numerical study, implementing the parameter estimation and GMMB price calculation. Finally, some concluding remarks are given in Section 5.5.

5.2 Model description

Suppose $(\Omega, \mathcal{F}, \{\mathcal{F}_t\}, \mathcal{P})$ is a filtered probability space that supports all observed underlying stochastic processes in our modelling set up. Here, $\mathcal{P}$ is the objective probability measure and $\{\mathcal{F}_t\}$ is the joint filtration generated by all processes. The short rate r_t, force of mortality μ_t and stock index S_t are stochastic processes whose parameters are driven by an HMM.

If r_t follows the Vasicek model then it has the dynamics

$$\mathrm{d}r_t = a(b_t - r_t)\,\mathrm{d}t + \sigma_t\,\mathrm{d}W_t^1, \tag{5.1}$$

where a is a positive constant and W_t^1 is a standard Brownian motion under $\mathcal{P}$. When pricing, parameters must be under the risk-neutral measure $\mathcal{Q}$, which can be recovered by calibrating the model with current market prices. The link between $\mathcal{P}$ and $\mathcal{Q}$ is via a market price of risk. However, insurance products are long-term contracts; using only current prices for calibration may not be adequate to reflect the parameter estimates appropriate for long-term products. Therefore, for all underlying variables, we do not consider parameter estimates under $\mathcal{Q}$ and rely instead on estimates from historical data under $\mathcal{P}$.

It assumed that the stochastic differential equation (SDE) for the force of mortality μ_t is given by

$$\mathrm{d}\mu_t = c\mu_t\,\mathrm{d}t + \xi_t\,\mathrm{d}Y_t, \tag{5.2}$$

where c is a positive constant and Y_t is a standard Brownian motion correlated to W_t^1. Equation (5.2) is a generalisation of a non-mean reverting Ornstein-Uhlenbeck process, which was first introduced to model mortality rate in Luciano and Vigna [20]. Actually, it may be viewed that the process for the force of mortality has a long-term equilibrium at point 0. Whilst this μ_t's specification allows for negative values, it is still a suitable model as c and ξ_t could be chosen such that the probability of negative values is minimised. Setting the correlation structure as $\mathrm{d}W_t^1\,\mathrm{d}Y_t = \rho_1\,\mathrm{d}t$, Y_t can be expressed as $Y_t = \rho_1 W_t^1 + \sqrt{1-\rho_1^2}W_t^2$,

where W_t^2 is a standard Brownian motion independent of W_t^1.

We suppose the stock index S_t has dynamics

$$\mathrm{d}S_t = m_t S_t \,\mathrm{d}t + \eta_t S_t \,\mathrm{d}Z_t, \tag{5.3}$$

where Z_t is a standard Brownian motion and $\mathrm{d}W_t^1 \,\mathrm{d}Z_t = \rho_2 \,\mathrm{d}t$. Consequently, $Z_t = \rho_2 W_t^1 + \sqrt{1-\rho_2^2} W_t^3$, where W_t^3 is a standard Brownian motion independent of W_t^1 and W_t^2.

Let $\mathbf{x}_t$ be a finite-state Markov chain on $(\Omega, \mathcal{F}, \{\mathcal{F}_t\}, \mathcal{P})$ with a state space $\mathcal{E}$. Following Elliott [8], we choose $\mathcal{E}$ as the set of standard basis vectors, i.e. $\mathcal{E} = \{\mathbf{e}_1, \mathbf{e}_2, \ldots, \mathbf{e}_N\} \subset \mathbb{R}^N$, where N is the number of states. Here, $\mathbf{e}_i = (0, \ldots, 1, \ldots, 0)^\top$ is the unit vector with the i^{th} entry being 1 and 0 elsewhere, and $\top$ stands for the transpose of a matrix. With this notation, $\mathbf{e}_i$ represents the i^{th} state, which is regarded as the i^{th} "regime" of the economic and mortality environments. Let $\mathbf{Q} = [q_{ij}]_{i,j=1,\ldots,N}$ be the intensity matrix, that is, q_{ij} is the transition intensity for $\mathbf{x}_t$ of going from state j to state i; and so, $\mathbf{Q}$ satisfies $\sum_{k=1}^N q_{kj} = 0$ for all $j = 1, \ldots, N$. As established in Elliott [8], $\mathbf{x}_t$ has the semi-martingale representation

$$\mathrm{d}\mathbf{x}_t = \mathbf{Q}\mathbf{x}_t \,\mathrm{d}t + \mathrm{d}\mathbf{M}_t,$$

where $\{\mathbf{M}_t\}$ is an $\mathbb{R}^N$-valued martingale with respect to $\mathcal{F}^{\mathbf{x}}$ under $\mathcal{P}$, and $\mathcal{F}^{\mathbf{x}}$ is the natural filtration generated by $\mathbf{x}_t$.

This chapter proposes a regime-switching framework by enriching equation (5.1) via having parameters b_t and σ_t depend on $\mathbf{x}_t$, i.e.,

$$b_t = b(\mathbf{x}_t) = \langle \mathbf{b}, \mathbf{x}_t \rangle \quad \text{and} \quad \sigma_t = \sigma(\mathbf{x}_t) = \langle \boldsymbol{\sigma}, \mathbf{x}_t \rangle,$$

where $\mathbf{b} = (b_1, b_2, \ldots, b_N)^\top$, $\boldsymbol{\sigma} = (\sigma_1, \sigma_2, \ldots, \sigma_N)^\top$ and $\langle \cdot, \cdot \rangle$ is the scalar product of two vectors. They describe the level of b and σ under various states. Similarly, ξ_t in equation (5.2) as well as m_t and η_t in equation (5.3) are also assumed to be governed by $\mathbf{x}_t$. Their corresponding dynamics are given by

$$\xi_t = \xi(\mathbf{x}_t) = \langle \boldsymbol{\xi}, \mathbf{x}_t \rangle \,, \quad m_t = m(\mathbf{x}_t) = \langle \mathbf{m}, \mathbf{x}_t \rangle \quad \text{and} \quad \eta_t = \eta(\mathbf{x}_t) = \langle \boldsymbol{\eta}, \mathbf{x}_t \rangle,$$

where $\boldsymbol{\xi} = (\xi_1, \xi_2, \ldots, \xi_N)^\top$, $\mathbf{m} = (m_1, m_2, \ldots, m_N)^\top$ and $\boldsymbol{\eta} = (\eta_1, \eta_2, \ldots, \eta_N)^\top$.

In order to achieve tractability in obtaining an analytical pricing solution, a and c in equations (5.1) and (5.2), respectively, will not be treated as regime-switching parameters. Additionally, we deem that the switching between regimes is only more pertinent for the mean-reverting level b and volatilities σ and ξ. As r_t, μ_t and S_t unfold through time, they all

depend on a single $\mathbf{x}_t$. Thus, when the regime of an environment changes, the three risk factors are all affected. Indeed, even if they are driven by different Markov chains, say $\mathbf{x}_t^{(1)}$, $\mathbf{x}_t^{(2)}$ and $\mathbf{x}_t^{(3)}$, we can combine these together to form a single Markov chain with a larger state space. Given the behaviour of the data time series, estimates of the state or regime will adjust accordingly through the use of an HMM filtering technique in Section 5.4.

5.3 Derivation of valuation formula

The price of a derivative security (i.e., financial or insurance contract) is calculated under Q and so the regime-switching Q-dynamics of r_t, μ_t and S_t are required. For risk-neutral pricing, the Esscher transform θ_t^i connects the $\mathcal{P}$ and Q dynamics of S_t. As shown in Elliott et al. [10], $\theta_t^i = \dfrac{r_t - m_t^i}{(\eta_t^i)^2}$ corresponding to the i^{th} regime and giving

$$\mathrm{d}S_t = r_t S_t \,\mathrm{d}t + \eta_t S_t \,\mathrm{d}Z_t, \tag{5.4}$$

where $\eta_t = \eta(\mathbf{x}_t) = \langle \boldsymbol{\eta}, \mathbf{x}_t \rangle$ and Z_t is a Q-Brownian motion. In order to adopt the Esscher transform in determing a risk-neutral probability so that the probability laws of the modulating Markov chain remain unchanged after measure changes, the independence between the Markov chain and Brownian motion must be imposed.

Going back to the purpose of this chapter, we are valuing a GMMB, which has a very long maturity and so the parameter dynamics are better reflected under the objective measure $\mathcal{P}$. We suppose the intensity matrix $\mathbf{Q}$ has the same dynamics under both Q and $\mathcal{P}$, implying the same semi-martingale representation for $\mathbf{x}_t$ under both measures. The dynamics of the process μ_t under $\mathcal{P}$ is also assumed. It has to be noted that although insurance contracts are not offered to the entire population, the insurer has a sufficient large pool of policyholders and so the unsystematic mortality risk is negligible. The risk-neutral dynamics for r_t is assumed to follow that of r_t under $\mathcal{P}$ and the same assumption goes for the correlation between our three underlying stochastic processes as discussed in Section 5.2.

The insurer's liability is $(G - F_T)^+$, where F_T is the policyholder's fund level at maturity T and G is the minimum guarantee. This is the same as the payoff of a put option on F_T with a strike price of G. In the segregated fund contract in Canada, G is typically 75% or 100% of the initial investment and F_T is linked to the performance of the stock index S_T.

In particular,

$$F_T = F_0 \frac{S_T}{S_0} e^{-\iota T},$$

where ι is the constant continuously compounded management charge rate. Further details on the design of investment guarantees can be found in Hardy [16]. Without loss of generality, we let $F_0 = S_0$ and $\iota = 0$. The pricing formula for the GMMB at time 0 is expressed as

$$\begin{aligned} P_{GMMB} &= \mathbb{E}^{\mathcal{Q}}\left[e^{-\int_0^T r_t \,\mathrm{d}t} e^{-\int_0^T \mu_t \,\mathrm{d}t} (G - F_T)^+ \middle| \mathcal{F}_0 \right] \\ &= \mathbb{E}^{\mathcal{Q}}\left[e^{-\int_0^T r_t \,\mathrm{d}t} e^{-\int_0^T \mu_t \,\mathrm{d}t} (G - S_T)^+ \middle| \mathcal{F}_0 \right]. \end{aligned} \tag{5.5}$$

5.3.1 Bond price

The fair value $B(t,T)$ of a zero-coupon bond at time t with a payment of \$1 at maturity T is

$$B(t,T) = \mathbb{E}^{\mathcal{Q}}\left[e^{-\int_t^T r_s \,\mathrm{d}s} \middle| \mathcal{F}_t \right]. \tag{5.6}$$

Under a Markov-modulated affine setting, Elliott and Siu [9] utilised a partial-differential-equation approach to show that (5.6) is also a Markov-driven exponential-affine bond price given

$$B(t,T) = e^{D(t,T,\mathbf{x}_t) - A(t,T) r_t}, \tag{5.7}$$

where

$$A(t,T) = \frac{1}{a}\left(1 - e^{-a(T-t)}\right)$$

and

$$D(t,T,\mathbf{x}_t) = \sum_{i=1}^{N} \ln\left(\langle \mathbf{\Phi}(t)\mathbf{1}, \mathbf{e}_i \rangle\right) \langle \mathbf{x}_t, \mathbf{e}_i \rangle. \tag{5.8}$$

In (5.8), $\mathbf{\Phi}(t)$ is the fundamental matrix solution of

$$\frac{\mathrm{d}\mathbf{\Phi}(t)}{\mathrm{d}t} = \mathbf{\Delta}(t)\mathbf{\Phi}(t), \quad \mathbf{\Phi}(T) = \mathbf{I},$$

where $\mathbf{I}$ is the $N \times N$ identity matrix and $\mathbf{\Delta}(t)$ is defined as

$$\mathbf{\Delta}(t) = \mathrm{diag}\left(\mathbf{f}(t)\right) - \mathbf{Q}^\top. \tag{5.9}$$

Note that in (5.9), $\mathrm{diag}\left(\mathbf{f}(t)\right)$ is the diagonal matrix with $\mathbf{f}(t)$ being its diagonal and $\mathbf{f}(t) = (f_1(t), f_2(t), \ldots, f_N(t))$, where

$$f_i(t) = b_i a A(t,T) - \frac{1}{2}\sigma_i^2 A^2(t,T), \quad i = 1, 2, \ldots, N.$$

5.3.2 Pure endowment

The time-t price $M(t,T)$ of a pure endowment with a survival benefit of \$1 at maturity T is

$$M(t,T) = \mathbb{E}^{Q}\left[e^{-\int_t^T r_s\,\mathrm{d}s}e^{-\int_t^T \mu_s\,\mathrm{d}s}\middle|\mathcal{F}_t\right].$$

To facilitate the price calculation of a pure endowment, we invoke the change-of-numéraire technique; a similar approach can be found in Shen and Siu [27]. Define the forward measure $\widetilde{Q}$ associated with $B(t,T)$; $\widetilde{Q}$ is equivalent to Q and constructed via the Radon-Nikodým derivative

$$\left.\frac{\mathrm{d}\widetilde{Q}}{\mathrm{d}Q}\right|_{\mathcal{F}_T} := \Pi_T^{(1)} = \frac{e^{-\int_0^T r_s\,\mathrm{d}s}B(T,T)}{B(0,T)}.$$

Notice that $\Pi_T^{(1)}$ is a martingale under Q, and so

$$\Pi_t^{(1)} = \mathbb{E}^{Q}\left[\Pi_T^{(1)}\middle|\mathcal{F}_t\right] = \frac{e^{-\int_0^t r_s\,\mathrm{d}s}B(t,T)}{B(0,T)}.$$

By the Bayes' rule for conditional expectation,

$$\begin{aligned} M(t,T) &= \mathbb{E}^{Q}\left[e^{-\int_t^T r_s\,\mathrm{d}s}e^{-\int_t^T \mu_s\,\mathrm{d}s}\middle|\mathcal{F}_t\right] \\ &= \mathbb{E}^{Q}\left[e^{-\int_t^T r_s\,\mathrm{d}s}\middle|\mathcal{F}_t\right]\mathbb{E}^{\widetilde{Q}}\left[e^{-\int_t^T \mu_s\,\mathrm{d}s}\middle|\mathcal{F}_t\right] \\ &= B(t,T)\widetilde{S}(t,T), \end{aligned}$$

where $\widetilde{S}(t,T) = \mathbb{E}^{\widetilde{Q}}\left[e^{-\int_t^T \mu_s\,\mathrm{d}s}\middle|\mathcal{F}_t\right]$ is the conditional expectation of survival probability under $\widetilde{Q}$. As we desire an explicit solution for $M(t,T)$, the dynamics of μ_t under $\widetilde{Q}$ is needed. By the Girsanov's theorem, the corresponding Brownian motions under $\widetilde{Q}$ are

$$\mathrm{d}\widetilde{W}_t^1 = W_t^1 + \sigma_t A(t,T)\,\mathrm{d}t, \quad d\widetilde{W}_t^2 = \mathrm{d}W_t^2 \quad \text{and} \quad \mathrm{d}\widetilde{W}_t^3 = \mathrm{d}W_t^3.$$

Plugging them in equation (5.2), the dynamics of μ_t under $\widetilde{Q}$ are

$$\mathrm{d}\mu_t = (-\xi_t\sigma_t A(t,T) + c\mu_t)\,\mathrm{d}t + \xi_t\,\mathrm{d}\widetilde{Y}_t,$$

where $\mathrm{d}\widetilde{Y}_t = \rho_1\,\mathrm{d}\widetilde{W}_t^1 + \sqrt{1-\rho_1^2}\,\mathrm{d}\widetilde{W}_t^2$.

The dynamics of $\mathbf{x}_t$ also change under $\widetilde{Q}$. Applying Proposition 5.1 in Palmowski and Rolski [24], the new intensity matrix $\widetilde{\mathbf{Q}}(t) = \left[\widetilde{q}_{ij}(t)\right]_{i,j=1,\ldots,N}$ is given by

$$\widetilde{q}_{ij}(t) = \begin{cases} q_{ij}\frac{e^{D(t,T,\mathbf{e}_i)}}{e^{D(t,T,\mathbf{e}_j)}}, & i \neq j, \\ -\sum_{k\neq j} q_{kj}\frac{e^{D(t,T,\mathbf{e}_k)}}{e^{D(t,T,\mathbf{e}_j)}}, & i = j. \end{cases}$$

It can be seen that $\widetilde{\mathbf{Q}}(t)$ is a time dependent matrix and under $\widetilde{Q}$, $\mathbf{x}_t$ has the semi-martingale representation

$$\mathrm{d}\mathbf{x}_t = \widetilde{\mathbf{Q}}(t)\mathbf{x}_t\,\mathrm{d}t + \mathrm{d}\widetilde{\mathbf{M}}_t,$$

where $\widetilde{\mathbf{M}}_t$ is a martingale under $\widetilde{Q}$.
Following similar results we have for the bond price, the Markov-modulated exponential-affine form for the survival function is obtained and given by

$$\widetilde{S}(t,T) = e^{\widetilde{H}(t,T,\mathbf{x}_t)-\widetilde{G}(t,T)\mu_t}, \tag{5.10}$$

where

$$\widetilde{G}(t,T) = \frac{1}{c}\left(e^{c(T-t)} - 1\right)$$

and

$$\widetilde{H}(t,T,\mathbf{x}_t) = \sum_{i=1}^{N} \ln(\langle\widetilde{\mathbf{\Phi}}(t)\mathbf{1}, \mathbf{e}_i\rangle)\langle\mathbf{x}_t, \mathbf{e}_i\rangle, \tag{5.11}$$

where $\mathbf{1}$ is a vector of 1's. In (5.11), if we define $\widetilde{\mathbf{\Delta}}(t) = \mathrm{diag}\left(\widetilde{\mathbf{f}}(t)\right) - \widetilde{\mathbf{Q}}(t)^\top$ and $\widetilde{f}_i(t) = -\xi_i\sigma_i A(t,T)\widetilde{G}(t,T) - \frac{1}{2}\xi_i^2\widetilde{G}^2(t,T)$, for $i = 1, 2, \ldots, N$ then $\widetilde{\mathbf{\Phi}}(t)$ is the fundamental matrix solution of

$$\frac{\mathrm{d}\widetilde{\mathbf{\Phi}}(t)}{\mathrm{d}t} = \widetilde{\mathbf{\Delta}}(t)\widetilde{\mathbf{\Phi}}(t), \quad \widetilde{\mathbf{\Phi}}(T) = \mathbf{I}.$$

Therefore, combining equations (5.7) and (5.10), the price of a pure endowment has the analytic solution

$$M(t,T) = e^{D(t,T,\mathbf{x}_t)+\widetilde{H}(t,T,\mathbf{x}_t)-A(t,T)r_t-\widetilde{G}(t,T)\mu_t}. \tag{5.12}$$

5.3.3 Guaranteed minimum maturity benefit

We could first assume that the modulating Markov chain is observable then its 'filtered' estimate utilising historical data could be used later. We do not translate these estimates into risk-neutral estimates given the long maturity of the contract and we rely on information provided by past data in the real world. A pertinent literature dealing with option valuation and filtering is given in Elliott and Siu [**?**] and Siu [**?**].

In order to turn the GMMB pricing expression in (5.5) into an efficiently implementable form, we shall use another measure called the endowment-risk-adjusted measure $\widehat{Q}$ defined through the Radon-Nikodŷm derivative

$$\left.\frac{\mathrm{d}\widehat{Q}}{\mathrm{d}Q}\right|_{\mathcal{F}_T} := \Pi_T^{(2)} = \frac{e^{-\int_0^T r_s\,\mathrm{d}s}e^{-\int_0^T \mu_s\,\mathrm{d}s}M(T,T)}{M(0,T)}.$$

Since $\Pi_T^{(2)}$ is a martingale under Q,

$$\Pi_t^{(2)} = \mathbb{E}^Q\left[\Pi_T^{(2)}\middle|\mathcal{F}_t\right] = \frac{e^{-\int_0^t r_s\,\mathrm{d}s}e^{-\int_0^t \mu_s\,\mathrm{d}s}M(t,T)}{M(0,T)}.$$

In a similar manner to finding the price of a pure endowment through the application of the Bayes' rule, the GMMB price is

$$\begin{aligned} P_{GMMB} &= \mathbb{E}^Q\left[e^{-\int_0^T r_t\,\mathrm{d}t}e^{-\int_0^T \mu_t\,\mathrm{d}t}(G - S_T)^+\middle|\mathcal{F}_0\right] \\ &= M(0,T)\mathbb{E}^{\widehat{Q}}\left[(G - S_T)^+|\mathcal{F}_0\right]. \end{aligned} \tag{5.13}$$

Since we already came up with an analytic solution to $M(0,T)$ in Subsection 5.3.2, it only remains to evaluate $\mathbb{E}^{\widehat{Q}}\left[(G - S_T)^+|\mathcal{F}_0\right]$. By using the Girsanov's theorem again, the corresponding Brownian motions under $\widehat{Q}$ are

$$\mathrm{d}\widehat{W}_t^1 = W_t^1 + \left(\sigma_t A(t,T) + \rho_1\xi_t\widetilde{G}(t,T)\right)\mathrm{d}t, \quad \mathrm{d}\widehat{W}_t^2 = W_t^2 + \sqrt{1-\rho_1^2}\xi_t\widetilde{G}(t,T)\,\mathrm{d}t \quad \text{and}$$
$$\mathrm{d}\widehat{W}_t^3 = W_t^3.$$

Substituting them into equations (5.1) and (5.4), the respective $\widehat{Q}$–dynamics of r_t and S_t are

$$\mathrm{d}r_t = \left(ab_t - \sigma_t^2 A(t,T) - \rho_1\sigma_t\xi_t\widetilde{G}(t,T) - ar_t\right)\mathrm{d}t + \sigma_t\,\mathrm{d}\widehat{W}_t^1 \tag{5.14}$$

and

$$\mathrm{d}S_t = \left(r_t - \rho_2\eta_t\sigma_t A(t,T) - \rho_1\rho_2\eta_t\xi_t\widetilde{G}(t,T)\right)S_t\,\mathrm{d}t + \eta_t S_t\,\mathrm{d}\widehat{Z}_t, \tag{5.15}$$

where $\mathrm{d}\widehat{Z}_t = \rho_2\,\mathrm{d}\widehat{W}_t^1 + \sqrt{1-\rho_2^2}\,\mathrm{d}\widehat{W}_t^3$. Noting that the dynamics of S_t have a complex structure in (5.15), an explicit solution to GMMB pricing formula would be difficult to attain. Hence, a simulation-based method is necessary to complete the valuation of GMMB. In the next Subsection, we utilise the Fourier-transform approach as an alternative to efficiently compute numerically the price of a GMMB.

Lastly, the distribution of $\mathbf{x}_t$ under $\widehat{Q}$ changes as well. The intensity matrix $\widehat{\mathbf{Q}}(t) = \left[\widehat{q}_{ij}(t)\right]_{i,j=1,\ldots,N}$ is given by

$$\widehat{q}_{ij}(t) = \begin{cases} q_{ij}\dfrac{e^{D(t,T,\mathbf{e}_i)+\widetilde{H}(t,T,\mathbf{e}_i)}}{e^{D(t,T,\mathbf{e}_j)+\widetilde{H}(t,T,\mathbf{e}_j)}}, & i \neq j, \\ -\sum_{k\neq j} q_{kj}\dfrac{e^{D(t,T,\mathbf{e}_k)+\widetilde{H}(t,T,\mathbf{e}_k)}}{e^{D(t,T,\mathbf{e}_j)+\widetilde{H}(t,T,\mathbf{e}_j)}}, & i = j. \end{cases}$$

Thus, $\mathbf{x}_t$ has the semi-martingale representation

$$\mathrm{d}\mathbf{x}_t = \widehat{\mathbf{Q}}(t)\mathbf{x}_t\,\mathrm{d}t + \mathrm{d}\widehat{\mathbf{M}}_t,$$

where $\widehat{\mathbf{M}}_t$ is a martingale under $\widehat{Q}$.

5.3.4 Fourier transform

In this Subsection, we apply a version of the Fourier transform method proposed in Carr and Madan [3] to price GMMBs; see also Fan et al. [12] for option pricing. This approach can be extended to fast Fourier transform (FFT) to price GMMBs with various guaranteed values.

Write $s_t := \log S_t$. The dynamics of s_t under $\widehat{Q}$, from equation (5.15), is given by

$$\mathrm{d}s_t = \left(r_t - \frac{1}{2}\eta_t^2 - \rho_2\eta_t\sigma_t A(t,T) - \rho_1\rho_2\eta_t\xi_t\widehat{G}(t,T)\right)\mathrm{d}t + \eta_t\,\mathrm{d}\widehat{Z}_t.$$

We first determine the characteristic function of $\left(\int_0^T r_t\,\mathrm{d}t, \int_0^T \eta_t\,\mathrm{d}\widehat{Z}_t\right)$ conditional on $\mathcal{F}_T^{\mathbf{x}}$ under $\widehat{Q}$. Equation (5.14) has the solution

$$r_t = e^{-at}\left(r_0 + \int_0^t e^{as}\left(ab_s - \sigma_s^2 A(s,T) - \rho_1\sigma_s\xi_s\widetilde{G}(s,T) - ar_s\right)\mathrm{d}s + \int_0^t e^{as}\sigma_s\,\mathrm{d}\widehat{W}_s^1\right). \tag{5.16}$$

Integrating both sides of equation (5.16) yields

$$\begin{aligned}\int_0^T r_t\,\mathrm{d}t = \int_0^T e^{-at}\Bigg(&r_0 + \int_0^t e^{as}\left(ab_s - \sigma_s^2 A(s,T) - \rho_1\sigma_s\xi_s\widetilde{G}(s,T) - ar_s\right)\mathrm{d}s \\ &+ \int_0^t e^{as}\sigma_s\,\mathrm{d}\widehat{W}_s^1\Bigg)\mathrm{d}t.\end{aligned}$$

It may be proved that $\left(\int_0^T r_t\,\mathrm{d}t, \int_0^T \eta_t\,\mathrm{d}\widehat{Z}_t\right)$ follows a bivariate normal distribution with respective mean and covariance matrix

$$\begin{bmatrix} \int_0^T e^{-at}\left(r_0 + \int_0^t e^{as}(ab_s - \sigma_s^2 A(s,T) - \rho_1\sigma_s\xi_s\widetilde{G}(s,T) - ar_s)\,\mathrm{d}s\right)\mathrm{d}t \\ 0 \end{bmatrix}$$

and

$$\begin{bmatrix} \int_0^T A(t,T)^2\sigma_t^2\,\mathrm{d}t & \int_0^T \rho_2\sigma_t\eta_t A(t,T)\,\mathrm{d}t \\ \int_0^T \rho_2\sigma_t\eta_t A(t,T)\,\mathrm{d}t & \int_0^T \eta_t^2\,\mathrm{d}t \end{bmatrix}.$$

The characteristic function of $\left(\int_0^T r_t\,\mathrm{d}t, \int_0^T \eta_t\,\mathrm{d}\widehat{Z}_t\right)$ conditional on $\mathcal{F}_T^{\mathbf{x}}$ is

$$\begin{aligned}&\mathbb{E}^{\widehat{Q}}\left[\exp\left\{iv\left(\int_0^T r_t\,\mathrm{d}t + \int_0^T \eta_t\,\mathrm{d}\widehat{Z}_t\right)\right\}\middle|\,\mathcal{F}_T^{\mathbf{x}}\right] = \\ &\exp\left\{ivA(0,T)r_0 - \frac{1}{2}v^2\int_0^T \eta_t^2\,\mathrm{d}t - \frac{1}{2}v^2\int_0^T A(t,T)^2\sigma_t^2\,\mathrm{d}t\right. \\ &\left. + iv\int_0^T A(t,T)[ab_t - \sigma_t^2 A(t,T) - \rho_1\sigma_t\xi_t\widehat{G}(t,T)]\,\mathrm{d}t - v^2\int_0^T A(t,T)\rho_2\sigma_t\eta_t\,\mathrm{d}t\right\}.\end{aligned}$$

Hence, the characteristic function of s_T under $\widehat{Q}$ is

$$\begin{aligned}
\phi(v,0,T) &= \mathbb{E}^{\widehat{Q}}\left[e^{ivs_T}\right] \\
&= \mathbb{E}^{\widehat{Q}}\left[\mathbb{E}^{\widehat{Q}}\left[\exp\left\{iv\left(s_0 + \int_0^T \left(r_t - \frac{1}{2}\eta_t^2 - \rho_2\eta_t\sigma_t A(t,T) - \rho_1\rho_2\eta_t\xi_t\widehat{G}(t,T)\right)\mathrm{d}t\right.\right.\right.\right. \\
&\quad \left.\left.\left.\left. + \int_0^T \eta_t\,\mathrm{d}\widehat{Z}_t\right)\right\}\middle|\mathcal{F}_T^{\mathbf{x}}\right]\right] \\
&= \mathbb{E}^{\widehat{Q}}\left[\exp\left\{iv\left(s_0 - \int_0^T\left(\frac{1}{2}\eta_t^2 + \rho_2\eta_t\sigma_t A(t,T) + \rho_1\rho_2\eta_t\xi_t\widehat{G}(t,T)\right)\mathrm{d}t\right)\right\}\right. \\
&\quad \left.\times\mathbb{E}^{\widehat{Q}}\left[\exp\left\{\int_0^T r_t\,\mathrm{d}t + \int_0^T \eta_t\,\mathrm{d}\widehat{Z}_t\right\}\middle|\mathcal{F}_t^{\mathbf{x}}\right]\right] \\
&= \mathbb{E}^{\widehat{Q}}\left[\exp\left\{iv\left(s_0 + A(0,T)r_0\right) + \int_0^T \langle\boldsymbol{\varphi}_t, \mathbf{x}_t\rangle\,\mathrm{d}t\right\}\right] = e^{iv(s_0+A(0,T)r_0)}\mathbb{E}^{\widehat{Q}}\left[e^{\int_0^T\langle\boldsymbol{\varphi}_t,\mathbf{x}_t\rangle\,\mathrm{d}t}\right], \quad (5.17)
\end{aligned}$$

where $\boldsymbol{\varphi}_t = (\varphi_1(t), \varphi_2(t), \ldots, \varphi_N(t))$ and

$$\begin{aligned}
\varphi_j(t) = &-iv\left(\frac{1}{2}\eta_j^2 + \rho_2\eta_j\sigma_j A(t,T) + \rho_1\rho_2\eta_j\xi_j\widetilde{G}(t,T)\right) - \frac{1}{2}v^2\eta_j - \frac{1}{2}v^2A(t,T)\sigma_j^2 \\
&+ ivA(t,T)\left(ab_j - \sigma_j^2 A(t,T) - \rho_1\sigma_j\xi_j\widetilde{G}(t,T)\right) - v^2A(t.T)\rho_2\sigma_j\eta_j
\end{aligned}$$

for $j = 1, 2, \ldots, N$.

All that remains to be done is the evaluation of the expectation of $e^{\int_0^T\langle\boldsymbol{\varphi}_t,\mathbf{x}_t\rangle\,\mathrm{d}t}$ under $\widehat{Q}$. If

$$\mathbf{W}_t := e^{\int_0^t\langle\boldsymbol{\varphi}_s,\mathbf{x}_s\rangle\,\mathrm{d}s}\mathbf{x}_t$$

then $\mathbf{W}_t$ satisfies the stochastic differential equation

$$\mathrm{d}\mathbf{W}_t = \langle\boldsymbol{\varphi}_t, \mathbf{x}_t\rangle\,\mathbf{W}_t\,\mathrm{d}t + e^{\int_0^t\langle\boldsymbol{\varphi}_s,\mathbf{x}_s\rangle\,\mathrm{d}s}\,\mathrm{d}\mathbf{x}_t.$$

Note that

$$\mathrm{d}\mathbf{x}_t = \widehat{\mathbf{Q}}(t)\mathbf{x}_t\,\mathrm{d}t + \mathrm{d}\widehat{\mathbf{M}}_t \quad \text{and} \quad \langle\boldsymbol{\varphi}_t, \mathbf{x}_t\rangle\,\mathbf{W}_t = \mathrm{diag}(\boldsymbol{\varphi}_t)\mathbf{W}_t$$

so that

$$\mathrm{d}\mathbf{W}_t = \left(\widehat{\mathbf{Q}}(t) + \mathrm{diag}(\boldsymbol{\varphi}_t)\right)\mathbf{W}_t\,\mathrm{d}t + e^{\int_0^t\langle\boldsymbol{\varphi}_s,\mathbf{x}_s\rangle\,\mathrm{d}s}\,\mathrm{d}\widehat{\mathbf{M}}_t$$

and therefore,

$$\mathbf{W}_t = \mathbf{W}_0 + \int_0^t\left(\widehat{\mathbf{Q}}(s) + \mathrm{diag}(\boldsymbol{\varphi}_s)\right)\mathbf{W}_s\,\mathrm{d}s + \int_0^t e^{\int_0^s\langle\boldsymbol{\varphi}_u,\mathbf{x}_u\rangle\,\mathrm{d}u}\,\mathrm{d}\widehat{\mathbf{M}}_s. \quad (5.18)$$

Taking expectations bot sides of equation (5.18),

$$\mathbb{E}^{\widehat{Q}}[\mathbf{W}_t] = \mathbf{x}_0 + \int_0^t\left(\widehat{\mathbf{Q}}(s) + \mathrm{diag}(\boldsymbol{\varphi}_s)\right)\mathbb{E}^{\widehat{Q}}[\mathbf{W}_t]\,\mathrm{d}s.$$

Let $\widehat{\mathbf{\Phi}}(t)$ be the fundamental matrix solution to

$$\frac{\mathrm{d}\widehat{\mathbf{\Phi}}(t)}{\mathrm{d}t} = \left(\widehat{\mathbf{Q}}(t) + \mathrm{diag}(\boldsymbol{\varphi}_t)\right)\widehat{\mathbf{\Phi}}(t), \quad \widehat{\mathbf{\Phi}}(0) = \mathbf{I}.$$

Then $\mathbb{E}^{\widehat{Q}}[\mathbf{W}_t]$ can be represented as $\widehat{\mathbf{\Phi}}(T)\mathbf{x}_0$. Consequently,

$$\begin{aligned}
&\mathbb{E}^{\widehat{Q}}\left[\exp\left(\int_0^T \langle \boldsymbol{\varphi}_t, \mathbf{x}_t\rangle \,\mathrm{d}t\right)\right] \\
&= \mathbb{E}^{\widehat{Q}}\left[\exp\left(\int_0^T \langle \boldsymbol{\varphi}_t, \mathbf{x}_t\rangle \,\mathrm{d}t\right)\langle \mathbf{x}_t, \mathbf{1}\rangle\right] = \mathbb{E}^{\widehat{Q}}\left[\left\langle \exp\left(\int_0^T \langle \boldsymbol{\varphi}_t, \mathbf{x}_t\rangle \,\mathrm{d}t\right)\mathbf{x}_t, \mathbf{1}\right\rangle\right] \\
&= \left\langle \mathbb{E}^{\widehat{Q}}\left[\exp\left(\int_0^T \langle \boldsymbol{\varphi}_t, \mathbf{x}_t\rangle \,\mathrm{d}t\right)\mathbf{x}_t\right], \mathbf{1}\right\rangle = \left\langle \mathbb{E}^{\widehat{Q}}\left[\mathbf{W}_T\right], \mathbf{1}\right\rangle = \left\langle \widehat{\mathbf{\Phi}}(T)\mathbf{x}_0, \mathbf{1}\right\rangle. \qquad (5.19)
\end{aligned}$$

Combining equations (5.17) and (5.19), the characteristic function of s_T under $\widehat{Q}$ is

$$\phi(v, 0, T) = e^{iv(s_0 + A(0,T)r_0)}\left\langle \widehat{\mathbf{\Phi}}(T)\mathbf{x}_0, \mathbf{1}\right\rangle.$$

Now, consider the Fourier transform of the GMMB price as provided by equation (5.13). Write $g := \log G$. In order to achieve a square-integrable function, we first modify the price by imposing a factor α, i.e.,

$$P'_{GMMB}(g) := e^{-\alpha g} P_{GMMB}(g),$$

where $\alpha > 0$. The Fourier transform of $P'_{GMMB}(g)$ is

$$\begin{aligned}
\chi(v) &= \int_{-\infty}^{\infty} e^{ivg} P'_{GMMB}(g)\,\mathrm{d}g = \int_{-\infty}^{\infty} e^{ivg} e^{-\alpha g} M(0,T)\mathbb{E}^{\widehat{Q}}\left[(e^g - e^{s_T})^+ \,|\mathcal{F}_0\right]\mathrm{d}g \\
&= M(0,T)\int_{-\infty}^{\infty} e^{ivg} e^{-\alpha g}\int_{-\infty}^{g} (e^g - e^s)\, f_{s_T}(s)\,\mathrm{d}s\,\mathrm{d}g \\
&= M(0,T)\int_{-\infty}^{\infty} f_{s_T}(s)\int_{s}^{\infty}\left(e^{(1+iv-\alpha)g} - e^{s+(iv-\alpha)g}\right)\mathrm{d}g\,\mathrm{d}s \\
&= M(0,T)\int_{-\infty}^{\infty} f_{s_T}(s)\left(-\frac{e^{(1+iv-\alpha)s}}{1+iv-\alpha} + \frac{e^{(1+iv-\alpha)s}}{iv-\alpha}\right)\mathrm{d}s \\
&= \frac{M(0,T)\phi(v + i(\alpha-1), 0, T)}{(1+iv-\alpha)(iv-\alpha)},
\end{aligned}$$

where $f_{s_T}(s)$ is the density of s_T. Then, the price of GMMB is obtained by using the inverse Fourier transform

$$P_{GMMB} = \frac{e^{\alpha g}}{2\pi}\int_{-\infty}^{\infty} e^{-ivg}\chi(v)\,\mathrm{d}v. \qquad (5.20)$$

Equation (5.20) could be computed numerically employing the discrete inverse Fourier transform

$$P_{GMMB} \approx \frac{e^{\alpha g}}{2\pi}\sum_{j=-M}^{M} e^{-iv_j g}\chi(v_j)\Delta v, \qquad (5.21)$$

where $v_j = \Delta v(j-1)$ and M is typically selected as a power of 2.

5.4 Numerical illustration

5.4.1 Recursive filtering

We apply the discrete-time HMM-filtering method to estimate parameters from historical data. Mortality data are usually recorded yearly, whilst the interest rates and stock index values are gathered daily or monthly. Given the issue on the synchrony of data frequency, it is difficult to estimate all parameters simultaneously. Due to this limitation, parameter estimation will be performed separately for the different models and the correlation coefficients will be estimated separately as well.

From equation (5.1),

$$r_t = r_s e^{-a(t-s)} + \int_s^t b_u e^{-a(t-u)}\,\mathrm{d}u + \int_s^t \sigma_u e^{-a(t-u)}\,\mathrm{d}W_t^1. \tag{5.22}$$

Let Δt be the constant time interval between data points. With the aid of the distribution of the stochastic integral over the time period $[t_k,\ t_{k+1}]$ corresponding to the increment $r_{k+1}-r_k$, equation (5.22) can be approximated as

$$r_{k+1} = e^{-a\Delta t} r_k + b_k(1 - e^{-a\Delta t}) + \sigma_k \sqrt{\frac{1 - e^{-2a\Delta t}}{2a}}\epsilon_{k+1}^{(1)}, \tag{5.23}$$

where $\left\{\epsilon_k^{(1)}\right\}$ is a sequence of independent and identically distributed (IID) standard normal random variables (RVs). We re-write equation (5.23) as

$$r_{k+1} = \alpha_1 r_k + \alpha_2(\mathbf{x}_k) + \alpha_3(\mathbf{x}_k)\epsilon_{k+1}^{(1)}, \tag{5.24}$$

where $\alpha_1 = e^{-a\Delta t}$, $\alpha_2(\mathbf{x}_k) = b_k(1 - e^{-a\Delta t})$ and $\alpha_3(\mathbf{x}_k) = \sigma_k \sqrt{\dfrac{1 - e^{-2a\Delta t}}{2a}}$.
Similarly, for equation (5.2), we have

$$\mu_{k+1} = \beta_1 \mu_k + \beta_2(\mathbf{x}_k)\epsilon_{k+1}^{(2)}, \tag{5.25}$$

where $\beta_1 = e^{c\Delta t}$, $\beta_2(\mathbf{x}_k) = \xi_k \sqrt{\dfrac{e^{2c\Delta t} - 1}{2c}}$ and $\left\{\epsilon_k^{(2)}\right\}$ is a sequence of IID standard normal RVs. From equation (5.3),

$$\log\left(\frac{S_{k+1}}{S_k}\right) = \gamma_1(\mathbf{x}_k) + \gamma_2(\mathbf{x}_k)\epsilon_{k+1}^{(3)}, \tag{5.26}$$

where $\gamma_1(\mathbf{x}_k) = \left(m_t - \dfrac{1}{2}\eta_t^2\right)\Delta t$, $\gamma_2(\mathbf{x}_k) = \eta_t \sqrt{\Delta t}$ and $\left\{\epsilon_k^{(3)}\right\}$ is also a sequence of IID standard normal RVs.

The discrete-time expression for the hidden Markov chain $\mathbf{x}_k$ is

$$\mathbf{x}_{k+1} = \mathbf{P}\mathbf{x}_k + \boldsymbol{\varepsilon}_{k+1}, \tag{5.27}$$

where $\boldsymbol{\varepsilon}_k$ is a martingale increment under $\mathcal{P}$; $\mathbf{P} = [p_{ij}]_{i,j=1,\ldots,N}$ is the transition probability matrix; and p_{ij} is the transition probability of $\mathbf{x}_k$ from state j to state i, i.e., $p_{ij} = \mathcal{P}(\boldsymbol{x}_{k+1} = \mathbf{e}_i | \mathbf{x}_k = \mathbf{e}_j)$. The connection between the intensity matrix $\mathbf{Q}$ and the transition probability matrix $\mathbf{P}$ is given by

$$\mathbf{P} = \exp(\mathbf{Q}\Delta t).$$

We introduce a new measure $\widetilde{\mathcal{P}}$ under which the observations are IID RVs and $\mathbf{x}_k$ retains the same distribution under $\mathcal{P}$. With observations being IID, $\widetilde{\mathcal{P}}$ is an ideal measure that makes calculations involving expectations manageable. We shall focus first on the interest rate model. Define the processes $\lambda_l^{(1)}$ and $\Lambda_k^{(1)}$ by

$$\lambda_l^{(1)} = \frac{\psi\left(\left(r_l - \alpha_1 r_{l-1} - \alpha_2(\mathbf{x}_{l-1})\right)/\alpha_3(\mathbf{x}_{l-1})\right)}{\alpha_3(\mathbf{x}_{l-1})\psi(r_l)},$$

$$\Lambda_k^{(1)} = \prod_{l=1}^{k} \lambda_l, \quad k \geq 1, \quad \Lambda_0^{(1)} = 1,$$

where $\psi(\cdot)$ is the probability density function of a standard normal RV.

Let $\mathcal{H}_k$ be the filtration generated by the observed processes r_t, μ_t and S_t. Write $\boldsymbol{\zeta}_k \coloneqq \mathbb{E}^{\widetilde{\mathcal{P}}}\left[\Lambda_k^{(1)}\mathbf{x}_k \middle| \mathcal{H}_k\right]$; It may be verified that $\mathbb{E}^{\widetilde{\mathcal{P}}}\left[\Lambda_k^{(1)} \middle| \mathcal{H}_k\right] = \langle \boldsymbol{\zeta}_k, \mathbf{1}\rangle$. Denote by $\mathbf{D}$ the diagonal matrix with the i^{th} element on the diagonal being $\frac{\psi\left(\left(r_l - \alpha_1 r_{l-1} - \alpha_{2,i}\right)\right)/\alpha_{3,i}}{\alpha_{3,i}\psi(r_l)}$. Based on Erlwein and Mamon [11], $\boldsymbol{\zeta}_k$ has the recursive relation

$$\boldsymbol{\zeta}_{k+1} = \mathbf{P}\mathbf{D}\boldsymbol{\zeta}_k.$$

To estimate the model parameters, we define the following three functions of $\mathbf{x}_k$:

(i) the number of jumps from state j to state i up to time k denoted by

$$\mathfrak{J}_k^{(ij)} = \sum_{l=1}^{k} \left\langle \mathbf{x}_{l-1}, \mathbf{e}_j \right\rangle \langle \mathbf{x}_l, \mathbf{e}_i \rangle ;$$

(ii) the amount of time spent on state i up to time k given by

$$\mathfrak{O}_k^{(i)} = \sum_{l=1}^{k} \langle \mathbf{x}_{l-1}, \mathbf{e}_i \rangle ;$$

and

(iii) the process for function g contingent upon state i up to time k represented by

$$\mathfrak{T}_k^{(i)}(g) = \sum_{l=1}^{k} \langle \mathbf{x}_{l-1}, \mathbf{e}_i \rangle \, g(y_l).$$

Let $\mathfrak{C}_k$ be one of the above three stochastic processes, i.e. $\mathfrak{C}_k = \mathfrak{I}_k^{(sr)}$, $\mathfrak{O}_k^{(r)}$ or $\mathfrak{T}_k^{(r)}(g)$. Then, the 'best' estimate in the sense of conditional expected value of $\mathfrak{C}_k$ at time k, by the Bayes' theorem, is given by

$$\widehat{\mathfrak{C}}_k = \mathbb{E}^{\mathcal{P}}\left[\mathfrak{C}_k \mid \mathcal{H}_k\right] = \frac{\mathbb{E}^{\widetilde{\mathcal{P}}}\left[\Lambda_k^{(1)}\mathfrak{C}_k \middle| \mathcal{H}_k\right]}{\mathbb{E}^{\widetilde{\mathcal{P}}}\left[\Lambda_k^{(1)} \middle| \mathcal{H}_k\right]} = \frac{\mathbb{E}^{\widetilde{\mathcal{P}}}\left[\Lambda_k^{(1)}\mathfrak{C}_k \middle| \mathcal{H}_k\right]}{\langle \boldsymbol{\zeta}_k, \mathbf{1} \rangle}.$$

Write $\omega(\mathfrak{C})_k := \mathbb{E}^{\widetilde{\mathcal{P}}}\left[\Lambda_k^{(1)}\mathfrak{C}_k \middle| \mathcal{H}_k\right]$. Note that, for any k,

$$\omega(\mathfrak{C})_k = \omega\left(\mathfrak{C}_k \langle \mathbf{x}_k, \mathbf{1} \rangle\right) = \omega\left(\langle \mathfrak{C}_k \mathbf{x}_k, \mathbf{1} \rangle\right) = \langle \omega\left(\mathfrak{C}_k \mathbf{x}_k\right), \mathbf{1} \rangle.$$

The estimate of $\mathfrak{C}_k$ is immediate once the value for $\omega(\mathfrak{C}_k \mathbf{x}_k)$ is determined. For the interest rate model, we adopt from Erlwein and Mamon [11] the estimation results below:

$$\omega\left(\mathfrak{I}_k^{(ij)}\mathbf{x}_k\right) = \mathbf{PD}\omega\left(\mathfrak{I}_{k-1}^{(ij)}\mathbf{x}_{k-1}\right) + \left\langle \boldsymbol{\zeta}_{k-1}, \mathbf{e}_j \right\rangle \frac{\psi\left((r_k - \alpha_1 r_{k-1} - \alpha_{2,j})/\alpha_{3,j}\right)}{\alpha_{3,j}\psi(r_k)} p_{ij}\mathbf{e}_i \tag{5.28}$$

$$\omega\left(\mathfrak{O}_k^{(i)}\mathbf{x}_k\right) = \mathbf{PD}\omega\left(\mathfrak{O}_{k-1}^{(i)}\mathbf{x}_{k-1}\right) + \langle \boldsymbol{\zeta}_{k-1}, \mathbf{e}_i \rangle \frac{\psi\left((r_k - \alpha_1 r_{k-1} + \alpha_{2,i})/\alpha_{3,i}\right)}{\alpha_{3,i}\psi(r_k)} \mathbf{Pe}_i \tag{5.29}$$

$$\omega\left(\mathfrak{T}_k^{(i)}(g)\mathbf{x}_k\right) = \mathbf{PD}\omega\left(\mathfrak{T}_{k-1}^{(i)}(g)\boldsymbol{x}_{k-1}\right) + \langle \boldsymbol{\zeta}_{k-1}, \mathbf{e}_i \rangle \frac{\psi\left((r_k - \alpha_1 r_{k-1} + \alpha_{2,i})/\alpha_{3,i}\right)}{\alpha_{3,i}\psi(r_k)} \mathbf{Pe}_i. \tag{5.30}$$

We set the initial values as $\omega\left(\mathfrak{I}_0^{(sr)}\right) = \omega\left(\mathfrak{O}_0^{(r)}\right) = \omega\left(\mathfrak{T}_0^{(r)}(g)\right) = 0$. By the EM algorithm the set of parameter estimates $\left\{\widehat{p}_{ij}, \widehat{\alpha}_{2,i}, \widehat{\alpha}_{3,i}\right\}$, for $i, j = 1, \ldots, N$, is generated and computed as follows:

$$\widehat{p}_{ij} = \frac{\left\langle \omega\left(\mathfrak{I}_k^{(ij)}\mathbf{x}_k\right), \mathbf{1} \right\rangle}{\left\langle \omega\left(\mathfrak{O}_k^{(j)}\mathbf{x}_{\boldsymbol{k}}\right), \mathbf{1} \right\rangle}, \tag{5.31}$$

$$\widehat{\alpha}_{2,i} = \frac{\left\langle \omega\left(\mathfrak{T}_k^{(i)}(r_k)\mathbf{x}_k\right), \mathbf{1} \right\rangle - \left\langle \alpha_1 \omega\left(\mathfrak{T}_k^{(i)}(r_{k-1})\mathbf{x}_k\right), \mathbf{1} \right\rangle}{\left\langle \omega\left(\mathfrak{O}_k^{(j)}\mathbf{x}_k\right), \mathbf{1} \right\rangle}, \tag{5.32}$$

and

$$\widehat{\alpha}_{3,i} = \sqrt{\frac{A_1 - 2A_2}{\omega\left(\mathfrak{O}_k^{(i)}\right)}}, \tag{5.33}$$

where

$$A_1 = \omega\left(\mathfrak{T}_k^{(i)}(r_k^2)\right) + \alpha_1^2 \omega\left(\mathfrak{T}_k^{(i)}(r_{k-1}^2)\right) + \alpha_{2,i}^2 \omega\left(\mathfrak{O}_k^{(i)}\right)$$

and

$$A_2 = \alpha_1 \omega\left(\mathfrak{T}_k^{(i)}(r_k r_{k-1})\right) + \alpha_{2,i}\omega\left(\mathfrak{T}_k^{(i)}(r_k)\right) - \alpha_1\alpha_{2,i}\omega\left(\mathfrak{T}_k^{(i)}(r_{k-1})\right).$$

The parameters b_k and σ_k could be estimated using the relation specified in (5.24).

Following similar estimation procedure, the mortality-model parameters are explicitly estimated as

$$\widehat{\beta}_{2,i} = \sqrt{\frac{\left\langle \omega\left(\mathfrak{T}_k^{(i)}(\mu_k^2)\mathbf{x}_k\right), \mathbf{1}\right\rangle + \beta_1^2\left\langle \omega\left(\mathfrak{T}_k^{(i)}(\mu_{k-1}^2)\mathbf{x}_k\right), \mathbf{1}\right\rangle - 2\beta_1\left\langle \omega\left(\mathfrak{T}_k^{(i)}(\mu_k\mu_{k-1})\mathbf{x}_k\right), \mathbf{1}\right\rangle}{\left\langle \omega\left(\mathfrak{O}_k^{(i)}\mathbf{x}_k\right), \mathbf{1}\right\rangle}}; \tag{5.34}$$

and for the stock index model,

$$\widehat{\gamma}_{1,i} = \frac{\left\langle \omega\left(\mathfrak{T}_k^{(i)}(\log(S_k/S_{k-1}))\mathbf{x}_k\right), \mathbf{1}\right\rangle}{\left\langle \omega\left(\mathfrak{O}_k^{(i)}\mathbf{x}_k\right), \mathbf{1}\right\rangle} \tag{5.35}$$

and

$$\widehat{\gamma}_{2,i} = \sqrt{\frac{\left\langle \omega\left(\mathfrak{T}_k^{(i)}(\log(S_k/S_{k-1})^2)\mathbf{x}_k\right), \mathbf{1}\right\rangle + \gamma_1^2\left\langle \omega\left(\mathfrak{O}_k^{(i)}\mathbf{x}_k\right), \mathbf{1}\right\rangle - 2\gamma_1\left\langle \omega\left(\mathfrak{T}_k^{(i)}(\log(S_k/S_{k-1}))\mathbf{x}_k\right), \mathbf{1}\right\rangle}{\left\langle \omega\left(\mathfrak{O}_k^{(i)}\mathbf{x}_k\right), \mathbf{1}\right\rangle}}. \tag{5.36}$$

5.4.2 Parameter estimates

The HMM filtering technique will be illustrated in this Subsection to calibrate the model to historical data. Monthly data on the 10-year Canada government bond yields from 1950 to 2011 were obtained from the Federal Reserve Economic Data website. For the mortality data, we use yearly cohort data for Canadian males between age 50 (in 1951) and age 110 (in 2011), which are available from the Human Mortality Database. For the stock index data, we choose the monthly data of iShares Core S&P 500 ETF from 2002 to 2011; these data are obtained from Yahoo Finance. The behaviours of the various historical data are presented in Figure 5.1.

In the filtering algorithm, the dataset is divided into batches. In each algorithm step, we calculate, by processing a batch of data points, $\omega\left(\mathfrak{I}_k^{(ij)}\mathbf{x}_k\right)$, $\omega\left(\mathfrak{O}_k^{(i)}\mathbf{x}_k\right)$ and $\omega\left(\mathfrak{T}_k^{(i)}(g)\mathbf{x}_k\right)$ recursively employing equations (5.28)– (5.30). Parameters are updated after each step applying equations (5.31)–(5.36). Initial values of the parameters are obtained by the using maximum likelihood method. We use these initial values for the first step of the algorithm.

The interest rate data is processed in batches of 20 data values; that is, the parameters are updated approximately every two years. For each step, the parameters $\widehat{p}_{ij}$, $\widehat{\alpha}_{2,i}$ and

Figure 5.1: Behaviour of various historical data

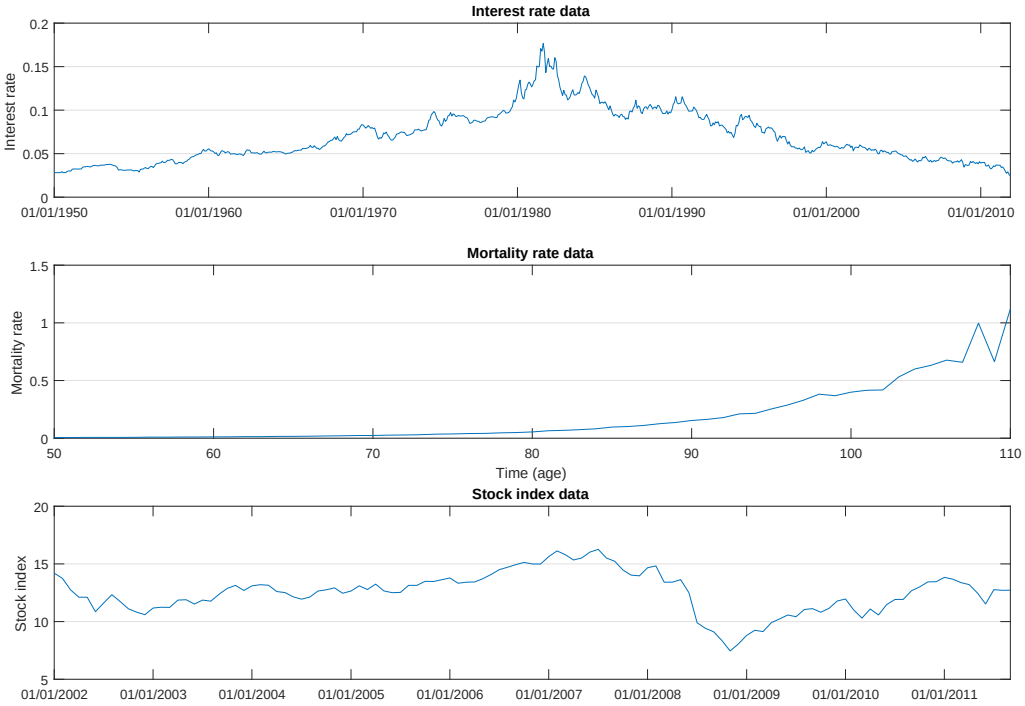

$\widehat{\alpha}_{3,i}$, for $i, j = 1, \ldots, N$, are calculated via equations (5.31), (5.32) and (5.33), respectively. They can then be utilised in the recovery of the original model's parameters $\widehat{b}_i$ and $\widehat{\sigma}_i$, for $i = 1, \ldots, N$. Figures 5.2 and 5.3 display the evolution of parameter estimates of interest rate model under the 2-state and 3-state settings, respectively. For the 2-state model, the mean-reversion level $\widehat{b}$ in state 2 increases steadily before the 20th step and then decreases afterwards. This is in agreement with the behaviour of the historical data. The state-2 volatility increases dramatically between the 17th and 20th steps because of the drastic change in interest rates. It can be observed that the 3-state model captures these behaviors in various different states more adequately.

The mortality rate data is processed in batches of 2 data points, which means the parameters are updated every two years. For $i = 1, \ldots, N$, $\widehat{\beta}_{2,i}$ is computed using equation (5.34) thereby giving $\widehat{\xi}$. Figures 5.4 and 5.5 depict the parameter estimates' dynamics in the mortality model. The volatility increases substantially after the 25th step. This suggests that the volatility could be higher at older ages. Therefore, the HHM is appropriate for mortality modelling because it is able to capture the random occurrence of both low volatility and high volatility states.

The processing of the stock index data is performed with 3 data points in each batch; thus, the parameters are updated every quarter. For $i = 1, \ldots, N$, $\widehat{\gamma}_{1,i}$ and $\widehat{\gamma}_{2,i}$ are determined through equations (5.35) and (5.36). Figures 5.6 and 5.7 exhibit the evolution of parameter estimates for the stock index model. There is a generally continuous trend of historical data values falling in large magnitude during the period Jan 2008 – Jan 2009. This leads to a decrease in m and an increase in η.

Figure 5.2: Evolution of interest-rate model's parameters under the 2-state setting

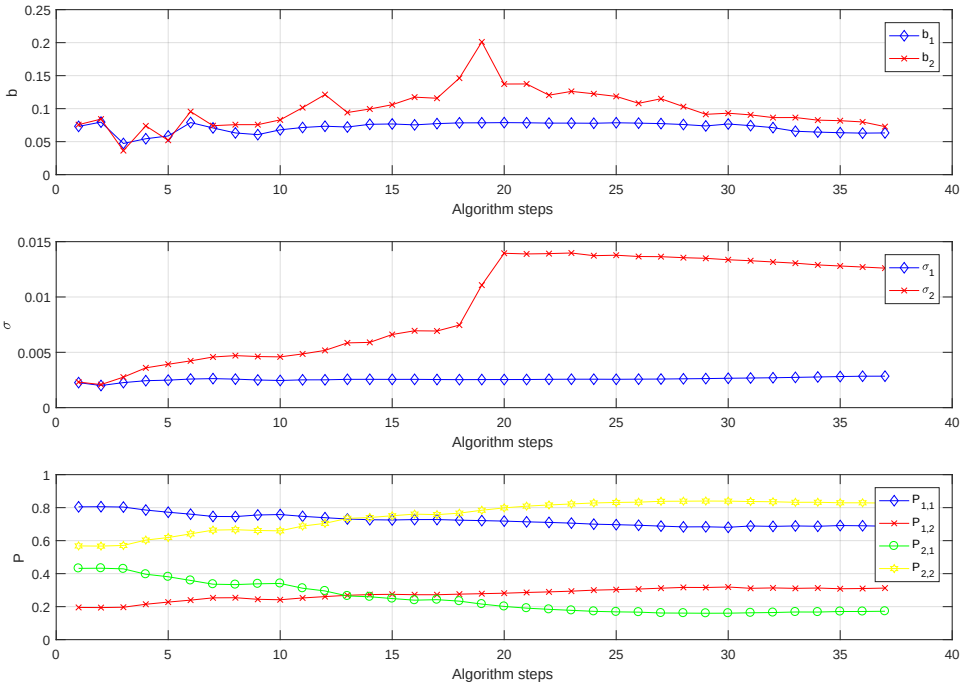

Table 5.1 shows the estimated parameters in the last algorithm step. Clearly, parameter values in different states could be significantly different. To quantify the variance of these parameter estimates, we compute the Fisher information $\mathcal{I}$. The maximum likelihood estimate is asymptotically normally distributed with variance $\mathcal{I}^{-1}$. Consistent to the concept of evolving parameter estimates, the Fisher information values could also be updated in each algorithm step. The Fisher information of an estimated parameter can be calculated by taking the expectation of the second derivatives of the log-likelihood function with respect to the parameter in consideration. The Fisher information for each regime-switching parameter is given by

Figure 5.3: Evolution of interest-rate model's parameters under the 3-state setting

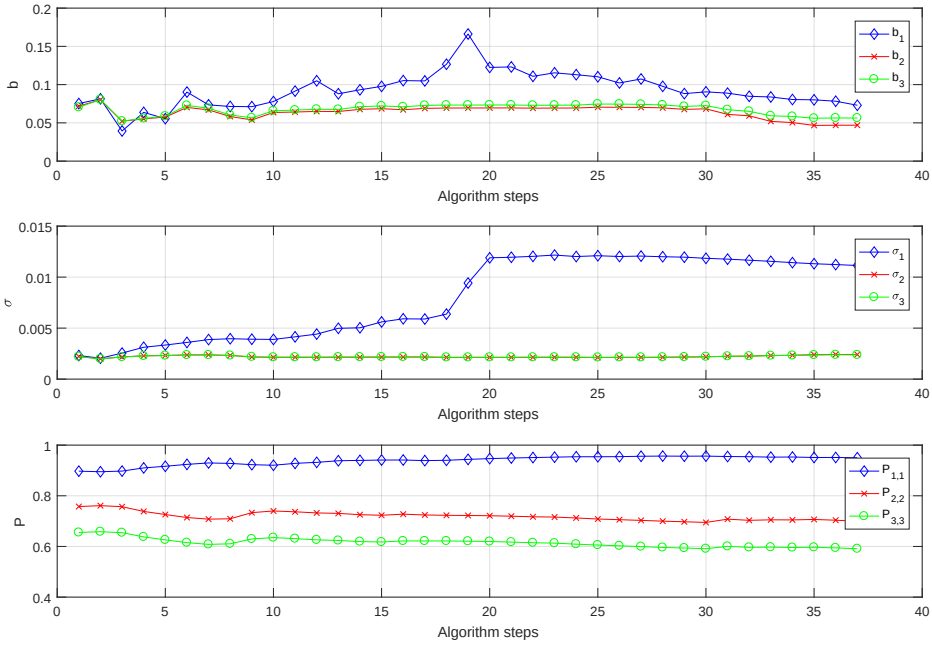

$$\mathcal{I}(\alpha_{2,i}) = \frac{\omega\left(\mathfrak{O}_k^{(i)}\right)}{\alpha_{3,i}^2}, \tag{5.37}$$

$$\begin{aligned}\mathcal{I}(\alpha_{3,i}) = &-\frac{\omega\left(\mathfrak{O}_k^{(i)}\right)}{\alpha_{3,i}^2} + \frac{\omega\left(\mathfrak{T}_k^{(i)}(r_k^2)\right) + \alpha_1^2\omega\left(\mathfrak{T}_k^{(i)}(r_{k-1}^2)\right) + \alpha_{2,i}^2\omega\left(\mathfrak{O}_k^{(i)}\right)}{\alpha_{3,i}^4/3} \\ &+ \frac{-2\alpha_1\omega\left(\mathfrak{T}_k^{(r)}(r_k r_{k-1})\right) - 2\alpha_{2,i}\omega\left(\mathfrak{T})_k^{(i)}(r_k)\right) + 2\alpha_1\alpha_{2,i}\omega\left(\mathfrak{T}_k^{(i)}(r_{k-1})\right)}{\alpha_{3,i}^4/3},\end{aligned} \tag{5.38}$$

$$\mathcal{I}(\beta_{2,i}) = -\frac{\omega\left(\mathfrak{O}_k^{(i)}\right)}{\beta_{2,i}^2} + \frac{\omega\left(\mathfrak{T}_k^{(i)}(\mu_k^2)\right) + \alpha_1^2\omega\left(\mathfrak{T}_k^{(i)}(\mu_{k-1}^2)\right) - 2\alpha_1\omega\left(\mathfrak{T}_k^{(i)}(\mu_k\mu_{k-1})\right)}{\beta_{2,i}^4/3}, \tag{5.39}$$

$$\mathcal{I}(\gamma_{1,i}) = \frac{\omega\left(\mathfrak{O}_k^{(i)}\right)}{\gamma_{2,i}^2}, \tag{5.40}$$

$$\begin{aligned}\mathcal{I}(\gamma_{2,i}) = &\frac{\omega\left(\mathfrak{T}_k^{(i)}(\log(S_k/S_{k-1})^2)\right) + \gamma_1^2\omega\left(\mathfrak{O}_k^{(i)}\right) - 2\gamma_1\omega\left(\mathfrak{T}_k^{(i)}(\log(S_k/S_{k-1}))\right)}{\gamma_{2,i}^4/3} \\ &- \frac{\omega\left(\mathfrak{O}_k^{(i)}\right)}{\gamma_{2,i}^2}.\end{aligned} \tag{5.41}$$

Figure 5.4: Evolution of mortality-rate model's parameters under the 2-state setting

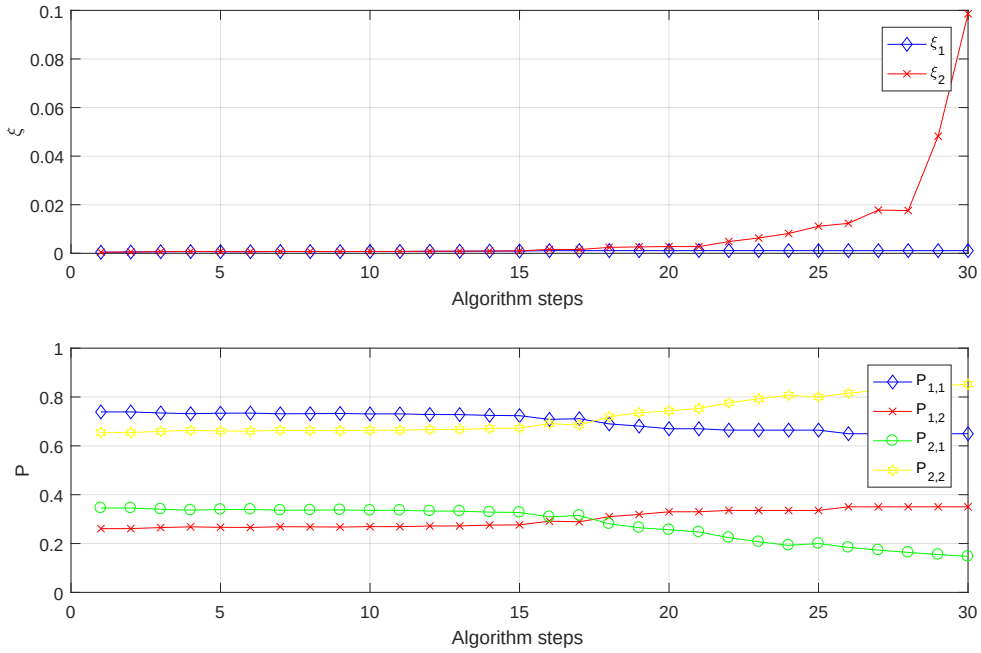

The respective standard error for each regime-switching parameter can be obtained via using equations (5.37)– –(5.41). The results are shown in Table 5.2, from which we see that the standard errors are relatively small implying very good precision of parameter estimates calculated using our proposed method.

Table 5.1: Parameter estimates in the final algorithm step

	state	$\widehat{a}$	$\widehat{b}$	$\widehat{\sigma}$	$\widehat{c}$	$\widehat{\xi}$	$\widehat{m}$	$\widehat{\eta}$
1-state	1	0.0559	0.0683	0.0102	0.0852	0.0818	0.0025	0.1666
2-state	1	0.0559	0.0632	0.0028	0.0852	0.0011	0.0812	0.1213
	2	0.0559	0.0728	0.0126	0.0852	0.0986	-0.0640	0.1970
3-state	1	0.0559	0.0730	0.0111	0.0852	0.0010	0.0762	0.1194
	2	0.0559	0.0470	0.0024	0.0852	0.0012	0.0417	0.1384
	3	0.0559	0.0563	0.0024	0.0852	0.1016	-0.0854	0.2132

Figure 5.5: Evolution of mortality-rate model's parameters under the 3-state setting

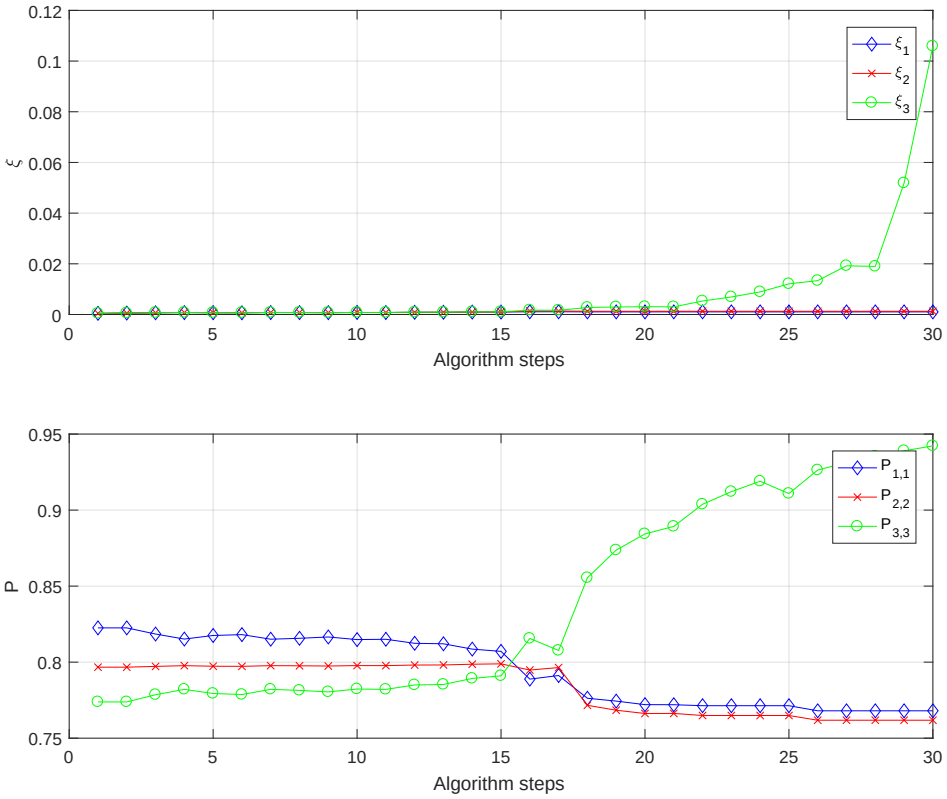

Table 5.2: Standard errors for the parameter estimates in the final algorithm step

	state	$\widehat{b}$	$\widehat{\sigma}(\times 10^{-3})$	$\widehat{\xi}(\times 10^{-3})$	$\widehat{m}$	$\widehat{\eta}$
1 state	1	0.0023	0.2665	7.4630	0.0054	0.0111
2-state	1	0.0018	0.1238	0.1770	0.0012	0.0119
	2	0.0035	0.4085	1.4124	0.0058	0.0177
3-state	1	0.0027	0.3161	0.2126	0.0071	0.0146
	2	0.0017	0.1961	0.2689	0.0079	0.0162
	3	0.0022	0.2539	11.5363	0.0110	0.0226

To determine the optimal number of regimes appropriate for a given data set, we use the log-likelihood value, Akaike information criterion (AIC), and Bayesian information criterion (BIC). Both the AIC and BIC consider the log likelihood function and the number of parameters as inputs for model selection. The respective AIC and BIC formulae are given by

$$\text{AIC} = -2\log\mathcal{L} + 2 \times (\text{number of parameters})$$

Figure 5.6: Evolution of stock-index model's parameters under the 2-state setting

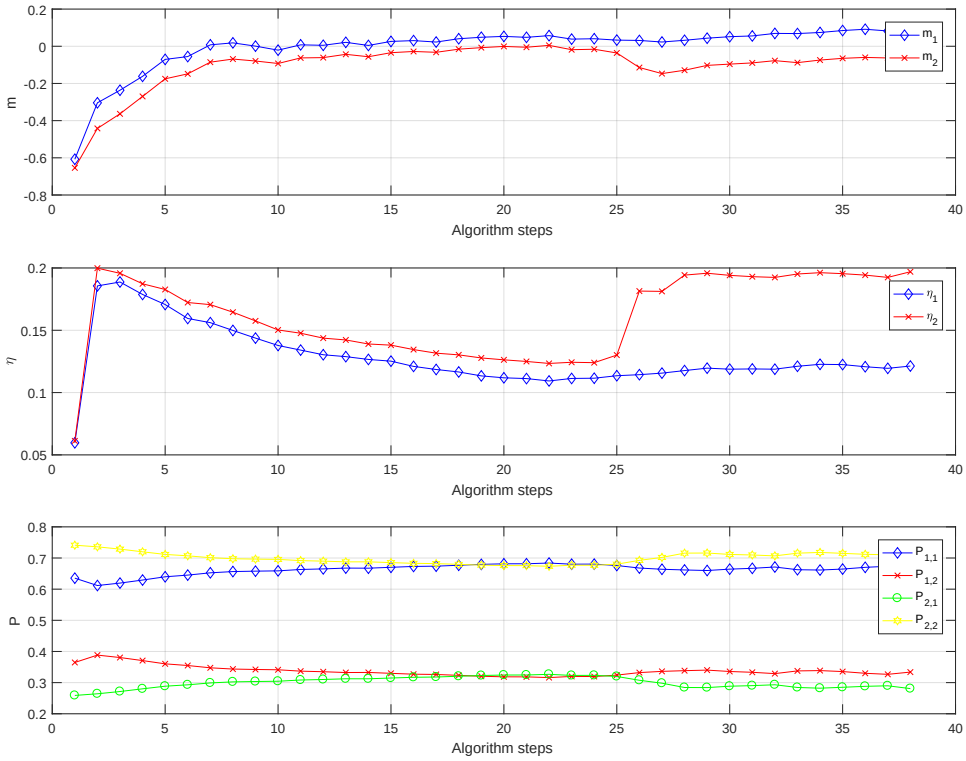

and

$$\text{BIC} = -2\log\mathcal{L} + (\text{number of parameters}) \times \log\ (\text{number of observations}),$$

where $\mathcal{L}$ refers to the likelihood function. The model with the lowest AIC or BIC would be the most preferable model. The results are shown in Table 5.3; numbers in bold are the lowest and correspond to the best model. Our numerical results illustrate that the 2-state model is the most appropriate (giving the best balance between maximising likelihood and estimating the number of parameters) for our historical data. Although the 3-state model may have higher log-likelihood values, the greater number of parameters involved penalises the AIC and BIC values.

To assess the prediction performance of various model settings, we examine the one-step ahead predictions. The one-step ahead forecasts for the interest rate, mortality rate, and stock index are computed as

$$\mathbb{E}^{\mathcal{P}}\left[r_{k+1}|\mathcal{F}_k\right] = \alpha_1 r_k + \langle \boldsymbol{\alpha}_2, \mathbf{P}\widehat{\mathbf{x}}_k \rangle, \tag{5.42}$$

Figure 5.7: Evolution of stock-index model's parameters under the 3-state setting

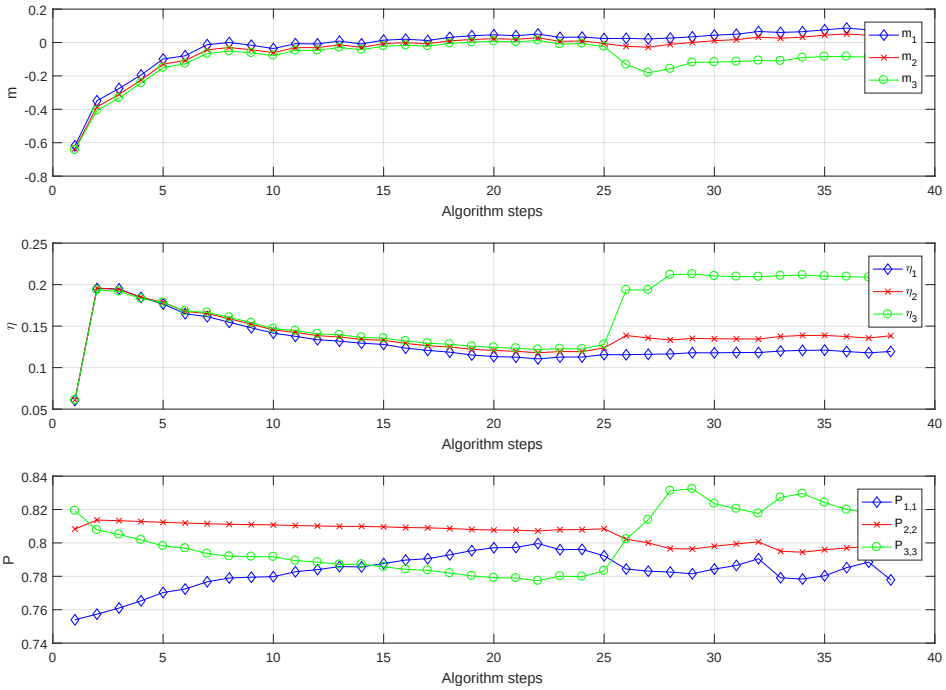

$$\mathbb{E}^{\mathcal{P}}\left[\mu_{k+1}|\mathcal{F}_k\right] = \beta_1\mu_k \tag{5.43}$$

and

$$\mathbb{E}^{\mathcal{P}}\left[\log\left(\frac{S_{k+1}}{S_k}\right)\middle|\mathcal{F}_k\right] = \langle\boldsymbol{\gamma}_1, \mathbf{P}\widehat{\mathbf{x}}_k\rangle + \langle\boldsymbol{\gamma}_2, \mathbf{P}\widehat{\mathbf{x}}_k\rangle, \tag{5.44}$$

where $\widehat{\mathbf{x}}_k = \mathbb{E}^{\mathcal{P}}[\mathbf{x}_k|\mathcal{F}_k]$.

We generate the one-step predictions for r_t, μ_t and S_t under the 1-state, 2-state and 3-state models using equations (5.42), (5.43), and (5.44), respectively. To assess the goodness of fit of the one-step ahead prediction, we adopt three criteria: root mean square error (RMSE), mean absolute error (MAE), and relative absolute error (RAE); the results are presented in Table 5.4. Although the differences are small, the 2-state model yields a better prediction performance than the 1-state and 3-state models.

Table 5.3: AIC and BIC values under different model settings. Numbers in bold represent the best among others.

Risk factor		Log likelihood	AIC	BIC
Interest rate	1-state	3256	-6508	-6499
	2-state	**3404**	**-6796**	**-6768**
	3-state	3388	-6753	-6697
Mortality rate	1-state	72.2417	-142.4833	-140.3890
	2-state	187.8974	**-367.7948**	**-359.4175**
	3-state	**191.1901**	-364.3801	-345.5310
Stock index	1-state	183.1841	-362.3682	**-356.8958**
	2-state	188.7342	**-365.4684**	-349.0512
	3-state	**192.4256**	-360.8513	-328.0169

Table 5.4: Error analysis under different model settings

Risk factor		RMSE ($\times 10^{-3}$)	MAE($\times 10^{-3}$)	RAE($\times 10^{-2}$)
Interest rate	1-state	2.95378	1.85806	7.50994
	2-state	2.95309	1.85697	7.50103
	3-state	2.95394	1.85712	7.50362
Mortality rate	1-state	22.5459	13.3687	7.7110
	2-state	22.5459	13.3687	7.7110
	3-state	22.5459	13.3687	7.7110
Stock price	1-state	48.5182	35.9969	1.6601×10^{19}
	2-state	48.3853	35.7898	1.8231×10^{3}
	3-state	48.4688	35.7969	1.2487×10^{3}

5.4.3 GMMB pricing

In this subsection, we present implementation results for the valuation of a GMMB. The parameter values for our pricing are those given in Table 5.1. Our proposed method, i.e., equation (5.21), is used to calculate GMMB prices efficiently; we set $\alpha = 1.5$, $M = 512$ and $\Delta v = 0.2$. Under this method, we do not need the trajectories of r_t, μ_t and S_t from time 0 to T; this then reduces significantly the computing time.

The Monte Carlo simulation method, applied to equation (5.5) is considered as our benchmark. To implement equation (5.5) directly, we generate sample paths of r_t, μ_t, S_t as well

as $\mathbf{x}_t$ from time 0 to T under measure Q. To do this, we divide each year into 252 time intervals with fixed length $\Delta t = \frac{1}{525}$. Applying the Euler discretisation scheme, we approximate the evolution of r_t, μ_t, S_t and $\mathbf{x}_t$ over $[0, T]$. The discresation of $\mathbf{x}_t$ is as per equation (5.27) whilst the respective discretisations for r_t, μ_t and S_t, under Q, are

$$r_{k+1} = r_k + a(b_k - r_k)\Delta t + \sigma_k \sqrt{\Delta t}\epsilon_{k+1},$$

$$\mu_{k+1} = \mu_k + c\mu_k\Delta t + \xi_k \sqrt{\Delta t}\left(\rho_1\epsilon_{k+1} + \sqrt{\rho_1^2}\epsilon'_{k+1}\right)$$

and

$$S_{k+1} = S_k + r_k S_k \Delta t + \eta_k S_k \sqrt{\Delta t}\left(\rho_2\epsilon_{k+1} + \sqrt{1-\rho_2^2}\epsilon''_{k+1}\right),$$

where $\{\epsilon_k\}$, $\{\epsilon'_k\}$ and $\{\epsilon''_k\}$ are independent sequences of standard normal random variables. The integrals in equation (5.5) are evaluated by applying the Trapezoidal Rule.

Numerical results from our proposed method and the Monte Carlo simulation method given various values of ρ_1 and ρ_2 are displayed in Table 5.5. For the GMMB pricing, we set the guaranteed level $G = 20$ and the maturity $T = 10$ viewed at year 2011. This means we are assuming $T = 0$ at year 2011. Further, it is supposed that the policyholder is aged 50 at time 0. We choose observed data points in 2011 for the values of r_0, μ_0 and S_0. The results from the Monte Carlo method are obtained employing 1,000,000 samples via parallel simulation with 8 cores in Matlab. The numbers enclosed in parenthesis are standard errors of values resulting from the simulation method. We can see that the prices from our proposed method and the benchmark are very close. It is worth noting that the results from our proposed method are within the 95% confidence interval of the results by the simulation method. Furthermore, prices increase as ρ_1 and ρ_2 vary from negative to positive. This is consistent with the fact that negative correlation aids in diversification, combatting the combined effect of risk factors that move together. The average computing time of our proposed method is considerably less (by 99%) than that of the simulation method. This implies that our proposed method is not only highly accurate but is also remarkably efficient.

Table 5.5: GMMB prices with different parameter values and number of states

Setting	(ρ_1, ρ_2)	Our proposed method	Monte-Carlo simulation
1-state	$(-0.9, -0.9)$	2.4395	2.4306 (0.0020)
	$(-0.5, -0.5)$	2.5430	2.5389 (0.0021)
	$(0, 0)$	2.9063	2.9178 (0.0026)
	$(0.5, 0.5)$	3.4995	3.5054 (0.0032)
	$(0.9, 0.9)$	3.7894	3.8112 (0.0042)
2-state	$(-0.9, -0.9)$	2.5945	2.6005 (0.0026)
	$(-0.5, -0.5)$	2.6929	2.6938 (0.0028)
	$(0, 0)$	2,9354	2.9300 (0.0031)
	$(0.5, 0.5)$	3.3067	3.3040 (0.0036)
	$(0.9, 0.9)$	3.6989	3.6875 (0.0041)
3-state	$(-0.9, -0.9)$	2.6032	2.5964 (0.0023)
	$(-0.5, -0.5)$	2.7331	2.7042 (0.0029)
	$(0, 0)$	2.9599	2.9653 (0.0037)
	$(0.5, 0.5)$	3.3045	3.2931 (0.0041)
	$(0.9, 0.9)$	3.5231	3.5198 (0.0045)
Average computing time		43 secs	4.71 hrs

We vary the values of guaranteed level G and maturity time T to see how the GMMB price responds. Results are depicted in Figure 5.8. The GMMB price increases as G increases; this is because a higher guaranteed level would lead insurers to set a higher reserve, and hence a higher premium. The GMMB price decreases as T increases; this is justified by the fact that interest and mortality rates contributed to the discounting of the future payoff. Therefore, the longer the maturity, the greater the effect of the discounting, and consequently the lower the price. We also investigate how interest rate, mortality rate and stock index level affect the GMMB price. We look into the corresponding percent change of GMMB price when we vary the values of r_0, μ_0 and S_0 ranging from -20% to 20% of their current value.

Figure 5.9 shows that the GMMB price decreases for any risk factor that increases. Given the -20% to 20% change, the GMMB price changes roughly from -10% to 10% when r_0 is varied, from -1% to 1% when μ_0 is perturbed, and from -40% to 40% when S_0 is changed. Thus, the stock index has the most significant influence on the price. The impact of mortality rate is relative low because the mortality rate is still low for an individual at aged 50.

However, the mortality will increase at older age, and hence, in that case it will have much greater influence on the price.

Figure 5.8: GMMB prices with various values of G and T

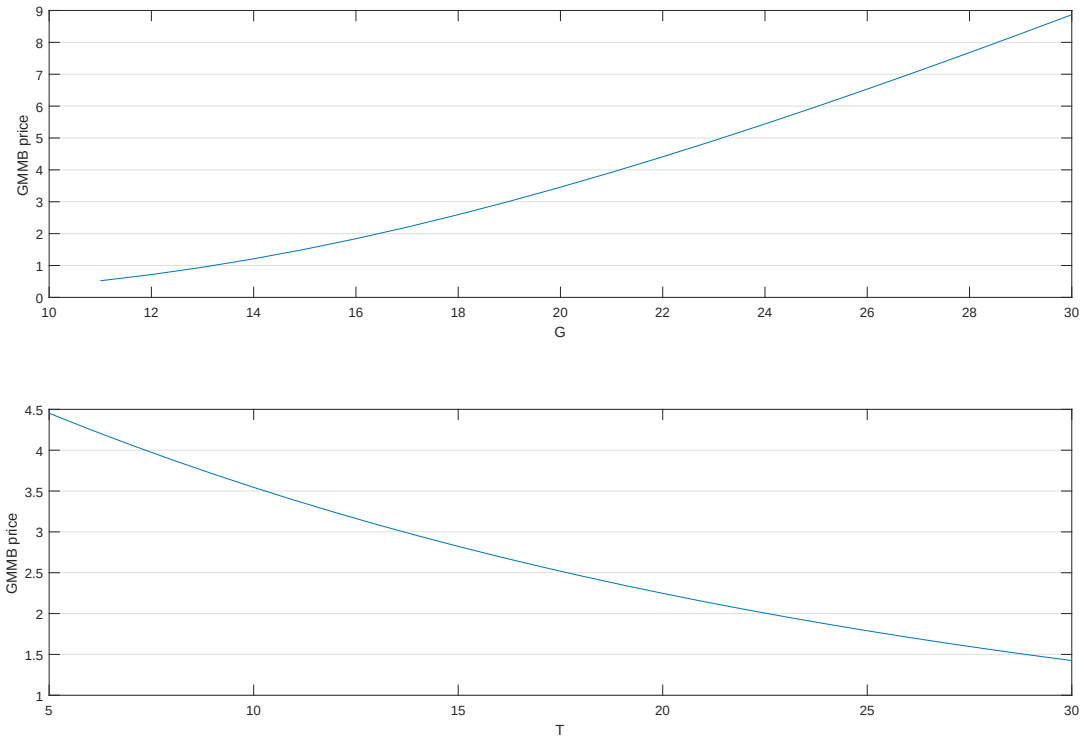

Figure 5.9: Sensitivity of GMMB prices to r_0, μ_0 and S_0

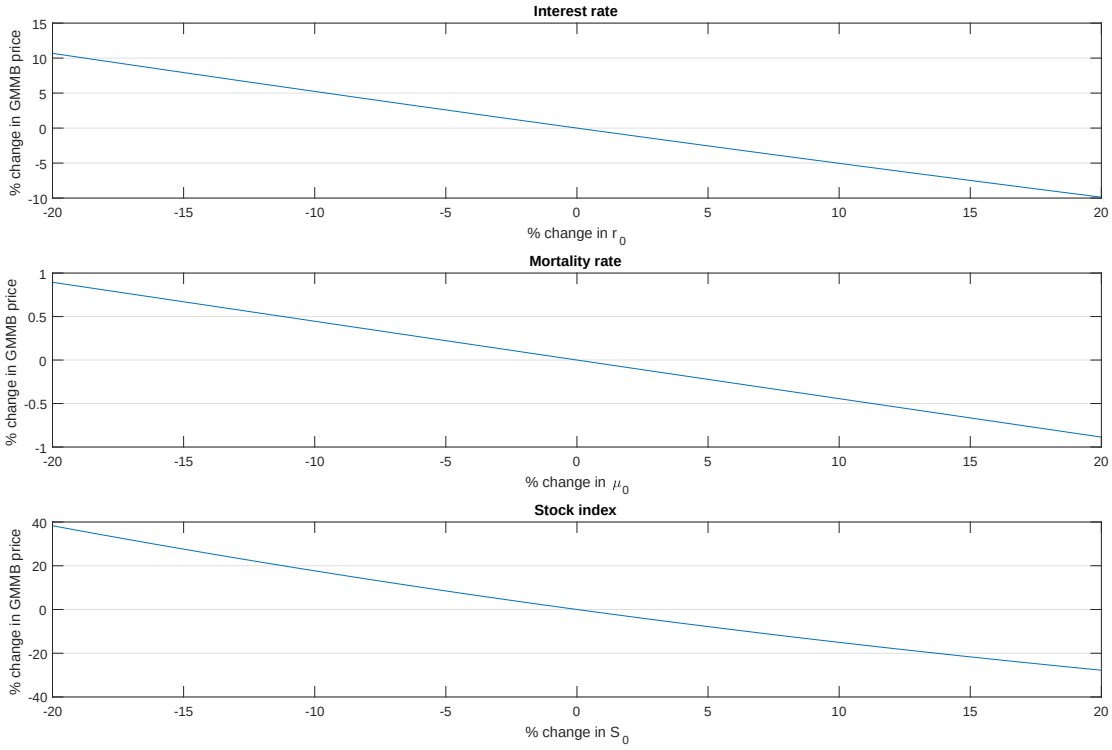

5.5 Conclusion

We developed an integrated framework for the valuation of GMMB. The dynamics of interest rate, mortality rate, and stock index are all driven by an HMM. These three risk factors are also correlated via their diffusion components; to some extent there is an additionally embedded correlation with the fact that one underlying Markov chain drives the switching of regimes in these risk processes. The change of measure technique, featuring the forward measure and endowment-risk-adjusted measure, was employed to obtain a closed-form regime-switching exponential-affine solution for the endowment, and in turn this facilitates the pricing evaluation of the GMMB.

The Fourier transform is used to price the GMMB numerically. Numerical results demonstrated that our proposed method is significantly more efficient, with high level of accuracy, than the Monte Carlo simulation method. Our parameter estimation made use of the recursive HMM-based filtering technique. Calibration to historical data was performed, and results showed that the 2-state set up is the most adequate in capturing the dynamics of the

risk factors involved in the proposed model.

Our work concentrated on the valuation of GMMB and calibration of model parameters. However, in practice, risk measures, such as the value-at-risk and conditional tail expectation, are also essential in risk management. These can be achieved under our proposed modelling framework by considering the distribution of the payoff under the objective measure. Evaluating the Greeks is also important to hedge the GMMB contract. This can be done by differentiating the pricing formula with respect to various parameters similar to the idea in Ignatieva et al. [17].

Our modelling framework is flexible and it can be extended in many ways. We may adopt the Cox-Ingersoll-Ross (CIR) model for the interest rate instead of the Vasicek model and introduce regime switching as well. To better describe the dynamics of mortality rate, we may use the model in Lee and Carter [18] in which both age and year factors for mortality are considered. A higher-order HMM could be added to enrich the model further; see Mamon and Elliott [21] for example. Our modelling framework can also be utilised for other GMBs such as the GMDB, GMAB and GMIB. One may include the analysis of the withdrawal feature in a contract, allows the policyholder to withdraw some money from his fund before the maturity date. All of these extensions, as this research's natural directions, will lead to certain computational challenge requiring new methods and approaches.

References

[1] D. Bauer, A. Kling, and J. Russ. A universal pricing framework for guaranteed minimum benefits in variable annuities. *ASTIN Bulletin*, 38(2):621–651, 2008.

[2] M. Brennan and E. Schwartz. The pricing of equity-linked life insurance policies with an asset value guarantee. *Journal of Financial Economics*, 3(3):195–213, 1976.

[3] P. Carr and D. Madan. Option valuation using the fast Fourier transform. *Journal of Computational Finance*, 2(4):61–73, 1999.

[4] Z. Chen, K. Vetzal, and P. Forsyth. The effect of modelling parameters on the value of GMWB guarantees. *Insurance: Mathematics and Economics*, 43(1):165–173, 2008.

[5] J. Da Fonseca and J. Ziveyi. Valuing variable annuity guarantees on multiple assets. *Scandinavian Actuarial Journal*, 2017(3):209–230, 2017.

[6] M. Dai, Y. Kwok, and J. Zong. Guaranteed minimum withdrawal benefit in variable annuities. *Mathematical Finance*, 18(4):595–611, 2008.

[7] P. Date, R. Mamon, and A. Tenyakov. Filtering and forecasting commodity futures prices under an hmm framework. *Energy Economics*, 40:1001–1013, 2013.

[8] R. Elliott. Exact adaptive filters for Markov chains observed in gaussian noise. *Automatica*, 30(9):1399–1408, 1994.

[9] R. Elliott and T. Siu. On Markov-modulated exponential-affine bond price formulae. *Applied Mathematical Finance*, 16(1):1–15, 2009.

[10] R. Elliott, L. Chan, and T. Siu. Option pricing and Esscher transform under regime-switching. *Annals of Finance*, 1(4):423–432, 2005.

[11] C. Erlwein and R. Mamon. An online estimation scheme for a Hull–White model with HMM-driven parameters. *Statistical Methods and Applications*, 18(1):87–107, 2009.

[12] K. Fan, Y. Shen, T. Siu, and R. Wang. An FFT approach for option pricing under a regime-switching stochastic interest rate model. *Communications in Statistics-Theory and Methods*, 46(11):5292–5310, 2017.

[13] R. Feng and J. Vecer. Risk based capital for guaranteed minimum withdrawal benefit. *Quantitative Finance*, 17(3):471–478, 2017.

[14] M. Fung, K. Ignatieva, and M. Sherris. Systematic mortality risk: An analysis of guaranteed lifetime withdrawal benefits in variable annuities. *Insurance: Mathematics and Economics*, 58:103–115, 2014.

[15] H. Gao, R. Mamon, and X. Liu. Pricing a guaranteed annuity option under correlated and regime-switching risk factors. *European Actuarial Journal*, 5(2):309–326, 2015.

[16] M. Hardy. *Investment Guarantees: Modeling and Risk Management for Equity-Linked Life Insurance*. John Wiley & Sons, New Jersey, 2003.

[17] K. Ignatieva, A. Song, and J. Ziveyi. Pricing and hedging of guaranteed minimum benefits under regime-switching and stochastic mortality. *Insurance: Mathematics and Economics*, 70:286–300, 2016.

[18] R. Lee and L. Carter. Modeling and forecasting US mortality. *Journal of the American Statistical Association*, 87(419):659–671, 1992.

[19] R. Liu, Q. Zhang, and G. Yin. Option pricing in a regime-switching model using the fast fourier transform. *International Journal of Stochastic Analysis*, 2006, 2006.

[20] E. Luciano and E. Vigna. Non-mean reverting affine processes for stochastic mortality. *Carlo Alberto Notebook*, 30/06:ICER WP 4/05, 2005.

[21] R. Mamon and R. Elliott. *Hidden Markov Models in Finance: Further Developments and Applications, Volume II*. Springer, 2014.

[22] C. Marshall, M. Hardy, and D. Saunders. Valuation of a guaranteed minimum income benefit. *North American Actuarial Journal*, 14(1):38–58, 2010.

[23] Mo. Milevsky and T. Salisbury. Financial valuation of guaranteed minimum withdrawal benefits. *Insurance: Mathematics and Economics*, 38(1):21–38, 2006.

[24] Z. Palmowski and T. Rolski. A technique for exponential change of measure for Markov processes. *Bernoulli*, 8(6):767–785, 2002.

[25] J. Peng, K. Leung, and Y. Kwok. Pricing guaranteed minimum withdrawal benefits under stochastic interest rates. *Quantitative Finance*, 12(6):933–941, 2012.

[26] G. Piscopo and S. Haberman. The valuation of guaranteed lifelong withdrawal benefit options in variable annuity contracts and the impact of mortality risk. *North American Actuarial Journal*, 15(1):59–76, 2011.

[27] Y. Shen and T. Siu. Longevity bond pricing under stochastic interest rate and mortality with regime-switching. *Insurance: Mathematics and Economics*, 52(1):114–123, 2013.

Chapter 6

Setting risk margin for claim liabilities in accordance with IFRS 17

6.1 Introduction

The international Accounting Standards Board is responsible for setting accounting standards for many countries that are part of the Organization for Economic Co-operation and Development. One of its standards, known as the International Financial Reporting Standards (IFRS) 17, deals with insurance contracts (see International Accounting Standards Board [6]). The Canadian Accounting Standards Board will adopt IFRS 17 without modification starting 01 January 2022. The preparation for implementing the new standard engendered substantial efforts and upgraded systems, processes and controls.

In IFRS 17, the general measurement model for liabilities of insurance contracts is the Building Block Approach (BBA). It affords a comprehensive and coherent framework that provides information reflecting many features of insurance contracts. Under the BBA, the value of insurance contracts is measured as the sum of four blocks described as follows:

- **Block 1:** Sum of the future cash flows that relate directly to the fulfillment of the contractual obligations;
- **Block 2:** The value of the future cash flows;
- **Block 3:** Risk adjustment, representing the compensation for bearing the uncertainty about the cash flows;
- **Block 4:** Contractual service margin (CSM), representing the unearned profit that will be recognised in profit or loss as services are provided.

In this chapter, we address the evaluation of risk margins (Block 3) of insurance policies by proposing an efficient and accurate method in risk margins' estimation under IFRS 17. It has to be noted that IFRS 17 does not provide specific prescriptions for risk margin calculations, nor does it mandate a particular method to determine risk margin.Although it does not restrict the usage of any technique, it requires that the risk margin should reflect the compensation that the entity requires for bearing the uncertainty about the amount and timing of the cash flows that arises from non-financial risk. Risk margins can be computed using various risk measures, which are justified by the principles and concepts in probability theory and statistics.

We consider the claims development triangle, which will be the basis for our risk margin calculation. The claim development triangle is specifically used for forecasting future claims and estimating outstanding claim liabilities. Some methods for the estimation of outstanding liabilities include the chain-ladder method, Bornhuetter-Ferguson method and frequency-severity method; an overview of such methods are given in Taylor [18] and Wüthrich and Merz [21]). Models for claims and supporting the above methods include the log-normal model (Barnett and Zehnwirth [1]), gamma model (Zehnwirth [22] and Mack [10]), distribution-free approach (Mack [11]), and over-dispersed model (Renshaw and Verrall [17]). In our case, we shall develop and customise the paid-incurred chain model proposed in Merz and Wüthrich [12] to predict the future claims using Ontario's automobile claim data. Our methodology combines the principal elements of Hertig [5] for paid losses and Gogol [4] for incurred claims.

Some stochastic claim reserving methods can replicate the reserve estimates from the deterministic claim reserving methods such as the chain-ladder and Bornhuetter-Ferguson methods. One noticeable advantage of the stochastic claim reserving methods is that they are able to attach a probability or confidence level to describe the accuracy of a reserve estimate for outstanding liabilities. To evaluate the risk margins of insurance policies, the distribution of the outstanding claim liabilities need to be determined. The general approach is to obtain the empirical cumulative distribution function via Monte-Carlo (MC) simulation. The distribution could be approximated using normal or log-normal distributions. Here, we also employ the moment-based density method Provost [16] as an alternative. This method was applied to risk measurement and management of insurance policies including guaranteed minimum benefits in Gao et al. [3] and Zhao et al. [23] as well as aggregate losses in Jin et al. [8].

This chapter is organised as follows. In section 2, the paid-incurred chain model is developed and the formula for the claim reserves is provided. Four risk-margin computation methods are described in section 3. In section 4, numerical examples based on historical data are discussed. Moment-based density approximation is applied for the approximation of distribution of claim reserves. In section 5, the simulation's distribution assumption is statistically validated. Finally, some concluding remarks are given in section 6.

6.2 Model description

A claim-development triangle is an essential method to organise data for actuarial analyses and claim reserving. The triangle (see Table 6.1) depicts how the claims in each accident year are developing to their ultimate value. This data organisation greatly facilitates the comparison of the development history experienced in an accident year. In this method, we consider two types of triangles: (i) incurred claims, which refer to the reported claim amounts and (ii) paid losses, which refer to the payments made for the claims. The paid losses should be less than the incurred claims in the same development year. Nonetheless, they should have the same values ultimately; that is, all reported claims must be paid off at the end of the lifetime of the policies.

Table 6.1: An illustration of the claims development triangle. The left-hand panel displays the cumulative paid losses whilst the right-hand shows the cumulative incurred claims.

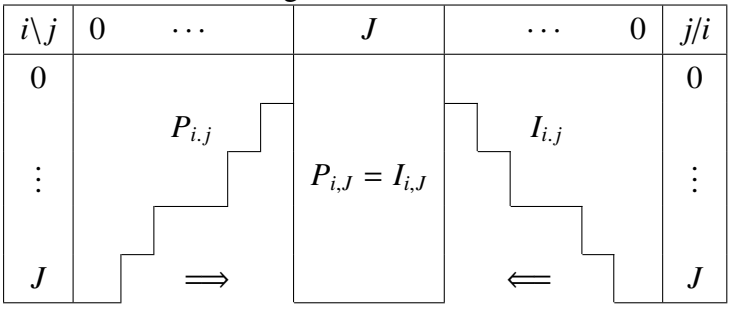

The fundamental ideas of the paid-incurred chain method can be found in Merz and Wüthrich [12]. It is designed for analysing information on both incurred claims and paid losses data. We denote the accident year by i ($0 \leq i \leq J$) and the development year by j ($0 \leq j \leq J$). Here, J refers to the largest development year. Let $I_{i,j}$ be the cumulative incurred claims in accident year i after j development years and $P_{i,j}$ be the corresponding cumulative paid losses. We further *assume* that all the claims are settled after J years, i.e., $P_{i,J} = I_{i,J}$. Table

6.1 imparts graphically the implementation structure of this method. Define the sets

$$\mathfrak{B}_j^P = \{P_{i,l} : 0 \le i \le J, 0 \le l \le j\},$$

$$\mathfrak{B}_j^I = \{I_{i,l} : 0 \le i \le J, 0 \le l \le j\}$$

and

$$\mathfrak{B}_j = \mathfrak{B}_j^P \cup \mathfrak{B}_j^I$$

as the paid losses data, incurred claims data and joint data information up to development year j, respectively.

Consider a series of independent and identically distributed random variables $\{\xi_{1,1}, \ldots, \xi_{J,J}, \zeta_{1,1}, \ldots, \zeta_{J,J}\}$. In our case, we shall assume that they follow the Gaussian distributions; that is,

$$\xi_{i,j} \sim N(\phi_j, \sigma_j^2), \quad 0 \le i \le J \text{ and } 0 \le j \le J,$$

$$\zeta_{i.j} \sim N(\varphi_j, \tau_j^2), \quad 0 \le i \le J \text{ and } 0 \le j \le J,$$

where ϕ_j, σ_j, φ_j and τ_j are constants for $1 \le j \le J$.

The cumulative paid losses $P_{i,j}$ are determined by the recursion

$$P_{i,j} = P_{i,j-1} e^{\xi_{i,j}}$$

with initial value $P_{i,0} = e^{\xi_{i,0}}$. For the cumulative incurred claims $I_{i,I}$, we have the backward recursion

$$I_{i,j-1} = I_{i,j} e^{-\zeta_{i.j-1}}$$

with initial value $I_{i,J} = P_{i,J}$. $e^{\xi_{i,j}}$ and $e^{-\zeta_{i,j-1}}$ are called link ratios. Conditional on the sets $\mathfrak{B}_j$ and given the distribution assumptions on $\xi_{i,j}$ and $\zeta_{i.j-1}$, the joint distribution of $\left(\log P_{i,j+1}, \log P_{i,j+2}, \ldots, \log P_{i,J}\right)^\top$ follows a multivariate normal distribution, i.e.,

$$\left(\log P_{i,j+1}, \log P_{i,j+2}, \ldots, \log P_{i,J}\right)^\top \Big|_{\mathfrak{B}_j} \sim N(\boldsymbol{u}, \boldsymbol{\Sigma}), \tag{6.1}$$

where $\top$ is a vector transpose.

In equation (6.1),

$$\boldsymbol{u} = \begin{bmatrix} \eta_{j+1} + \left(1 - \beta_{j,j+1}\right)\left(\log P_{i,j} - \eta_j\right) + \beta_{j,j+1}\left(\log I_{i,j} - \mu_j\right) \\ \vdots \\ \eta_J + \left(1 - \beta_{j,J}\right)\left(\log P_{i,j} - \eta_j\right) + \beta_{j,J}\left(\log I_{i,j} - \mu_j\right) \end{bmatrix} \tag{6.2}$$

and

$$\boldsymbol{\Sigma} = \begin{bmatrix} \omega_{j+1}^2 - \left(1-\beta_{j,j+1}\right)\omega_j^2 - \beta_{j,j+1}\omega_{j,j+1}^2 & \cdots & \omega_{j+1}^2 - \left(1-\beta_{j,j+1}\right)\omega_j^2 - \beta_{j,j+1}\omega_{j,J}^2 \\ \vdots & \ddots & \vdots \\ \omega_{j+1}^2 - \left(1-\beta_{j,J}\right)\omega_j^2 - \beta_{j,J}\omega_{j,j+1}^2 & \cdots & \omega_J^2 - \left(1-\beta_{j,J}\right)\omega_j^2 - \beta_{j,J}\omega_{j,J}^2 \end{bmatrix}. \tag{6.3}$$

The parameters in equations (6.2) and (6.3) are given by

$$\eta_j = \sum_{m=0}^{j}\phi_m, \quad \omega_j^2 = \sum_{m=0}^{j}\sigma_m^2, \quad \mu_j = \sum_{m=0}^{J}\phi_m - \sum_{n=j}^{J-1}\varphi_n, \quad \nu_j^2 = \sum_{m=0}^{J}\sigma_m^2 - \sum_{n=j}^{J-1}\tau_n^2 \text{ and } \beta_{j,l} = \frac{\omega_l^2 - \omega_j^2}{\nu_j^2 - \omega_j^2}.$$

Let $C_{i,j}$ denote the incremental paid loss in accident year i during the j^{th} development year. Thus,

$$C_{i,j} = P_{i,j} - P_{i,j-1}. \tag{6.4}$$

As we are interested in future unpaid losses, the distribution of $C_{i,j}$ needs to be determined. Furthermore, note that the total paid losses in year k is given by

$$C_k = \sum_{i+j=k} C_{i,j}. \tag{6.5}$$

At time J, the total discounted future-unpaid losses is

$$R_J = \sum_{k=1}^{J} \frac{C_{J+k}}{(1+r_k)^k}, \tag{6.6}$$

where r_k is the interest rate at time k. In other words, this is the time-J outstanding loss liabilities of the claims spanning accident years 0 to J. It is also the reserve for the claims at time J.

6.3 Risk-margin calculation

IFRS 17 mandates that the risk margins must be calculated based on the discounted fulfillment cash flows over the lifetime of policies. As this new standard does not designate any estimation technique in determining the risk margin, we adopt four methods discussed in International Actuarial Association [7]. They are value at risk (VaR), conditional tail expectation (CTE), Wang transform (WT) and cost of capital (CoC).

VaR is the loss level for which the loss random variable exceeds with probability $1-\alpha$, where α is the confidence level. So, if S is the loss random variable then the $100\alpha\%$ VaR, denoted by $\text{VaR}_\alpha(S)$, is given by

$$\text{VaR}_\alpha(S) = \inf\{s : \mathbb{P}(S \leq s) \geq \alpha\}.$$

The risk margin is equal to the difference between VaR and the corresponding probability weighted expected value. The drawback of VaR is that it disregards the extreme values beyond the confidence level and this could lead to an underestimation of risks.

CTE is an alternative quantile technique, whose advantage over VaR is its primary concentration on the tail of the loss distribution and it is also a coherent risk measure. More specifically, CTE is the expected loss given that the loss is greater than $\text{VaR}_\alpha(S)$. Therefore,

$$\text{CTE}_\alpha(S) = \mathbb{E}[S|S > \text{VaR}_\alpha(S)].$$

The risk margin is then calculated as the difference between the CTE and the corresponding probability weighted expected value. The CTE may not be coherent though when the loss distribution is discrete. See for example, Boyle et al. [2].

Another coherent risk measure that we include is WT, which is typified as a distortion risk measure; see Wang [19] and Wang [20]. Under WT, probability distribution is adjusted due to risk preferences. This means that lower adjusted probability values are assigned to favourable outcomes whilst higher adjusted probability values are assigned to unfavorable outcomes. A WT was chosen in Miccolis and Heppen [14] to provide risk adjustment as per IFRS 17 by calibrating parameters. A general expression for the distortion risk measure for a non-negative loss random variable S is given by

$$\zeta_\chi(s) = \int_0^\infty \chi\left(1 - F_S(s)\right) ds,$$

where $F_S(s)$ is the cumulative distribution function of S and $\chi(x)$ is a distortion function $\chi\colon [0,1] \to [0,1]$, which is a non-decreasing function with $\chi(0) = 0$ and $\chi(1) = 1$. The distortion function for WT is given by

$$\chi(x) = \Phi\left(\Phi^{-1}(x) + \Phi^{-1}(\eta)\right),$$

where η is a risk aversion parameter. The higher the η, the lesser is the risk aversion. *The risk margin is calculated as the difference between the probability-weighted expected value using adjusted probability and the expected vale under the original probability.*

Under the concept of CoC, an entity will determine its risk preference based on its selection of a capital amount appropriate for the risks that are relevant to IFRS 17's measurement objectives. The assigned capital amount that would be used in computing the CoC is the difference between

(a) the amount calculated under the probability distribution associated with the selected confidence level and
(b) the amount using the probability weighted expected value.

The risk margin is computed as the present value of the future cost of capital associated with relevant cash flows. This is expressed as

$$\text{risk margin} = \sum_{i=1}^{n} \frac{c_i A_i}{(1 + r_i)^i},$$

where A_i is the assigned capital amount for period ending at time i, c_i is the CoC's rate at time i and r_i is the discount rate at time i.

The challenge in choosing the appropriate c_i is akin to meeting the specific requirement objectives. This should reflect a rate of return consistent with the entity being indifferent between insurance contract's liabilities with uncertain cash flows and liabilities with fixed cash flows. Also, the CoC's rate should take into account the entity's risk preference and experience. A general approach to quantifying a risk margin based on the CoC technique is described in Meyers [13], which incorporates stochastic path dependencies given that the capital amount is impacted over the time, and such an approach is applied to the claims development triangles of the unpaid losses.

6.4 Numerical illustration

In this section, we present a numerical illustration utilising incurred claims and paid losses data on Ontario automobile from 2002 to 2016 inclusive. There are three different groups of insurance policies categorised as: bodily injury, direct compensation and accident benefit. This tells us that we have 6 different data sets: (i) bodily injury incurred claims, (ii) bodily injury paid losses, (iii) direct compensation incurred claims, (iv) direct compensation paid losses, (v) accident benefit incurred claims, and (vi) accident benefit paid losses. The data sets were compiled by the General Insurance Statistical Agency and are displayed as claims development triangles.

These three types of insurance policies have various features and show different trends over development years. In this illustration, we have $J = 14$, i.e., we assume all claims are settled after 14 years. Moreover, it is assumed that the horizontal year is 2016 and we

must forecast the future claims after 2016. The estimates of parameters $\phi_j, \sigma_j, \varphi_j, \tau_j$ for $0 \leq j \leq J$ are obtained by using the maximum likelihood method. The formulae for the estimators are given by

$$\hat{\phi}_j = \frac{1}{J+1-j} \sum_{i=1}^{J+1-j} \log \frac{P_{i,j}}{P_{i,j-1}}, \quad \hat{\sigma}_j^2 = \frac{1}{J-j} \sum_{i=1}^{J+1-j} \left(\log \frac{P_{i,j}}{P_{i,j-1}} - \hat{\phi}_j \right)^2$$

and

$$\hat{\varphi}_j = \frac{1}{J+1-j} \sum_{i=1}^{J+1-j} \log \frac{I_{i,j}}{I_{i,j-1}}, \quad \hat{\phi}_j^2 = \frac{1}{J-j} \sum_{i=1}^{J+1-j} \left(\log \frac{I_{i,j}}{I_{i,j-1}} - \hat{\varphi}_j \right)^2.$$

Since there are not enough data points to estimate σ_{14} and τ_{14}, we extrapolate their values. Tables 6.2 and 6.3 display the estimates of these parameters.

Table 6.2: Parameter estimates recovered from paid-losses data

	Bodily injury		Direct compensation		Accident benefit	
Development year	ϕ_j	σ_j	ϕ_j	σ_j	ϕ_j	σ_j
1	1.788270	0.157308	0.129518	0.013202	1.004686	0.177061
2	1.110350	0.094517	0.001331	0.000329	0.327183	0.094545
3	0.715325	0.052882	0.000377	0.000225	0.193076	0.067292
4	0.437724	0.040531	0.000142	0.000300	0.130786	0.043079
5	0.254945	0.023194	0.000091	0.000307	0.082337	0.018089
6	0.135959	0.013062	0.000062	0.000090	0.053216	0.011642
7	0.073244	0.008697	-0.000028	0.000052	0.037004	0.007191
8	0.035751	0.002376	-0.000036	0.000076	0.026940	0.007446
9	0.021297	0.004364	-0.000024	0.000020	0.017885	0.002140
10	0.012067	0.003368	-0.000004	0.000017	0.015164	0.002982
11	0.007262	0.001986	-0.000008	0.000011	0.012159	0.001694
12	0.004751	0.000407	0.000011	0.000026	0.009612	0.001672
13	0.002382	0.000726	0.000001	0.000006	0.005552	0.000048
14	0.001546	0.000371	-0.000001	0.000001	0.005677	0.000000

Using the parameter estimates in Tables 6.2 and 6.3, the MC simulation method is conducted to forecast future unpaid losses and estimate the outstanding claims liabilities via the following procedure:

1. For each i ($0 \leq i \leq J$), generate values of $P_{i,j}$ ($i+1 \leq j \leq J$) using equation (6.1).

Table 6.3: Parameter estimates recovered from incurred-claims data

	Bodily injury		Direct compensation		Accident benefit	
Development year	φ_j	τ_j	φ_j	τ_j	φ_j	τ_j
1	0.363657	0.048902	0.023472	0.006457	0.223483	0.082017
2	0.279259	0.047978	0.000111	0.000712	0.077566	0.053506
3	0.135730	0.027995	0.000006	0.000400	0.058734	0.028937
4	0.059139	0.021971	0.000032	0.000468	0.026611	0.009055
5	0.023823	0.016908	-0.000108	0.000168	0.016343	0.007765
6	0.010466	0.010082	0.000053	0.000136	0.008198	0.007305
7	0.004622	0.006287	-0.000071	0.000095	0.007328	0.004943
8	0.003734	0.001926	-0.000035	0.000062	0.006238	0.003780
9	0.000282	0.001536	-0.000036	0.000047	0.004755	0.002683
10	0.001657	0.002030	0.000001	0.000031	0.004365	0.002093
11	-0.000375	0.000608	-0.000015	0.000009	0.001936	0.001826
12	0.000367	0.000321	0.000009	0.000022	0.001397	0.001573
13	-0.000200	0.000141	0.000002	0.000006	-0.000980	0.000767
14	0.000600	0.000051	-0.000003	0.000000	0.000251	0.000364

2. Calculate $C_{i,j}$, C_{J+l} and R_J using equations (6.4), (6.5) and (6.6), respectively.

3. Repeat steps 1 and 2 N times.

Considering that $J = 14$ and the horizontal year is 2016, we forecast the unpaid losses from years 2017 up to 2030. These unpaid losses correspond to insurance contracts with accident years from 2002 to 2016. The directive from IFRS 17 states that the discount rate applied to the estimates of the future cash flows should: (i) reflect the cash flows and liquidity's characteristics of the insurance contracts and (ii) be consistent with the current observed market prices. *IFRS 17 does not specify though any technique to determine the discount rate.* The "top-down" and "bottom up" methods are suggested by KMPG [9] to determine the discount rate value. For the ease of calculation, we assume r is constant and $r = 0.024$ in this example.

We implemented the MC simulation with 1,000,000 replicates. The histograms of unpaid losses for bodily-injury type policies in different years (C_{J+l}) are displayed in Figure 6.1. The means and standard deviations of unpaid losses in different years are shown in Table 6.4; the means and standard deviations of total discounted unpaid losses (i.e., outstanding

claims liabilities) are shown in the last row. From Table 6.4, the direct-compensation policy has much lower means and standard deviations. This is consistent with the fact that the claims are almost always reported and paid in the first few years under this policy type. The accident-benefit policy has the highest volatilities and this observation suggests that the future cash flows for this policy is more uncertain than those of the other two policies. The histograms of discounted total paid losses (R_J) are portrayed in Figure 6.2.

Figure 6.1: Histogram of unpaid losses (Bodily injury)

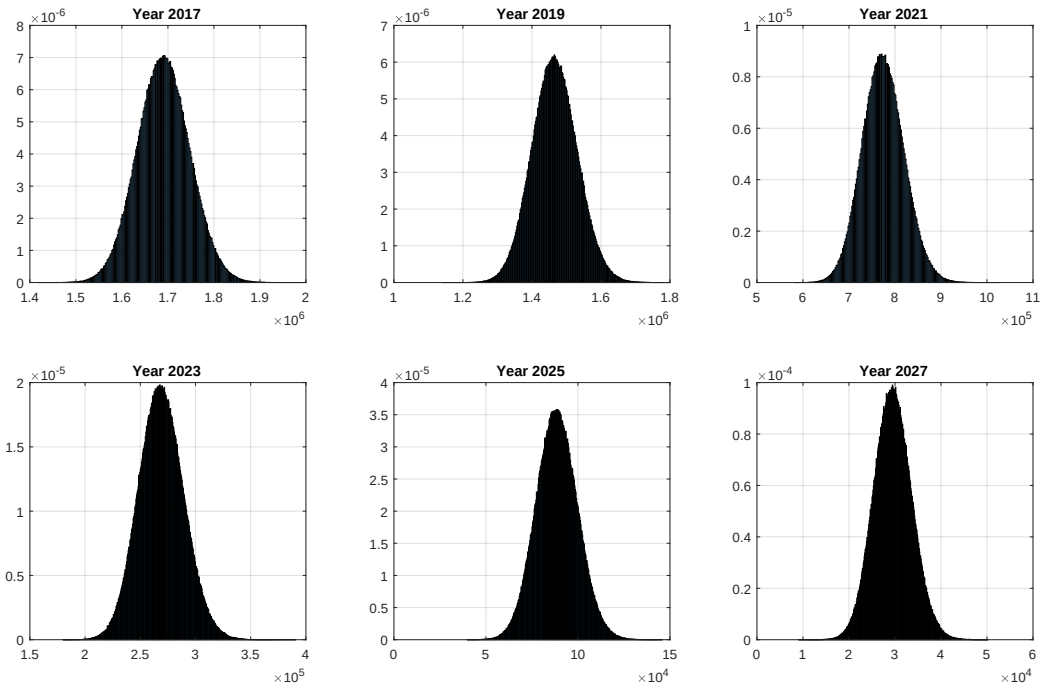

Note that it is impossible to obtain the exact distribution of outstanding claim liabilities. Therefore, some approximation methods must be utilised to obtain an approximated distribution. The most commonly used method is the empirical CDF. Some parametric approximations including normal and log-normal distributions could also be tried. We adopt the moment-based density approximation method introduced in Provost [16]. Under this method, the exact density function with known first n moments can be approximated by the product of (i) a base density, whose tail behaviour is congruent to that of the distribution to be approximated, and (ii) a polynomial of degree q. The parameters of the base density can be determined by matching the moments of the loss random variable and the approximated density.

Table 6.4: Mean and standard deviation for unpaid losses over years

	Bodily injury		Direct compensation		Accident benefit	
Year	Mean	Standard deviation	Mean	Standard deviation	Mean	Standard deviation
2017	1,690,702	56,868	161,823	7,514	2,081,685	145,573
2018	1,649,301	63,409	2,361	630	1,418,710	133,264
2019	1,466,276	65,562	601	538	1,038,584	109,498
2020	1,141,904	59,677	177	524	743,964	76,528
2021	774,620	45,353	104	416	525,908	44,481
2022	468,378	30,950	-14	154	375,404	31,389
2023	269,014	20,317	-107	114	272,098	22,738
2024	149,886	12,572	-75	104	194,005	17,352
2025	88,547	11,226	-32	42	133,650	9,693
2026	51,090	7,605	-3	36	98,451	8,316
2027	29,517	4,117	2	33	68,578	5,546
2028	16,176	1,753	14	33	43,156	3,906
2029	7,443	1,402	-1	8	23,514	1,264
2030	2,883	214	-2	0	11,580	1,083
Discounted total	7,251,056	179,836	161,072	7,357	6,530,111	225,069

The choice of the base function depends on the loss distribution. Based on the preliminary examination on the distribution of claims liabilities, we adopt the normal distribution for the approximation. In particular, the base function $\Psi(x)$ with parameters θ and c is given by

$$\Psi(x) = \frac{1}{\sqrt{2\pi c}} e^{-\frac{(x-\theta)^2}{2c^2}}.$$

Let the moments of the random variable X be $\alpha_X(i)$ for $i = 0, 1, \ldots, q$. Since it is not possible to obtain the theoretical moments of X, we can use the sample moments obtained from the data. Denote the theoretical moments of the base function $\Psi(x)$ by $m_X(i)$ for $i = 0, 1, \ldots, 2q$. The parameters θ and c of $\Psi(x)$ can be determined by setting $\alpha_X(i) = m_X(i)$ for $i = 1, 2$. Hence,

$$\theta = \alpha_X(1) \quad \text{and} \quad c = \sqrt{\alpha_X(2) - \alpha_X(1)^2}.$$

The density $f_X(x)$ of X is approximated as

$$f_q(x) = \Psi(x) \sum_{i=0}^{q} k_i \left(\frac{x-\theta}{c}\right)^i,$$

where k_i's, $i = 0, \ldots, n$, are polynomial coefficients and they are determined via

$$(k_0, k_1, \ldots, k_n)^\top = \mathbf{M}^{-1}(\alpha_X(0), \alpha_X(1), \ldots, \alpha_X(q))^\top,$$

where $\mathbf{M}$ is a $(q+1) \times (q+1)$ symmetric matrix whose $(i+1)^{\text{th}}$ row is $(m_X(i), m_X(i+1), \ldots, m_X(i+q))$.

Consequently, the approximated density of X is given by

$$f_q(x) = \frac{1}{\sqrt{2\pi c}} e^{-\frac{(x-\theta)^2}{2c^2}} \sum_{i=0}^{q} k_i \left(\frac{x-\theta}{c}\right)^i. \tag{6.7}$$

The approximated CDF of X can be obtained from equation (6.7). As an explicit formula for the quantile function is not available, quantiles can be calculated numerically (e.g., using Newton's method). We consider the normal and log-normal approximations as benchmarks. The approximated densities for the total unpaid losses based on these three methods are displayed in Figure 6.2. The corresponding CDFs are shown in Figure 6.3 and the moment-based approximation is the closest to the empirical CDF.

The Kolmogorov-Smirnov test is used to assess the goodness of fit of the approximations. The results of the test are provided in Table 6.5 showing that the moment-based density

Figure 6.2: Density of total unpaid losses

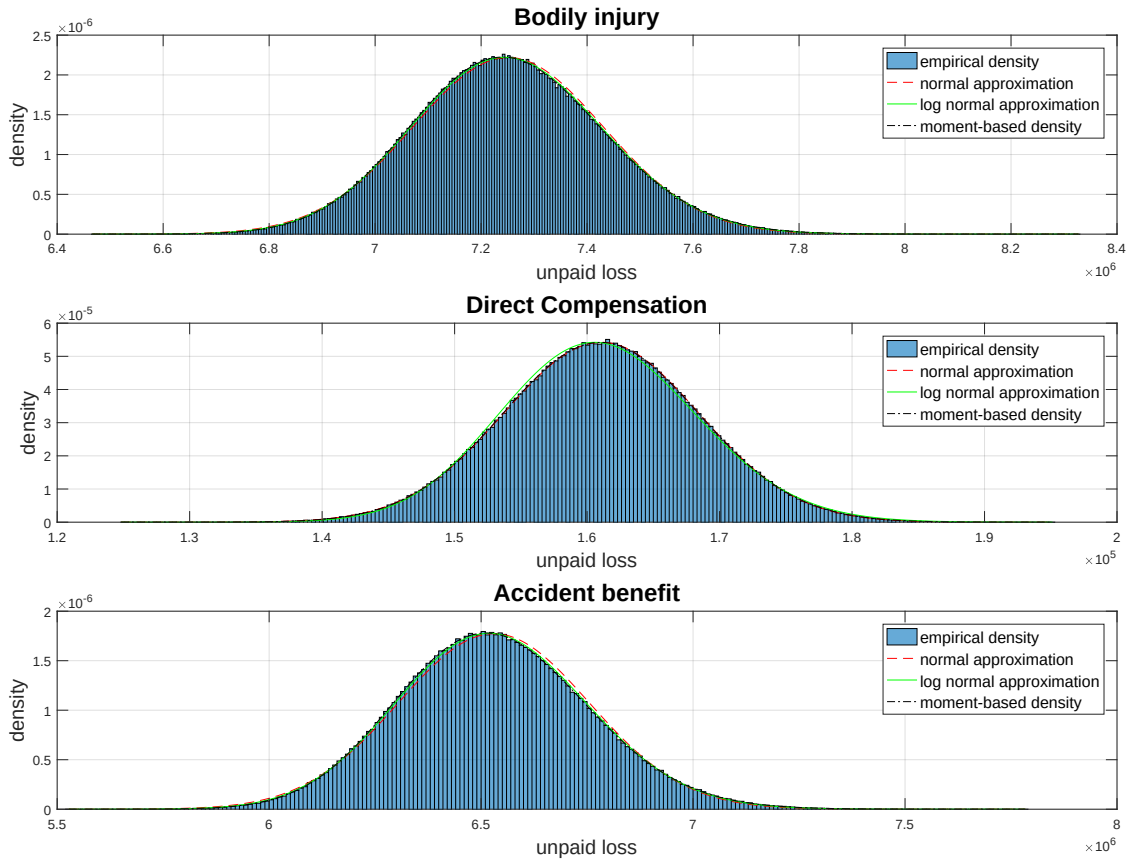

approximation outperforms the two other approximations.

Table 6.5: Results of the Kolmogorov-Smirnov test under different methods

	Bodily injury		Direct compensation		Accident benefit	
	test statistic	p-value	test statistic	p-value	test statistic	p-value
Moment-based	0.00072	0.67787	0.000363	0.999400	0.000485	0.972524
Normal	0.00757	0.00000	0.001221	0.101413	0.010594	0.000000
Log normal	0.00292	0.00000	0.008348	0.000000	0.003856	0.000000

The risk margins of three policy types are computed using the VaR, CTE, WT and CoC metrics based on the simulation results. The normal and log-normal approximations serve as benchmarks. We select three confidence levels for VaR and CTE: 90%, 95% and 99%. The three risk aversion parameter values for WT are 0.1, 0.05 and 0.01. The capital amounts

Figure 6.3: CDF of total unpaid losses

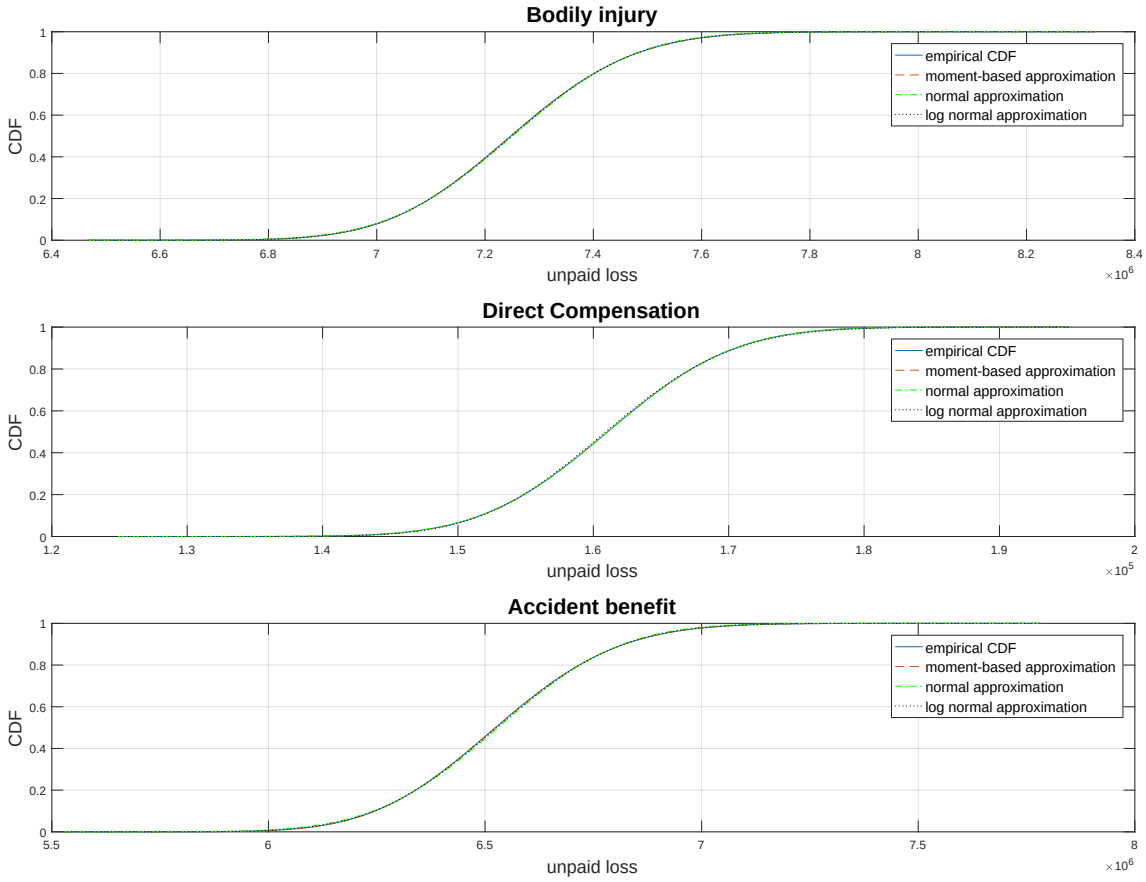

every year under the CoC method are determined using the VaR. The CoC rate is set at 0.08. The results are shown in Tables 6.6-6.9; percentages refer to the ratios of the risk margins to the probability weighted expected values. Results obtained from moment-based density method are better than those from the normal and log-normal approximations. This is because the differences between the results from the empirical CDF and those from the moment-based density method are much smaller than the differences between results from the other two methods and those from the empirical CDF. Note that risk margins using the CTE method have the highest values because CTE considers potential loss beyond the confidence level. Risk margins using the CoC method have much lower values.

It has to be noted that, notwithstanding IFRS 17's not indicating the method in determining risk margins, it requires that the confidence level to be disclosed. Therefore, if the WT or CoC method is used to calculate risk margins, the equivalent confidence level must be

revealed consistent with the VaR method.

The computed risk margins are based on historical data. In order to analyse the sensitivity of these risk margins to various risk-metric calculation, we employ the non-parametric bootstrap method. Bootstrap is a simulation-based statistical analysis that could be used to measure the accuracy of sample estimates. As statistics calculated from samples can be used to estimate parameter in the population, the bootstrap distribution can be utilised to describe the behaviour of quantities being estimated such as standard errors and confidence intervals.

Suppose $\{P_{i,j}, I_{i,j} : 0 < i \leq J, 0 < j \leq J - i\}$ is the observed data set. Define a_j and b_j as the mean and standard deviation of $P_{i,j}$ in year j, and also define e_j and g_j as the mean and standard deviation of $I_{i,j}$ in year j. We consider the residuals

$$D_{i,j} = \frac{P_{i,j} - \widehat{a}_j}{\widehat{b}_j} \quad \text{and} \quad E_{i,j} = \frac{I_{i,j} - \widehat{e}_j}{\widehat{g}_j},$$

where $\widehat{a}_j$,$\widehat{b}_j$,$\widehat{e}_j$ and $\widehat{g}_j$ are the estimates of a_j, b_j, e_j and g_j, respectively. Then we obtain the bootstrap distributions $\widehat{F}_{\mathcal{D}}$ for the set of observations $\mathcal{D} = \{D_{i,j} : i + j < J\}$ and $\widehat{F}_{\mathcal{E}}$ for the set of observations $\mathcal{E} = \{E_{i,j} : i + j < J\}$. We generate two series of IID residuals

$$D^*_{i,j} \sim \widehat{F}_{\mathcal{D}} \quad \text{and} \quad E^*_{i,j} \sim \widehat{F}_{\mathcal{E}}.$$

New 'observations' of $P_{i,j}$ and $I_{i,j}$ are given by

$$P^*_{i,j} = \widehat{a}_j + \widehat{b}_j D^*_{i,j} \quad \text{and} \quad P^*_{i,j} = \widehat{e}_j + \widehat{g}_j E^*_{i,j}.$$

The new estimates of parameters for the corresponding distribution are determined through these new observations. Consequently, the risk margins are computed under the new estimated distribution.

We apply the MC simulation method to generate 1,000 samples of new observations. For each trial, the risk margins are computed using simulation with 10,000 replicates. Then the bootstrap distribution for risk margins are obtained through these 1,000 samples. Figures 6.4-6.6 display the distribution of risk margins obtained using the bootstrap method. The corresponding means and standard deviations are shown in Table 6.10. From Figures 6.4-6.6 and Table 6.10, we see that the risk margins for bodily injury policy have the highest volatility whilst those for direct compensation have the lowest volatility. This suggests that the risk margins set for direct compensation policy are more accurate and stable. We also

Table 6.6: Risk margins using VaR

		90%		95%		99%	
		risk margin	risk margin %	risk margin	risk margin %	risk margin	risk margin %
Bodily injury	Emprical CDF	232,586	3.21%	301,332	4.16%	432,912	5.97%
	Moment-based	232,443	3.21%	301,327	4.16%	433,025	5.97%
	Normal	230,468	3.18%	295,803	4.08%	418,360	5.77%
	Log normal	231,730	3.20%	299,417	4.13%	428,042	5.90%
Direct compensation	Emprical CDF	9,441	5.86%	12,135	7.53%	17,229	10.70%
	Moment-based	9,439	5.86%	12,133	7.53%	17,213	10.69%
	Normal	9,429	5.85%	12,102	7.51%	17,115	10.63%
	Log normal	9,554	5.93%	12,415	7.71%	17,913	11.12%
Accident Benefit	Emprical CDF	291,133	4.46%	379,810	5.82%	550,904	8.44%
	Moment-based	291,759	4.47%	379,676	5.81%	550,023	8.42%
	Normal	288,438	4.42%	370,206	5.67%	523,589	8.02%
	Log normal	290,482	4.45%	376,316	5.76%	540,251	8.27%

Table 6.7: Risk margins using CTE

		90%		95%		99%	
		risk margin	risk margin %	risk margin	risk margin %	risk margin	risk margin %
Bodily injury	Emprical CDF	323,070	4.46%	382,240	5.27%	500,211	6.90%
	Moment-based	322,145	4.44%	380,489	5.25%	492,338	6.79%
	Normal	315,608	4.35%	370,949	5.12%	479,300	6.61%
	Log normal	320,451	4.42%	378,351	5.22%	493,044	6.80%
Direct compensation	Emprical CDF	12,961	8.05%	15,250	9.47%	19,737	12.25%
	Moment-based	12,938	8.03%	15,214	9.45%	19,596	12.17%
	Normal	12,912	8.02%	15,176	9.42%	19,609	12.17%
	Log normal	13,323	8.27%	15,791	9.80%	20,730	12.87%
Accident Benefit	Emprical CDF	408,207	6.25%	484,873	7.43%	639,130	9.79%
	Moment-based	407,440	6.24%	483,105	7.40%	633,080	9.69%
	Normal	394,993	6.05%	464,253	7.11%	599,858	9.19%
	Log normal	403,247	6.18%	476,953	7.30%	623,622	9.55%

Table 6.8: Risk margins using WT

		0.1		0.05		0.01	
		risk margin	risk margin %	risk margin	risk margin %	risk margin	risk margin %
Bodily injury	Emprical CDF	235,954	3.25%	304,946	4.21%	437,103	6.03%
	Moment-based	236,065	3.26%	305,273	4.21%	438,888	6.05%
	Normal	230,450	3.18%	295,749	4.08%	417,977	5.76%
	Log normal	233,992	3.23%	301,624	4.16%	429,625	5.92%
Direct compensation	Emprical CDF	9,466	5.88%	12,163	7.55%	17,225	10.69%
	Moment-based	9,466	5.88%	12,163	7.55%	17,221	10.69%
	Normal	9,427	5.85%	12,097	7.51%	17,083	10.61%
	Log normal	9,727	6.04%	12,580	7.81%	17,989	11.17%
Accident Benefit	Emprical CDF	298,548	4.57%	387,228	5.93%	558,767	8.56%
	Moment-based	298,582	4.57%	387,293	5.93%	558,804	8.56%
	Normal	288,424	4.42%	370,170	5.67%	523,377	8.01%
	Log normal	294,494	4.51%	380,325	5.82%	543,899	8.33%

Table 6.9: Risk margins using CoC

	90%		95%		99%	
	risk margin	risk margin %	risk margin	risk margin %	risk margin	risk margin %
Bodily Injury	35,911	0.50%	46,463	0.64%	66,633	0.92%
Direct Compensation	999	0.62%	1,285	0.80%	1,822	1.13%
Accident benefit	58,341	0.89%	75,550	1.16%	108,413	1.66%

note that the volatility under the CTE is higher than those of the VaR and WT. This tells us that the VaR and WT estimates are more stable than the CTE's.

Figure 6.4: Bootstrap distribution of risk margins (Bodily injury)

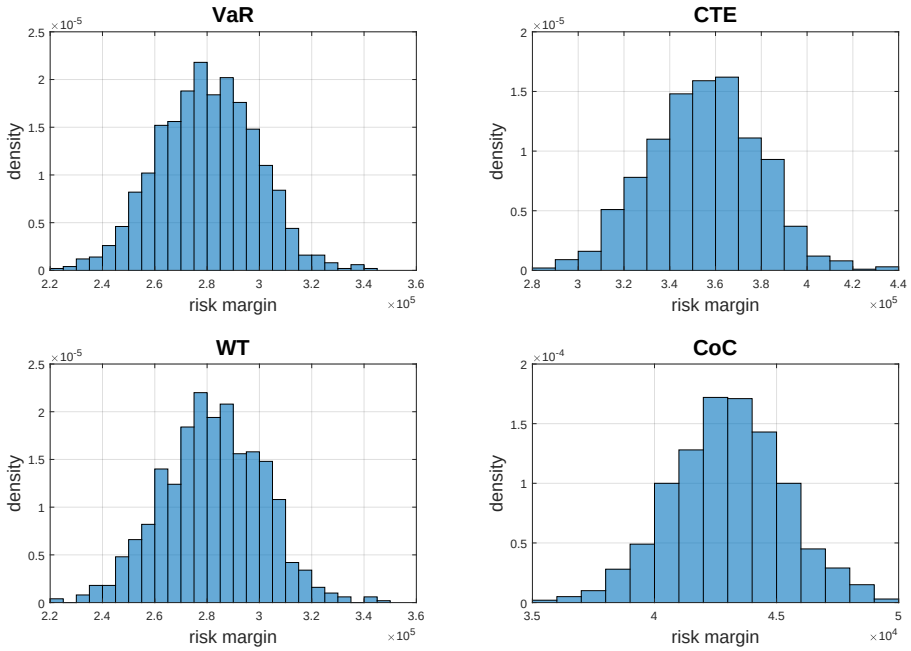

Figure 6.5: Bootstrap distribution of risk margins (Direct compensation)

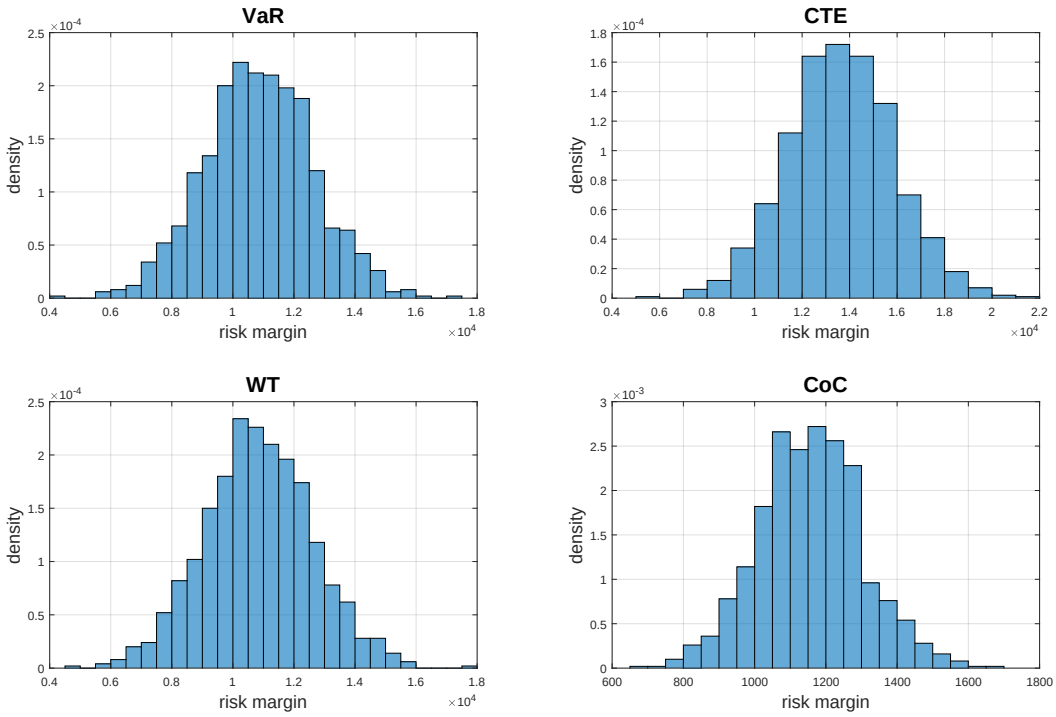

Figure 6.6: Bootstrap distribution of risk margins (Accident benefit)

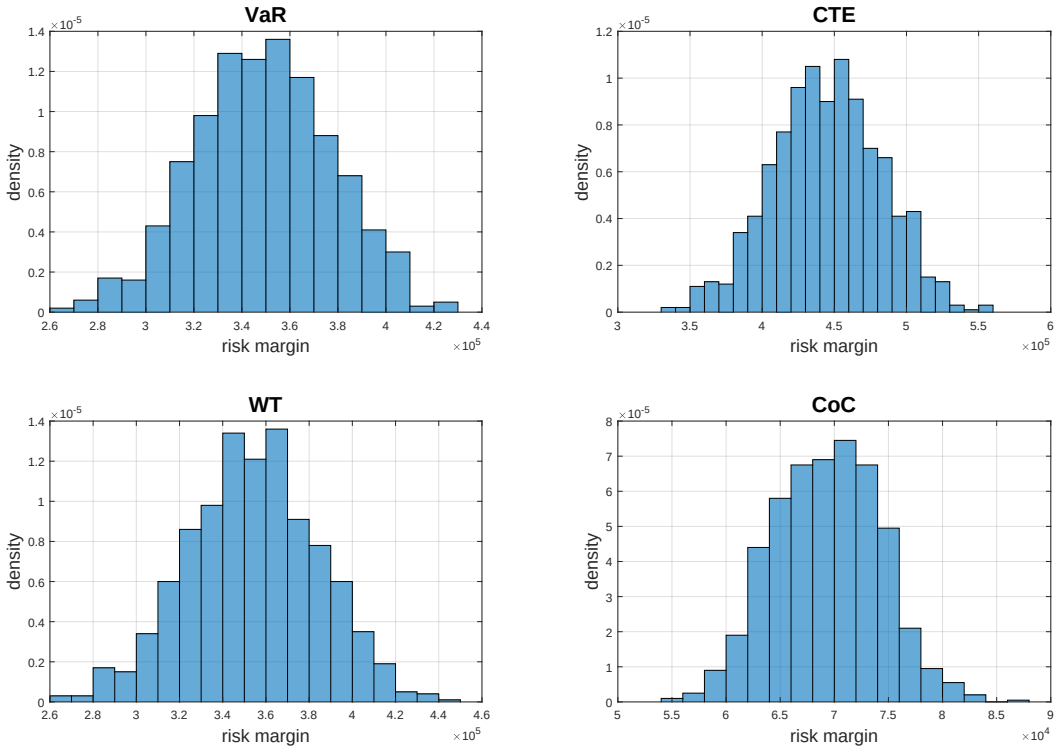

Table 6.10: Risk margins under the bootstrap method

	Bodily injury		Direct compensation		Accident benefit	
	mean	s.d.	mean	s.d.	mean	s.d.
VaR(95%)	280,034	18,678	10,848	1,786	349,095	28,620
CTE(95%)	355,017	23,859	13,631	2,243	444,891	37,543
WT(0.05)	282,258	19,054	10,839	1,781	353,871	30,081
CoC(95%)	43,023	2,329	1,157	146	69,330	4,910

6.5 Verifying the normality assumption

To verify that our data set for the numerical illustration in the previous section follows the normality assumption in section 6.2, we perform a KolmogorovSmirnov (KS) test and Shapiro-Wilk (WS) test the observations $\log \frac{P_{i,j}}{P_{i,j-1}}$ and $\log \frac{I_{i,j}}{I_{i,j-1}}$ covering the first three accident years. The KS test is a nonparametric test of the null hypothesis that the cumulative distribution function (CDF) of the data is equal to the hypothesised CDF. The KS test could

be used to assess normality of empirical data when the hypothesised CDF is a normal distribution. The SW test is also used for normality test but it is designed for situations of small sample sizes. The results from the two statistical tests are shown in Table 6.11. We see that high p-values are obtained so that we could not reject the null hypothesis of a normal CDF. Therefore, it is reasonable to adopt the normal assumption in the model.

Table 6.11: p-values for the KS and SW normality tests

		Bodily Injury		Direct Compensation		Accident benefit	
	Accident year	KS test	SW test	KS test	SW test	KS test	SW test
Paid	1	0.875474	0.793625	0.925442	0.204618	0.652408	0.136140
losses	2	0.868966	0.167638	0.963453	0.525485	0.939638	0.573753
	3	0.585226	0.075189	0.913402	0.665581	0.693782	0.083805
Inccured	1	0.925442	0.204618	0.958631	0.807814	0.920132	0.382023
claims	2	0.963453	0.525485	0.894853	0.432259	0.874620	0.547997
	3	0.913402	0.665581	0.610291	0.137533	0.931737	0.846044

Of course, if the normality assumption is not adequate, other non-Gaussian distributions with heavy tails could be considered (e.g., lognormal).

6.6 Conclusion

In this chapter, we proposed an efficient and accurate methodology and elaborated on the entire process in estimating risk margins for claims according to the IFRS 17's requirements. The paid-incurred chain model was adopted to describe the development of unpaid losses based on historical information involving incurred-claims and paid-losses data. The Monte-Carlo simulation method was employed to generate samples of future unpaid losses. To approximate the distribution of claims reserves, the Moment-based approximation method was utilised. Risk margins were computed in four different ways using the approximated distribution with the bootstrap method being applied to obtain the distribution of risk margins.

The methodology and procedures described here could be used as implementation guidelines for the computation of risk margins of insurance companies' claims. Certain fundamental ideas in this research could stimulate further examinations of various aspects of allocating risk margins of claims liabilities. In future studies, models and methods considered here could be extended in many ways. The independent assumption on the link ratios

could be relaxed and assumed that they follow a multivariate skew normal distribution (see Pigeon et al. [15]). A prior distribution of the model parameters could be taken into account leading a the Bayesian paid-chain incurred method as alluded in Merz and Wüthrich [12]. When dealing with several types of policies, risk dependencies and aggregation techniques should be treated with an appropriate approach. A copula method could be used to model the dependence structure and calculate the aggregated risks for all policies; some in International Actuarial Association [7].

It should be noted that, we only considered the historical data of incurred claims and paid losses. The reliability of estimation results will increase if we could incorporate other useful information including earned premium, earned exposure, reserves, etc. Furthermore, the additional information may decrease as well the variability of model parameter estimates and improve the performance of future forecasting of cash flows. Lastly, the risk margins we computed are solely based on future unpaid losses. Other relevant future cash flows satisfying the requirements of IFRS 17 could be embedded when available in the implementation of the method to calculate risk margin practically in insurance companies.

References

[1] G. Barnett and B. Zehnwirth. Best estimates for reserves. In *Proceedings of the Casualty Actuarial Society*, volume 87, pages 245–321, 2000.

[2] Siu T. Boyle, P. and H. Yang. Risk and probability measures. *Risk*, 15(7):53–57, 2002.

[3] H. Gao, R. Mamon, and X. Liu. Risk measurement of a guaranteed annuity option under a stochastic modelling framework. *Mathematics and Computers in Simulation*, 132:100–119, 2017.

[4] D. Gogol. Using expected loss ratios in reserving. *Insurance: Mathematics and Economics*, 12(3):297–299, 1993.

[5] J. Hertig. A statistical approach to ibnr-reserves in marine reinsurance. *ASTIN Bulletin: The Journal of the IAA*, 15(2):171–183, 1985.

[6] International Accounting Standards Board. *IFRS 17 Insurance Contracts*. IFRS Foundation, London, UK, 2017.

[7] International Actuarial Association. *Risk Adjustments for Insurance Contracts under IFRS17*. Toronto, Ontario, 2018.

[8] T. Jin, S. Provost, and J. Ren. Moment-based density approximations for aggregate losses. *Scandinavian Actuarial Journal*, 2016(3):216–245, 2016.

[9] KMPG. IFRS 17 Insurance Contracts First Impressions. URL `https://home.kpmg.com/content/dam/kpmg/xx/pdf/2017/07/ifrs17-first-impressions-2017.pdf`.

[10] T. Mack. A simple parametric model for rating automobile insurance or estimating ibnr claims reserves. *ASTIN Bulletin: The Journal of the IAA*, 21(1):93–109, 1991.

[11] T. Mack. Distribution-free calculation of the standard error of chain ladder reserve estimates. *ASTIN Bulletin: The Journal of the IAA*, 23(2):213–225, 1993.

[12] M. Merz and M. Wüthrich. Paid–incurred chain claims reserving method. *Insurance: Mathematics and Economics*, 46(3):568–579, 2010.

[13] G. Meyers. A cost of capital risk margin formula for non-life insurance liabilities. In *Casualty Actuarial Society E-Forum*, 2017.

[14] R. Miccolis and D. Heppen. A practical approach to risk margins in the measurement of insurance liabilities for property and casualty (general insurance) under developing international financial reporting standards. In *International Congress of Actuaries, Cape Town, South Africa*, 2010.

[15] M. Pigeon, K. Antonio, and M. Denuit. Individual loss reserving using paid–incurred data. *Insurance: Mathematics and Economics*, 58:121–131, 2014.

[16] S. Provost. Moment-based density approximants. *Mathematica Journal*, 9(4):727–756, 2005.

[17] A. Renshaw and R. Verrall. A stochastic model underlying the chain-ladder technique. *British Actuarial Journal*, 4(4):903–923, 1998.

[18] G. Taylor. *Loss Reserving: An Actuarial Perspective*, volume 21. Springer Science & Business Media, 2012.

[19] S. Wang. A class of distortion operators for pricing financial and insurance risks. *Journal of risk and insurance*, 67(1):15–15, 2000.

[20] S. Wang. A universal framework for pricing financial and insurance risks. *ASTIN Bulletin: The Journal of the IAA*, 32(2):213–234, 2002.

[21] M. Wüthrich and M.l Merz. *Stochastic Claims Reserving Methods in Insurance*, volume 435. John Wiley & Sons, 2008.

[22] B. Zehnwirth. Probabilistic development factor models with applications to loss reserve variability, prediction intervals and risk based capital. In *Casualty Actuarial Society Forum*, volume 2, pages 447–606. Citeseer, 1994.

[23] Y. Zhao, R. Mamon, and H. Gao. A two-decrement model for the valuation and risk measurement of a guaranteed annuity option. *Econometrics and Statistics*, 8:231–249, 2018.

Chapter 7

Conclusion

7.1 Research summary

In this thesis, we developed appropriately various pricing and hedging frameworks for insurance products with investment guarantees under correlated risks. First, the construction of a pricing framework for an annuity with stochastic and dependent interest and mortality rates was tackled. Second, a CIR interest rate model is combined with the LC mortality rate model in the pricing of GAO. Third, under a two-decrement model lapse risk is added into financial and insurance risks as a particular factor for the valuation of a GAO; all three risk factors are dependent and modelled as affine-diffusion processes. Fourth, a regime-switching framework for three risk processes, namely the short-rate, force of mortality and stock index processes and are all governed by HMMs, was created for for GMMB pricing. Finally, we explored the paid-incurred chain model to analyse the claim triangular data and compute the risk margins as per the requirements of IFRS 17.

The major research contributions accomplished in this thesis are: (i) Successful application of sequential probability measure changes to obtain computational efficient representation of the longevity product's value; (ii) Design of an efficient algorithm for GAO pricing, which reduces computing time through a comonotonic approximation; (iii) Utility of a moment-based density to approximate accurately and speedily the distribution of loss random variables; (iv) Implementable closed-form solutions, via Fourier transform, for a GMMB value under the framework of HMM-modulated risk processes; (v) Derivation of HMM filters for the GMMB modelling set up, and provided recursive estimators for every model parameter; and (vi) Allocation of risk margins using paid-incurred chain method on P&C claim data.

This research work offers valuable insights and contributions to the theoretical underpinnings of financial insurance covering some important issues in the life and non-life insurance sectors. Our results could benefit insurers academic researchers, and financial regulators. It is important for insurance companies to come up with the fair valuation and effective risk management of insurance products. Our applications of stochastic models in finance and actuarial science give some ideas on how to further take advantage of various useful concepts and methods in probability, statistics and related areas in addressing contemporary issues in pension economics and regulatory considerations towards financial stability and insurance resiliency.

7.2 Future research directions

Although we made considerable gains on accuracy and efficiency of our parameter estimation and methodology for valuation and risk management computations under more flexible modelling frameworks, we also recognise certain limitations. Yet, these limitations could be turned into opportunities for possible extensions or continued search for alternative techniques. The theoretical and practical contributions of our research are expected to inspire further investigations of developing new or tailoring available stochastic approaches in actuarial theory and practice. We provide several ramifications of what we learnt throughout the course of this study.

- An HMM could be incorporated to enrich further the pricing framework in Chapter 2 that synthesises CIR and LC processes. This extension enables capacity to to capture dynamic regime changes in the economic and mortality environments.

- A higher-order HMM (HOHMM) may be used in the modelling framework of Chapter 5. HMM is generally capable of describing first-order transitions amongst hidden states. However, it might not be adequate for some real-world applications because imposing that current state dependent only on the last state may be too restrictive. The HOHMM allows the present state to be dependent on information reflected on previous states many time steps into the past.

- Our pricing framework could be applied in other GMBs such as GMDB, GMAB and GMIB and other equity-linked insurance products. In principle, getting pricing representations for these insurance products may be straightforward under our proposed modelling frameworks; however, numerical evaluations could present some

challenges that need to be handled with the help of additional details and product's pay off specifications.

- Hedging strategy is an important part in risk management. Although we did not concentrate on sensitivity of parameters under our model settings, computing the 'Greeks' for insurance products could provide insurers, investors and regulators with characteristics of the insurance policies and investments that they are dealing with.

- In improving the accuracy of the estimation of risk margins in chapter 6, the inclusion of certain information such as earned premium and case reserve could reduce the variability of the estimators. Furthermore, some alternative distributions could be adopted to better describe the claim data. In particular, for calculating risk margins we only consider incurred claims and paid losses. Various earned premiums in different accident years suggest different amounts of potential losses. Therefore, we could link the earned premium to the claim amount through the ratio of incremental claim and earned premium rather than claims themselves.

  We also deem it more realistic for log-normal or gamma distribution in fitting the ratio data. These distributions have better performance than that of the normal distribution in capturing the behaviour of heavy right tails. The resulting risk margins under the new distributions will be higher and thereby preferred by risk-adverse companies.

Appendix

Calculation details for the computation of the first two moments of k_t for Chapter 3

$$
\begin{aligned}
\mathrm{E}^{\widetilde{Q}}[\sqrt{r_t}] &= \frac{1}{\sqrt{\widetilde{c}_t}} \int_0^\infty \sqrt{z} \sum_{i=0}^{\infty} \frac{e^{-\widetilde{\lambda}_t/2}(\widetilde{\lambda}_t/2)^i}{i!} p_{\Gamma(i+\widetilde{\nu}_t/2,1/2)}(z)dz \\
&= \frac{1}{\sqrt{\widetilde{c}_t}} \int_0^\infty \sqrt{z} \sum_{i=0}^{\infty} \frac{e^{-\widetilde{\lambda}_t/2}(\widetilde{\lambda}_t/2)^i}{i!} \frac{(1/2)^{i+\widetilde{\nu}_t/2} z^{i+\widetilde{\nu}_t/2-1}}{\Gamma(i+\widetilde{\nu}_t/2)} e^{-z/2} dz \\
&= \frac{\sqrt{2}}{\sqrt{\widetilde{c}_t}} \int_0^\infty \sum_{i=0}^{\infty} \frac{e^{-\widetilde{\lambda}_t/2}(\widetilde{\lambda}_t/2)^i}{i!} \frac{\Gamma(i+\widetilde{\nu}_t/2+1/2)}{\Gamma(i+\widetilde{\nu}_t/2)} \frac{(1/2)^{i+\widetilde{\nu}_t/2+1/2} z^{i+\widetilde{\nu}_t/2-1/2}}{\Gamma(i+\widetilde{\nu}_t/2+1/2)} e^{-z/2} dz \\
&= \sqrt{\frac{2}{\widetilde{c}_t}} \sum_{i=0}^{\infty} \frac{e^{-\widetilde{\lambda}_t/2}(\widetilde{\lambda}_t/2)^i}{i!} \frac{\Gamma(i+\widetilde{\nu}_t/2+1/2)}{\Gamma(i+\widetilde{\nu}_t/2)} \int_0^\infty \frac{(1/2)^{i+\widetilde{\nu}_t/2+1/2} z^{i+\widetilde{\nu}_t/2-1/2}}{\Gamma(i+\widetilde{\nu}_t/2+1/2)} e^{-z/2} dz \\
&= \sqrt{\frac{2}{\widetilde{c}_t}} \sum_{i=0}^{\infty} \frac{e^{-\widetilde{\lambda}_t/2}(\widetilde{\lambda}_t/2)^i}{i!} \frac{\Gamma(i+\widetilde{\nu}_t/2+1/2)}{\Gamma(i+\widetilde{\nu}_t/2)}.
\end{aligned}
$$

Note that $\frac{(1/2)^{i+\widetilde{\nu}_t/2+1/2} z^{i+\widetilde{\nu}_t/2-1/2}}{\Gamma(i+\widetilde{\nu}_t/2+1/2)} e^{-z/2}$ is the density function of a gamma random variable with parameters $i+\widetilde{\nu}_t/2+1/2$ and $1/2$. Hence, the expectation of k_t under the forward measure is

$$
\begin{aligned}
\mathrm{E}^{\widetilde{Q}}[k_t] &= \mathrm{E}^{\widetilde{Q}}\left[k_0 + ct - \rho\sigma\xi \int_0^t A(u,T)\sqrt{r_u}du + \xi\widetilde{Z}_t\right] \\
&= k_0 + ct - \rho\sigma\xi \int_0^t A(u,T)\mathrm{E}^{\widetilde{Q}}[\sqrt{r_u}]du.
\end{aligned}
$$

The variance of k_t under the forward measure is

$$\begin{aligned}
\mathrm{Var}^{\widetilde{Q}}[k_t] &= \mathrm{Var}^{\widetilde{Q}}\left[k_0 + ct - \rho\sigma\xi \int_0^t A(u,T)\sqrt{r_u}du + \xi\widetilde{Z}_t\right] \\
&= (\rho\sigma\xi)^2 \int_0^t A(u,T)^2 \mathrm{Var}^{\widetilde{Q}}[\sqrt{r_u}]du + \xi^2 \mathrm{Var}^{\widetilde{Q}}[\widetilde{Z}_t] + \rho\sigma\xi^2 \int_0^t A(u,T)\mathrm{Cov}^{\widetilde{Q}}[\sqrt{r_u}], \widetilde{Z}_u]du \\
&= (\rho\sigma\xi)^2 \int_0^t A(u,T)^2 (\mathrm{E}^{\widetilde{Q}}[r_u] - \mathrm{E}^{\widetilde{Q}}[\sqrt{r_u}]^2)du + \xi^2 t + \rho\sigma\xi^2 \int_0^t A(u,T)\mathrm{Cov}^{\widetilde{Q}}[\sqrt{r_u}], \widetilde{Z}_u]du.
\end{aligned}$$

Curriculum Vitae

Name:	Yixing Zhao
Post-Secondary Education and Degrees:	PhD in Statistics (Actuarial Science), 2015 - 2019 *The* University *of* Western Ontario, London, ON, Canada
	MSc in Statistics (Actuarial Science), 2014 - 2015 *The* University *of* Western Ontario, London, ON, Canada
	BSc in Mathematics and Applied Mathematics, 2010 - 2014 South China University *of* Technology, China
Honours and Awards:	Western Graduate Research Scholarship, 2015 - 2019 MITACS-Accelerate Internship Award, 2018 - 2019
Related Work Experience:	Research and Teaching Assistant, 2015 - 2018 *The* University *of* Western Ontario

Publications:

[1] Y. Zhao, R. Mamon, An efficient algorithm for the valuation of a guaranteed annuity option with correlated financial and mortality risks, *Insurance: Mathematics and Economics*, 78 (2018) 1–12.

[2] Y. Zhao, R. Mamon, H. Gao, A two-decrement model for the valuation and risk measurement of a guaranteed annuity option, *Econometrics and Statistics*, 8 (2018) 231–249.

[3] Y. Zhao, R. Mamon, Annuity valuation under correlated risks, *Japan Journal of Industrial and Applied Mathematics*, accepted, April 2019.

[4] Y. Zhao, R. Mamon, The valuation of a guaranteed minimum maturity benefit under a regime-switching framework, under second review in the *North American Actuarial Journal*.

[5] Y. Zhao, R. Mamon, Setting risk margin for claims liabilities in accordance with IRFS 17, under second review in *ASTIN Bulletin*.